

**DEVELOPMENT OF IN VITRO TOXICITY ASSAYS WITH A
RAINBOW TROUT GILL CELL LINE AND THEIR USE IN
DETERMINING THE CYTOTOXICITY AND PHOTOCYTOTOXICITY
OF POLYCYCLIC AROMATIC HYDROCARBONS INDIVIDUALLY
AND IN A COMPLEX MIXTURE**

by

KRISTIN SCHIRMER

A thesis

presented to the University of Waterloo

in fulfillment of the

thesis requirement for the degree of

Doctor of Philosophy

in

Biology

Waterloo, Ontario, Canada, 1997

©Kristin Schirmer 1997



National Library
of Canada

Acquisitions and
Bibliographic Services

395 Wellington Street
Ottawa ON K1A 0N4
Canada

Bibliothèque nationale
du Canada

Acquisitions et
services bibliographiques

395, rue Wellington
Ottawa ON K1A 0N4
Canada

Your file Votre référence

Our file Notre référence

The author has granted a non-exclusive licence allowing the National Library of Canada to reproduce, loan, distribute or sell copies of this thesis in microform, paper or electronic formats.

The author retains ownership of the copyright in this thesis. Neither the thesis nor substantial extracts from it may be printed or otherwise reproduced without the author's permission.

L'auteur a accordé une licence non exclusive permettant à la Bibliothèque nationale du Canada de reproduire, prêter, distribuer ou vendre des copies de cette thèse sous la forme de microfiche/film, de reproduction sur papier ou sur format électronique.

L'auteur conserve la propriété du droit d'auteur qui protège cette thèse. Ni la thèse ni des extraits substantiels de celle-ci ne doivent être imprimés ou autrement reproduits sans son autorisation.

0-612-22239-X

The University of Waterloo requires the signatures of all persons using or photocopying this thesis. Please sign below, and give address and date.

ABSTRACT

Polycyclic aromatic hydrocarbons (PAHs) are common contaminants in aquatic environments. However, studying their impact on fish is problematic. They are difficult to study because they can occur singly or as complex mixtures and can be modified by ultraviolet (UV) radiation. They are costly to study because of the expense associated with the exposure of fish to PAHs and subsequently with the disposal of large volumes of contaminated water. To overcome these problems, *in vitro* methods have been developed in this thesis to study the toxicity of individual PAHs and a PAH mixture to fish cells and to examine the influence of UV on toxicity.

Methodology was developed for quantifying the photocytotoxicity of fluoranthene to the rainbow trout gill cell line, RTgill-W1, for future use in screening PAHs for their relative photocytotoxicity to fish. Solubilization in a modified culture medium was achieved with and without fetal bovine serum (FBS) and with and without dimethyl sulfoxide (DMSO). FBS caused most of the fluoranthene to remain in solution and blocked photocytotoxicity if present during UV irradiation. DMSO had little effect on fluoranthene distribution in cell cultures but caused cells to be slightly more sensitive to the phototoxicity of fluoranthene. The indicator dyes, alamar Blue™ and 5-carboxyfluorescein diacetate acetoxymethyl ester (CFDA-AM), were used to quantify cytotoxicity in two different ways: singly in two separate assays, and mixed together in a novel single assay, which saved time and material. With UV irradiation for 2 hr at a photon fluence rate of either 1.4 $\mu\text{mol m}^{-2} \text{s}^{-1}$ UV-B (UV-A : UV-B, 1.5) or 1.1 $\mu\text{mol m}^{-2} \text{s}^{-1}$ UV-B (UV-A : UV-B, 9.7), both dyes indicated increasing loss of viability with increasing doses of fluoranthene. EC_{50} s ranged from 18 to 44 ng/ml (89 to 217 nM), with the alamar Blue assay being slightly more sensitive.

Sixteen PAHs were screened for their ability to be directly cytotoxic to the rainbow trout gill cell line, RTgill-W1. Exposure times of 2 hours or less were sufficient for direct cytotoxicity to be detected, which appeared to be caused by a common mechanism, the general perturbation of membranes. This was judged by the similarity of results obtained for three fluorescent indicator dyes, alamar Blue™, CFDA-AM, and neutral red. Among the 16 PAHs tested, just two- and three-ring PAHs were cytotoxic. These were naphthalene \cong acenaphthylene \cong acenaphthene > fluorene \cong phenanthrene. The relative potency of these five PAHs suggested that water solubility is important but another contributing factor is lipophilicity. Thus, for PAHs to be directly cytotoxic, they must accumulate in membranes and the failure of larger PAHs to be cytotoxic likely was caused by their failure to accumulate in membranes sufficiently. Only naphthalene was effective at concentrations well below its water solubility limit. Therefore, direct cytotoxicity is likely to be most environmentally relevant only with naphthalene.

Sixteen PAHs were screened for their ability to be photocytotoxic to the rainbow trout gill cell line, RTgill-W1. PAHs could be divided into one of 3 groups: incapable of being photocytotoxic, able to be photocytotoxic but also to be directly cytotoxic, or capable of only being photocytotoxic. Photocytotoxicity was distinct from direct cytotoxicity in that EC_{50} values were lower with the neutral red assay immediately after the PAH/UV treatment than with alamar Blue or CFDA-AM, indicating a more specific action on lysosomes. As well, in photocytotoxicity but not in direct cytotoxicity, the three assays showed increased impairment 24 hr after the treatment. This is consistent with the contention that reactive oxygen species are involved in photocytotoxicity. Most PAHs were found to be strictly photocytotoxic; however, only six compounds were photocytotoxic at concentrations theoretically achievable in water. When photocytotoxic PAHs were ranked relative to fluoranthene to establish fluoranthene equivalent factors (FEFs), benzo[a]pyrene and benzo[g,h,i]perylene were found to be most potent. However, when the water solubility of each compound was taken into account in order to calculate the potential environmental photocytotoxic potency (PEPP), fluoranthene and pyrene appeared to have the most potential to impact fish through photocytotoxicity.

The influence of ultra violet (UV) irradiation on creosote toxicity was investigated with the rainbow trout gill cell line, RTgill-W1, and two indicator dyes: alamar Blue and CFDA-AM. Respectively, these monitor metabolic activity and membrane integrity. After solubilization and chemical analysis, creosote was presented to cells in the dark to measure cytotoxicity or concurrently with UV irradiation to evaluate photocytotoxicity. As well, creosote was photomodified by two hours of UV irradiation prior to presentation to cells in the dark or together with UV. Cytotoxicity was detected only at high nominal creosote concentrations, but photocytotoxicity occurred at creosote concentrations 35 fold lower. All the aromatic hydrocarbons in creosote appeared to contribute to cytotoxicity, but photocytotoxicity was due only to the fluoranthene, pyrene, anthracene and benzo[a]anthracene of creosote. Photomodified creosote was much more cytotoxic than intact creosote and this difference was most pronounced in the alamar Blue assay. Likely, this was due to photomodification products that impaired the mitochondrial electron transport chain. Photomodified creosote was slightly less photocytotoxic than intact creosote. Overall these results indicate that UV irradiation potentially enhances the toxicity of creosote to fish in several different but significant ways.

ACKNOWLEDGMENTS

Here I am! My head is still spinning from writing my thesis and I haven't thanked anyone yet for helping me get to this point. The point I am talking about is that of daily prayer that my brain will last just one more day. Looking back, I think that these last three years were the most dynamic in my three-decade life. Actually, they were like a movie with me as the main actor! All right, you lab mates, I knew you would laugh. Kristin and movies and actors. But for all you Canadians who still can't believe that the stars were not at war in East Germany - I have seen Star Wars, all three parts, and it was not for nothing. What is the major truth I learned from the movie for my Ph.D.? THE FORCE HAS BEEN WITH ME!

Well, I would not be here without the director of the cast, my supervisor Dr. Niels Bols. Niels, how is this for a topic sentence? I am very grateful for your imperturbable support (don't you just love that phrase?) and enthusiasm throughout the project up to this very minute. Your generosity and understanding are invaluable commodities. You always find time for your crew members, be it between the baby wanting to have his diapers changed, Alee and Bjorn wanting to go camping, Lucy waiting desperately for some family time and....a basketball tournament. Working with you means great energy and fun and I am looking forward to the many Tim Hortons' coffee discussions still to come: of course, large and black.

Luckily, I also had the chance to work with the directors of two other crews, Drs. George Dixon and Bruce Greenberg. George and Bruce, making me see things from your perspective helped me to find out where my piece of lab bench toxicology can fit into the big picture of helping people understand what they see on stage, and added a great deal of environmental toxicology and photochemistry to my cell culture work. I believe that it is this combination that made my research somewhat unique.

There is, of course, no cast with just one actor. In fact, I had so many fellow crew members that I am afraid I will forget one, so please forgive me if you are not mentioned here and remember - I tried. Let me start with the highest ranked V.I.P.s: Lucy Lee (Doctor of Philosophy, Professor, and many other things), who showed me every day that women, motherhood and science can fit together; Liz Heikkila (first class technical expert in all kinds of cell bioassays), who, despite having a family, shared some of those tiring, endless time courses with me; Janine Clemons (Doctor of Philosophy), à la J9, who taught me (amongst other things) how to manage a computer rather than having the computer manage me; Denise Tom (Master of Science), à la Smiley, who is irreplaceable in having a whole crew work together and at the same time have everybody laugh but who, despite my sober efforts, still believes that German actors grow up on German beer rather than valuable mother's milk; Rosemarie Ganassin (Doctor of Philosophy, soon to be), à la Rm, who showed me that there are other things to adjust on a microscope than just the focus; and Jeff Whyte (Doctor of Philosophy, also soon to be) who made me listen to the North American classic, "War of the Worlds". This was during one

of those nights where I went to the studio hoping to practice my role in quiet, only to find out that everybody else had similar plans. Needless to say I got nothing done. And then there are the more temporary V.I.P.s: Jo-Anne Herbrick, Angelina Chan, John Brubacher and Andrew Dueck, all smart, hard workers and potential academy award winners. Jo-Jo, I saw Sean Connery last week and he did remember you, "ka-ching!". Angelina, you are the only person who shares my field experience and I would say it was a special one with all the hole drilling preparations and then the rain and the BBQ. John-Andrew, you guys were always great fun to work with but there is this one thing I haven't figured out yet. How do you cut your hair, now that you can't support each other anymore? Finally, there are the many, many actors from other teams that gave me constructive advise and help on my acting performance. Thank you Xiao-Dong for giving me one of your UV-boxes so generously as a gift; thank you Mike W. for showing me how to operate that delicate spectroradiometer; Brendan and Jim B. for letting me in on the secrets of HPLC analysis, and all of you plus Cheryl, Karen, Ali, Yousef, and Sudhakar for the many valuable discussions. Thank you Gert-Jan de Maagd and Hans Klamer in the Netherlands and Paul White in the U.S. for being such good friends and also for promoting my work outside Canadian borders. You really made me feel good! Thanks to Helmut Segner and Anja Behrens in Germany with whom we started a very productive and hopefully, long-lasting collaboration. And last but not least, thanks to all you crew members on that legendary Germany tour within the Canada/Germany Science Exchange for the great memories and lasting friendships.

Now (* sob *), I am getting really sentimental. Come on, you all know what comes next. Yes, I would like to give my love and thanks to my husband Mario (Super-Mario, that is). And I let you in on a little secret. Without our traditional Sunday brunch science colloquium I would probably still be trying to figure out what happens when you add a PAH to water. And that Mario did a much better job in encouraging me and explaining things than I did is easily measured by the fact that I will be done before him! But Mario, I promise that if I can't help you with all your modeling match factors, I will take (better) care of the dishes and shopping, and I will help you proofread your thesis. Does this sound like a deal to you?

Nicht träumen statt leben, sondern leben und träumen. Liebe Mutti und lieber Vati: Ich möchte Euch auch ganz sehr danke sagen für Eure Liebe, Unterstützung und Vertrauen. Natürlich bin ich schon ein bißchen stolz auf mich aber viel stolzer bin ich auf Euch und für Euch.

Finally, I would like to say thanks to all you Canadians, Australians, Brazilians, Americans, Irish, British and who knows from where else for making my stay here in Waterloo so special.

DON'T DREAM RATHER THAN LIVE, BUT LIVE AND DREAM.

TABLE OF CONTENTS

ABSTRACT.....	iv
ACKNOWLEDGMENTS.....	vi
LIST OF TABLES.....	xii
LIST OF FIGURES.....	xiii
GENERAL INTRODUCTION.....	1
REFERENCES.....	4
CHAPTER 1: Methodology for demonstrating and measuring the photocytotoxicity of fluoranthene to fish cells in culture.	6
1.1. ABSTRACT.....	6
1.2. INTRODUCTION.....	6
1.3. MATERIALS AND METHODS.....	9
<i>A. Cell lines and culture media.....</i>	<i>9</i>
<i>B. UV radiation exposure.....</i>	<i>9</i>
<i>C. Solubilization of fluoranthene.....</i>	<i>10</i>
<i>D. HPLC analysis of fluoranthene solutions.....</i>	<i>11</i>
<i>E. Fluoranthene distribution in cell cultures.....</i>	<i>11</i>
<i>F. Cytotoxicity of fluoranthene and photomodified fluoranthene.....</i>	<i>12</i>
<i>G. Photocytotoxicity of fluoranthene.....</i>	<i>13</i>
<i>H. Alamar Blue cytotoxicity assay.....</i>	<i>13</i>
<i>I. CFDA-AM cytotoxicity assay.....</i>	<i>13</i>
<i>K. Alamar Blue and CFDA-AM cytotoxicity assay.....</i>	<i>14</i>
<i>L. Data analysis.....</i>	<i>14</i>
1.4. RESULTS.....	15
<i>A. Utility of L-15/ex.....</i>	<i>15</i>
<i>B. UV exposure.....</i>	<i>16</i>
<i>C. Distribution of fluoranthene in cell cultures.....</i>	<i>17</i>
<i>D. Cytotoxicity of fluoranthene and photomodified fluoranthene.....</i>	<i>17</i>
<i>E. Photocytotoxicity of fluoranthene.....</i>	<i>19</i>
1.5. DISCUSSION.....	23
1.6. ACKNOWLEDGMENTS.....	26
1.7. REFERENCES.....	27

CHAPTER 2: Ability of 16 priority PAHs to be directly cytotoxic to a cell line from the rainbow trout gill.	31
2.1. ABSTRACT	31
2.1. INTRODUCTION	31
2.3. MATERIALS AND METHODS	34
<i>A. Cell culture and cytotoxicity testing</i>	34
<i>B. Cytotoxicity assays</i>	34
<i>C. Solubilization of PAHs and HPLC analysis</i>	36
<i>D. Data analysis</i>	36
2.4. RESULTS	38
<i>A. Cytotoxic PAHs</i>	38
<i>B. Non-cytotoxic PAHs</i>	46
2.5. DISCUSSION	49
2.6. ACKNOWLEDGMENTS	52
2.7. REFERENCES	53
CHAPTER 3: Ability of 16 priority PAHs to be photocytotoxic to a cell line from the rainbow trout gill.	56
3.1. ABSTRACT	56
3.2. INTRODUCTION	56
3.3. MATERIALS AND METHODS	58
<i>A. Cell culture, cytotoxicity tests and assays</i>	58
<i>B. UV radiation exposure</i>	58
<i>C. Preparation of PAH solutions and HPLC analysis</i>	59
<i>D. Data analysis</i>	60
3.4. RESULTS	61
<i>A. Non-photocytotoxic PAHs</i>	61
<i>B. Photocytotoxic and cytotoxic PAHs</i>	61
<i>C. Strictly photocytotoxic PAHs</i>	61
<i>D. Photocytotoxicity rankings relative to fluoranthene</i>	67
3.5. DISCUSSION	71
3.6. ACKNOWLEDGMENTS	75
3.7. REFERENCES	76

CHAPTER 4: An evaluation of the cytotoxicity and photocytotoxicity of intact and photomodified creosote through the use of a rainbow trout gill cell line, RTgill-W1, and two fluorescent indicator dyes, alamar Blue and 5-carboxyfluorescein diacetate acetoxymethylester.	79
4.1. ABSTRACT	79
4.2. INTRODUCTION	79
4.3. MATERIALS AND METHODS.....	82
<i>A. Cell line and culture media</i>	<i>82</i>
<i>B. UV radiation exposure</i>	<i>82</i>
<i>C. Preparation of creosote in L-15/ex</i>	<i>82</i>
<i>D. Extraction and chemical analysis of creosote.....</i>	<i>83</i>
<i>E. Cytotoxicity and photocytotoxicity of creosote.....</i>	<i>84</i>
<i>F. Cytotoxicity and photocytotoxicity of photomodified creosote.....</i>	<i>84</i>
<i>G. Alamar Blue and CFDA-AM cytotoxicity assays</i>	<i>84</i>
<i>H. Data analysis</i>	<i>85</i>
4.4. RESULTS.....	88
<i>A. Preparation and chemistry of creosote solutions</i>	<i>88</i>
<i>B. Cytotoxicity of creosote solutions.....</i>	<i>92</i>
<i>C. Photocytotoxicity of creosote solutions.....</i>	<i>98</i>
<i>D. Cytotoxicity of photomodified creosote solutions</i>	<i>101</i>
<i>E. Photocytotoxicity of photomodified creosote solutions</i>	<i>101</i>
<i>F. Comparison of cyto- and photocyto-toxicity of intact and photomodified creosote solutions</i>	<i>104</i>
4.5. DISCUSSION	105
<i>A. Preparation and chemistry of creosote solutions</i>	<i>105</i>
<i>B. Cytotoxicity of creosote solutions.....</i>	<i>105</i>
<i>C. Photocytotoxicity of creosote solutions.....</i>	<i>106</i>
<i>D. Cytotoxicity of photomodified creosote solutions</i>	<i>107</i>
<i>E. Photocytotoxicity of photomodified creosote solutions</i>	<i>108</i>
<i>F. Comparison of cyto- and photocyto-toxicity of intact and photomodified creosote solutions</i>	<i>109</i>
4.6. ACKNOWLEDGMENTS.....	110
4.7. REFERENCES	111
CONCLUDING REMARKS AND FUTURE DIRECTIONS	116
REFERENCES	120
Appendix I. Chemical configuration and absorption spectra of the 16 priority PAHs.	121

Appendix II. Emission of UV radiation by UV-B and UV-A photoreactor lamps.	127
Appendix III. RTgill-W1 cell bioassay for measuring the cytotoxicity and photocytotoxicity of PAHs.	128
Appendix IV. Preparation of the modified culture medium, L-15/ex, and alamar Blue, CFDA-AM, and neutral red dye solutions.	129
IV.1. PREPARATION OF L-15/ex	129
<i>A. Preparation of constituents of L-15/ex</i>	<i>129</i>
<i>B. Preparation of L-15/ex</i>	<i>130</i>
IV.2. PREPARATION OF DYE WORKING SOLUTIONS	130
<i>A. Preparation of alamar Blue</i>	<i>130</i>
<i>B. Preparation of CFDA-AM</i>	<i>130</i>
<i>C. Preparation of neutral red</i>	<i>131</i>

LIST OF TABLES

CHAPTER 2:

Table 2.1. Summary of physical-chemical data of the 16 priority PAHs and their ability to elicit direct cytotoxicity in RTgill-W1 cells.....	39
--	----

CHAPTER 3:

Table 3.1. Summary of photo-physical properties of PAHs	59
Table 3.2. EC ₅₀ values for PAHs that were photocytotoxic but not directly cytotoxic to RTgill-W1 cells at concentrations below water solubility	69
Table 3.3. EC ₅₀ values for the photocytotoxicity of PAHs and their potencies relative to fluoranthene	70

CHAPTER 4:

Table 4.1. Chemical analysis of creosote solutions	89
Table 4.2. Derivation of naphthalene equivalent membrane accumulation factors (NEMAFs) for directly cytotoxic compounds	94
Table 4.3. Directly cytotoxic compounds in creosote and development of naphthalene equivalent concentrations (NECs)	95
Table 4.4. Comparison of obtained and predicted direct cytotoxicity of creosote	97
Table 4.5. Photocytotoxic compounds in creosote and development of fluoranthene equivalent concentrations (FECs).....	101
Table 4.6. EC ₅₀ values for the toxicity of creosote and comparison of toxic potencies.....	104

LIST OF FIGURES

GENERAL INTRODUCTION:

Figure A.I. Molecular structure of the smallest PAH, naphthalene.	1
Figure A.II. Schematic representation of common sources and routes of exposure to PAHs in the environment.	2

CHAPTER 1:

Figure 1.1. Utility of UV-irradiated L-15/ex to support fish cell viability.	15
Figure 1.2. Effect of UV treatment on fish cell viability.	16
Figure 1.3. Distribution of fluoranthene 24 hr after its addition to confluent cell cultures.	18
Figure 1.4. Phase-contrast appearance of RTgill-W1 cells before and 2 hr after being concurrently exposed to fluoranthene and UV radiation.	19
Figure 1.5. Viability of RTgill-W1 cells upon exposure to increasing concentrations of fluoranthene in the dark and during UV irradiation.	21
Figure 1.6. Viability of RTgill-W1 cells immediately and 24 hr after being UV irradiated in increasing concentrations of fluoranthene.	22

CHAPTER 2:

Figure 2.1. Viability of RTgill-W1 cells immediately and 24 hr after being exposed to increasing concentrations of naphthalene.	40
Figure 2.2. Phase-contrast appearance of RTgill-W1 cells 2 hr after being exposed to 54 μ M naphthalene.	41
Figure 2.3. Cell viability of RTgill-W1 immediately and 24 hr after exposure to 26 μ M acenaphthylene or 23 μ M acenaphthene.	42
Figure 2.4. Viability of RTgill-W1 cells immediately and 24 hr after being exposed to increasing concentrations of acenaphthylene.	43
Figure 2.5. Cell viability of RTgill-W1 immediately and 24 hr after exposure to 12 μ M fluorene or 7 μ M phenanthrene.	44
Figure 2.6. Phase-contrast appearance of RTgill-W1 cells 2 hr after being exposed to 113 μ M fluorene.	45
Figure 2.7. Viability of RTgill-W1 cells immediately and 24 hr after being exposed to increasing concentrations of phenanthrene.	47
Figure 2.8. Viability of RTgill-W1 cells immediately and 24 hr after being exposed to increasing concentrations of anthracene.	48

CHAPTER 3:

Figure 3.1. Viability of RTgill-W1 cells after being exposed to increasing concentrations of naphthalene in the presence or absence of UV radiation.	62
Figure 3.2. Viability of RTgill-W1 cells immediately and 24 hr after being exposed to increasing concentrations of chrysene in the presence or absence of UV radiation.	63

Figure 3.3. Viability of RTgill-W1 cells immediately and 24 hr after being exposed to increasing concentrations of acenaphthylene in the presence or absence of UV radiation.	64
Figure 3.4. Viability of RTgill-W1 cells immediately and 24 hr after being exposed to increasing concentrations of benzo[b]fluoranthene in the presence or absence of UV radiation.	65
Figure 3.5. Viability of RTgill-W1 cells immediately and 24 hr after being exposed to increasing concentrations of fluoranthene in the presence or absence of UV radiation.	66
Figure 3.6. Viability of RTgill-W1 cells immediately and 24 hr after being simultaneously exposed for 2 hr to UV radiation and increasing concentrations of pyrene or benzo[g,h,i]perylene, and as measured with the neutral red assay.	68

CHAPTER 4:

Figure 4.1. Schematic representation of the four conditions under which cells were exposed to creosote (cytotoxicity and photocytotoxicity of creosote) or photomodified creosote (cytotoxicity and photocytotoxicity of photomodified creosote).	87
Figure 4.2. Contribution of each of the priority PAHs to the total PAH content measured by GC in the four creosote samples.	90
Figure 4.3. Contribution of each of the non-priority aromatic hydrocarbons to the total content of these compounds measured by GC in the four creosote samples.	91
Figure 4.4. Viability of RTgill-W1 cells upon exposure to increasing concentrations of creosote in L-15/ex.	93
Figure 4.5. Viability of RTgill-W1 cells upon creosote exposure and as predicted from previously obtained dose-response curves of naphthalene cytotoxicity using naphthalene equivalent concentrations (NECs).	96
Figure 4.6. Viability of RTgill-W1 cells upon exposure to increasing concentrations of creosote in L-15/ex in the presence of UV radiation.	99
Figure 4.7. Viability of RTgill-W1 cells upon creosote exposure and as predicted from previously obtained dose-response curves of fluoranthene photocytotoxicity using fluoranthene equivalent concentrations (FECs).	100
Figure 4.8. Viability of RTgill-W1 cells upon exposure to increasing concentrations of photomodified creosote in L-15/ex.	102
Figure 4.9. Viability of RTgill-W1 cells upon exposure to increasing concentrations of photomodified creosote in L-15/ex in the presence of UV radiation.	103

CONCLUDING REMARKS AND FUTURE DIRECTIONS

Figure B.I. Schematic representation of the direct cytotoxicity of PAHs.	117
Figure B.II. Schematic representation of the photocytotoxicity of PAHs.	118

APPENDIX I:

Figure C.I. Representation of the chemical configuration and absorption spectrum for each of the 16 priority PAHs.	121
--	-----

APPENDIX II:

Figure C.II. Emission of UV radiation by two UV-B photoreactor lamps or one UV-B and one UV-A photoreactor lamp, measured after passage through a 48-well culture plate lid.	127
--	-----

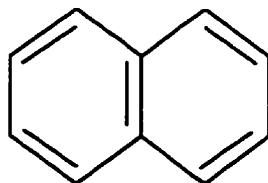
APPENDIX III:

Figure C.III. Schematic representation of the standard assay procedure.	128
---	-----

GENERAL INTRODUCTION

In 1775, the British surgeon Sir Percival Pott noted an association between the incidence of scrotal cancer in chimney sweeps and their exposure to soot (Harvey, 1991). More than a century later, laboratory experiments showed that application of coal tar to the ears of rabbits or the skin of mice, with the latter assay still being in use today, produced tumors. This phenomenon led a group of chemists and physicists to attempt the identification of the tumor producing compound and, after collecting evidence for over 10 years and fractionating 2 tons of coal tar, their work succeeded. In 1932, benzo[a]pyrene, a polycyclic aromatic hydrocarbon (PAH) was identified as the major tumor-producing agent in coal tar (Kennaway, 1955).

PAHs are a large group of chemicals whose common composition is the arrangement of carbon and hydrogen atoms in the form of two or more fused aromatic rings (Neff, 1985). The smallest polycyclic aromatic hydrocarbon, consisting of two fused aromatic rings, is naphthalene (Figure A.I.). With its low molecular weight, relatively high water solubility and volatility, naphthalene can be considered the most mobile PAH in the environment. Other PAHs that are of primary environmental concern because of their ability to move within and between compartments, such as water, air and soil, are those with a molecular weight below 300 g/mol. This group of mobile PAHs comprises thousands of compounds if the number and position of aromatic rings, as well as the number, chemistry and position of their substituents is taken into account (Neff, 1985). Because this large number of PAHs would be impossible to study and in order to unify research that is concerned with the hazards posed by PAHs, the U.S. Environmental Protection Agency (EPA) and the World Health Organization (WHO) have identified 16 unsubstituted PAHs as priority pollutants (Appendix I; Tuvikene, 1995). It is these 16 priority PAHs that are dealt with in this thesis.



NAPHTHALENE

Figure A.I. Molecular structure of the smallest PAH, naphthalene.

The occurrence of PAHs in coal tar gives insight into the source of PAHs. Coal tar is formed during the combustion of coal in the absence of air at approximately 1000°C. Thus, incomplete combustion of organic matter at high temperature will lead to PAH formation (Figure A.II.; Suess, 1976). Anthropogenic combustion sources are, among others, residential heating, agricultural

burning, incineration, transportation and smoking. Examples for industrial processes that lead to PAH formation are aluminum smelting, coke and asphalt production and petroleum refining. Natural sources of PAH formation are volcanic activity and forest fires. Although anthropogenic sources are considered the most relevant PAH producers in industrialized countries, natural sources can play a major role. For example, it has been estimated that 47 % of the atmospheric PAH emission in 1990 in Canada was due to forest fires (Environment Canada, 1994). Two other sources of PAH formation have been proposed. Firstly, the discovery of complex PAH mixtures in fossil fuel has led to the conclusion that, given enough time, decomposition of organic matter at relatively low temperatures (100-150°C) can lead to PAH production (Blumer, 1976). Secondly, PAH production due to direct biosynthesis by microorganisms and plants has been shown but later was attributed to experimental artifacts and therefore, evidence for this latter route of PAH formation remains equivocal (Neff, 1985). However, there is consensus that high temperature combustion of organic material is the major source of PAH formation and release into the environment and that PAH emission increases with industrial development (Suess, 1976; Neff, 1985). Thus, the question arises if and how organisms are able to deal with PAH exposures and what potential hazards are being posed to organisms living in PAH contaminated environments.

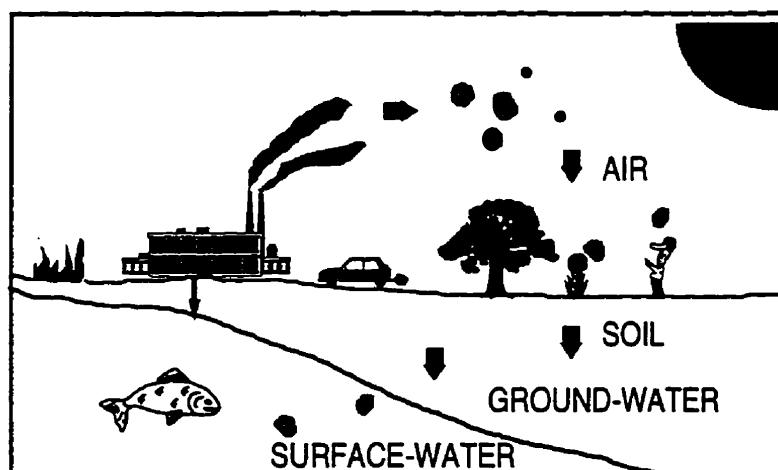


Figure A.II. Schematic representation of common sources and routes of exposure to PAHs in the environment.

Since the discovery of benzo[a]pyrene as a highly potent carcinogen in coal tar, many studies have investigated carcinogenesis and its initiation due to metabolic activation. However, other adverse effects of PAH exposure have begun to surface. These include the suppression of the immune system (Davila et al., 1997), the ability of PAHs to mimic steroid hormones and thus the

potential to modulate endocrine functions (Santodonato, 1997), and the toxicity elicited by the absorption by PAHs of UV radiation, causing singlet oxygen as well as radical formation and possibly toxic photomodification products (Arfsten et al., 1996).

Although by the early 1980s, the potential of PAHs to be toxic in the presence of UV radiation had been demonstrated in mammalian and avian cells (Allison, et al., 1966; Lewis, 1935; Malling and Chu, 1970; Morimura et al., 1964; Utsumi and Elkind, 1979), in *Neurospora crassa* (Malling and Chu, 1970); *Paramecium caudatum* (Epstein et al., 1964), *Drosophila melongaster* (Maltoltsky and Fabian, 1946), and *Escherichia coli* (Harrison and Raabe, 1967), UV radiation exposures were not accounted for in environmental risk analysis. Bowling et al. (1983) were the first to show that fish exposed to anthracene contaminated water in the presence of natural sunlight died within hours or days, whereas fish that were kept in the dark or not exposed to anthracene survived. Subsequent studies identified the fish gill epithelium as a major target site (Oris and Giesy, 1985, Weinstein et al., 1997). However, due to the costs involved and the large number of fish needed, whole fish exposures of large numbers of PAHs and of PAH mixtures were not feasible. Such studies would be useful in identifying the PAHs that are toxic, under environmental relevant conditions, to fish either directly or due to a UV radiation exposure. Furthermore, by establishing a larger PAH toxicity data set, PAHs could be ranked according to their toxic potencies, structure activity relationships recognized, and recommendations given for as to which compounds could serve as indicators of direct and photoinduced toxicity in environmental samples.

It is the overall goal of this thesis to study the direct and photoinduced toxicity of PAHs and a complex mixture to fish gill epithelial cells. The fish gill cells are from a cell line (RTgill-W1) that has been established from the rainbow trout (Bols et al., 1994). The PAHs are the 16 priority PAHs and the mixture is creosote. The specific goals of this thesis are:

- 1.) To develop methodologies for quantifying the photocytotoxicity of a model PAH, fluoranthene, to RTgill-W1 cells, using fluorescent indicator dyes that can be measured rapidly and reliably with a fluorescence plate reader (Chapter 1).
- 2.) To identify priority PAHs that are cytotoxic to RTgill-W1 cells in the absence of UV radiation and to rank them according to their toxic potency and environmental relevance (Chapter 2).
- 3.) To identify priority PAHs that are cytotoxic to RTgill-W1 cells in the presence of UV radiation and to rank them according to their toxic potency and environmental relevance (Chapter 3).
- 4.) To predict and measure the potential of creosote and photomodified creosote to be cytotoxic and/or photocytotoxic by using previously developed methodologies and toxic equivalent factors, which summarized the relationships between the physical-chemical properties of PAHs and their toxicity (Chapter 4).

REFERENCES

- Allison, A.C., Magnus, I.A. and Young, M.R. (1966) Role of lysosomes and of cell membranes in photosensitization. *Nature* **209**, 874-878.
- Arfsten, D.P., Schaeffer, D.J. and Mulveny, D.C. (1996) The effects of near ultraviolet radiation on the toxic effects of polycyclic aromatic hydrocarbons in animals and plants: a review. *Ecotoxicology and Environmental Safety* **33**, 1-12.
- Blumer, M. (1976) Polycyclic aromatic compounds in nature. *Scientific American* **234**, 34-45.
- Bols, N.C., Barlian, A., Chirino-Trejo, S.J., Caldwell, S.J., Goegan, P. and Lee, L.E.J. (1994) Development of a cell line from primary cultures of rainbow trout, *Oncorhynchus mykiss* (Walbaum), gills. *Journal of Fish Diseases* **17**, 601-611.
- Bowling, J.W., Leversee, G.J., Landrum, P.F. and Giesy, J.P. (1983) Acute mortality of anthracene-contaminated fish exposed to sunlight. *Aquatic Toxicology* **3**, 79-90.
- Davila, D.R., Mounho, B.J. and Burchiel, S.W. (1997) Toxicity of polycyclic aromatic hydrocarbons to the human immune system: models and mechanisms. *Toxicology and Ecotoxicology News* **4**, 5-9.
- Environment Canada (1994) Canadian Environmental Protection Act, Priority Substance List Assessment Report: Polycyclic aromatic hydrocarbons. En40-215/42E.
- Epstein, S.S., Small, M., Falk, H.L. and Mantel, N. (1964) On the association between photodynamic and carcinogenic activities in polycyclic compounds. *Cancer Research* **24**, 855-862.
- Harrison, A.P. and Raabe, V.E. (1967) Factors influencing the photodynamic action of benzo[a]pyrene on *Escherichia coli*. *Journal of Bacteriology* **93**, 618-626
- Harvey, R.G. (1991) Polycyclic aromatic hydrocarbons: chemistry and carcinogenicity. Cambridge University Press, Cambridge, Chapter 2.
- Kennaway, E. (1955) The identification of a carcinogenic compound in coal-tar. *British Medical Journal* **Sept. 24**, 749-752.
- Lewis, M.R. (1935) The photosensitivity of chick-embryo cells growing in media containing certain carcinogenic substances. *American Journal of Cancer* **25**, 305-309.
- Malling, H.V. and Chu, E.H.Y. (1970) Carcinogenic and noncarcinogenic polycyclic hydrocarbons in *Neurospora crassa* and Chinese Hamster Cells: their photodynamic effects. *Cancer Research* **30**, 1236-1240.
- Maltoltsky, G. and Fabian, G. (1946) Measurement of the photodynamic effect of carcinogenic substances with biological indicators. *Nature* **158**, 877-878.
- Morimura, Y., Kotin, P. and Falk, H.L. (1964) Photodynamic toxicity of polycyclic aromatic hydrocarbons in tissue culture. *Cancer Research* **24**, 1249-1259.

- Neff, J.M. (1985) Polycyclic aromatic hydrocarbons. In: *Fundamentals of aquatic toxicology*. G.M. Rand and S.R. Petrocelli (Eds), Hemisphere Publishing Corporation, Washington D.C., Chapter 14.
- Oris, J.T. and Giesy, J.P. JR. (1985). The photoenhanced toxicity of anthracene to juvenile sunfish (*Lepomis* spp.). *Aquatic Toxicology* **6**, 133-146.
- Santodonato, J. (1997) Review of the estrogenic and antiestrogenic activity of polycyclic aromatic hydrocarbons: relationship to carcinogenicity. *Chemosphere* **34**, 835-848.
- Suess, M.J. (1976) The environmental load and cycle of polycyclic aromatic hydrocarbons. *The Science of the Total Environment* **6**, 239-250.
- Tuvikene, A. (1995) Responses of fish to polycyclic aromatic hydrocarbons (PAHs). *Annales Zoologici Fennici* **32**, 295-309.
- Utsumi, H. and Elkind, M.M. (1979) Photodynamic cytotoxicity of mammalian cells exposed to sunlight-simulating near ultraviolet light in the presence of the carcinogen 7,12 dimethylbenz[a]anthracene. *Photochemistry and Photobiology* **30**, 271-278.
- Weinstein, J.E., Oris, J.T. and Taylor, D.H. (1997) An ultrastructural examination of the mode of UV-induced toxic action of fluoranthene in fathead minnows, *Pimephales promelas*. *Aquatic Toxicology*, in press.

CHAPTER 1

METHODOLOGY FOR DEMONSTRATING AND MEASURING THE PHOTOCYTOTOXICITY OF FLUORANTHENE TO FISH CELLS IN CULTURE ⁽¹⁾

1.1. ABSTRACT

Methodology was developed for quantifying the photocytotoxicity of fluoranthene to a gill cell line (RTgill-W1) from rainbow trout for future use in screening polycyclic aromatic hydrocarbons (PAHs) for their relative photocytotoxicity to fish. Solubilization in a modified culture medium was achieved with and without fetal bovine serum (FBS) and with and without dimethyl sulfoxide (DMSO). FBS caused most of the fluoranthene to remain in solution and blocked photocytotoxicity if present during UV irradiation. DMSO had little effect on fluoranthene distribution in cell cultures but caused cells to be slightly more sensitive to the phototoxicity of fluoranthene. The indicator dyes, alamar BlueTM and 5-carboxyfluorescein diacetate acetoxymethyl ester (CFDA-AM), were used to quantify cytotoxicity in two different ways: singly in two separate assays, and mixed together in a novel single assay, which saved time and material. With UV irradiation for 2 hr at a photon fluence rate of either 1.4 $\mu\text{mol m}^{-2} \text{s}^{-1}$ UV-B (UV-A : UV-B, 1.5) or 1.1 $\mu\text{mol m}^{-2} \text{s}^{-1}$ UV-B (UV-A : UV-B, 9.7), both dyes indicated increasing loss of viability with increasing doses of fluoranthene. $\text{EC}_{50\text{s}}$ ranged from 18 to 44 ng/ml (89 to 217 nM), with the alamar Blue assay being slightly more sensitive.

1.2. INTRODUCTION

Photosensitizing compounds have drawn enormous interest because of their clinical uses in human medicine (Epstein, 1989), but as well, photosensitizing compounds that are industrial pollutants are beginning to be evaluated for their environmental impact (Landrum et al., 1985; Huang et al., 1993). Upon absorbing light, photosensitizers undergo chemical reactions (Foote, 1976). The damaging or killing of cells by the photosensitized reactions is defined as photocytotoxicity (MacRobert, et al., 1989; Spikes, 1989). The cytotoxic products of photosensitization include singlet oxygen and other reactive oxygen species (Valenzo, 1987).

⁽¹⁾ This paper has been published in *Toxicology in Vitro* (1997) Vol. 11 (1/2), 107-119. Co-authors are A.G.J. Chan, B.M. Greenberg, D.G. Dixon and N.C. Bols.

Among environmental pollutants, most work has been completed on polycyclic aromatic hydrocarbons (PAHs). PAHs are ubiquitous contaminants in aquatic environments, and at least two, anthracene and fluoranthene, show enhanced toxicity to fish upon solar ultraviolet radiation (Bowling et al., 1983; Oris and Giesy, 1985; 1986; Kagan et al., 1985). Determining the potential of other PAHs to be phototoxic might be done more easily with fish cells in culture.

Although the ability of PAHs to photosensitize animal cells in culture to UV radiation was described first over 60 years ago (Lewis, 1935), the *in vitro* approach has yet to be optimized sufficiently to evaluate quickly and reliably the photocytotoxicity of large numbers of PAHs. Among the problems is the difficulty in dissolving them. Some solubilizing techniques have involved bovine serum (Morimura et al., 1964; Kocan et al., 1983), and other methods have used carrier solvents such as dimethyl sulfoxide (DMSO) (Malling and Chu, 1970). Usually the concentrations at which the photocytotoxicity of single PAHs have been studied have been higher than the highest concentrations theoretically possible in water, which are well below 300 ng/ml for most PAHs (Neff, 1985; Mackay et al., 1992). Various endpoints have been used to monitor photoinduced toxicity, including the inhibition of mitosis (Lewis, 1935), the phase-contrast appearance of cells (Van Gurp and Hankinson, 1983), and colony formation (Malling and Chu, 1970; Utsumi and Elkind, 1979). Although most responses occur rapidly after UV irradiation, quantifying them quickly has been difficult.

Recently, a number of cytotoxicity assays has been developed with fluorescent indicator dyes that allow the cellular responses to be quantified rapidly with fluorescent multiwell plate readers (O'Connor et al., 1991). One indicator dye is the virtually nonfluorescent 5-carboxyfluorescein diacetate acetoxymethyl ester (CFDA-AM), which is an esterase substrate that can enter living cells. Cells with an intact plasma membrane maintain a cytoplasmic milieu that supports esterase activity and the production of a fluorescent product. Therefore, CFDA-AM is an indirect measure of plasma membrane integrity (O'Connor et al., 1991). Another indicator dye that can be read with a fluorescent plate reader is alamar Blue (Pagé et al., 1993). Alamar Blue is an indicator of cellular metabolic activity. The dye is taken up by cells and acted upon by oxidoreductases and the mitochondrial electron transport chain to yield the reduced form (Goegan et al., 1995), which is much more fluorescent than the oxidized form (Pagé et al., 1993). With both assays, a reduction in fluorescent readings relative to controls is a measure of cytotoxicity. These tests have yet to be applied to phototoxicity studies, but potentially they could allow the phototoxic potential of a large number of PAHs to be tested rapidly.

Our overall goal in this paper is to develop a rapid, inexpensive *in vitro* procedure that can be used in the future to establish the relative phototoxicity of different PAHs to fish. Fluoranthene is used as a model PAH, and the main *in vitro* system is the detection of cytotoxicity in confluent cultures of the rainbow trout gill epithelial cell line, RTgill-W1. Confluent gill cell cultures are used because *in vivo* studies of the phototoxicity of anthracene to fish have identified the gill

epithelium as one of the principal sites of damage (Oris and Giesy, 1985). The specific goals of this paper are five fold. The first is to develop a protocol for solubilizing fluoranthene without the use of a carrier solvent in an exposure medium that supports the viability of cells but by itself does not generate photocytotoxic products upon being UV irradiated. The second goal is to find UV exposure conditions that do not cause cytotoxicity and confound the studies of fluoranthene photocytotoxicity. The third aim is to quantify the distribution of fluoranthene in cell cultures and to determine the influence of DMSO and FBS on this distribution. The fourth goal is to quantify cytotoxicity through the use of a multiwell plate reader and of two indicator dyes, alamar Blue and CFDA-AM, singly in separate assays and together in a common assay. The final goal is to use these methodological developments to determine the conditions under which fluoranthene is photocytotoxic.

1.3. MATERIALS AND METHODS

A. Cell lines and culture media

Two salmonid cell lines with epithelial-like morphologies were used. CHSE-214 was derived from Chinook salmon embryos (Lannan et al., 1984) and was purchased from the American Type Culture Collection (Rockville, MD, USA). RTgill-W1 was developed in this laboratory from the rainbow trout gill (Bols et al., 1994). Cytochrome P4501A activity was not detectable in either cell line (Lee et al., 1993; Bols, unpublished data), and drug metabolizing enzymes were unlikely to have influenced the results to follow because fluoranthene exposures by themselves were never cytotoxic, and because when photocytotoxicity was observed, the total time of the fluoranthene exposure usually had been only 2 hr. Both cell lines were grown in 75 cm² culture flasks at 22°C in Leibovitz's L-15 medium supplemented with 10 % FBS. The source of the tissue culture supplies and a description of the subcultivation procedure have previously been presented in detail (Bols and Lee, 1994; Schirmer et al., 1994).

A modification of the basal medium, L-15, was used for the exposure of cells to UV radiation. This was necessary because the treatment of conventional growth media with UV radiation generates toxicants that appear to arise from UV modification of medium components such as vitamins and aromatic amino acids (Stoien and Wang, 1974; Wang, 1976; Lorenzen et al., 1993). Therefore, L-15 was prepared with all constituents left out except for the salts, galactose, and pyruvate (Appendix IV). These components (cell culture grade, Sigma, St. Louis, MO, USA) were prepared in cell culture grade, distilled water (Canadian Life Technologies, Burlington, ON, Canada). They were sterilized and mixed together in the manner recommended by Leibovitz (1963, 1977) for the preparation of the complete basal medium. This modified medium was used either without or with a 10 % FBS supplement and referred to respectively as L-15/ex or L-15/ex with FBS.

B. UV radiation exposure

UV irradiation was done with either two UV-B photoreactor lamps or one UV-A and one UV-B photoreactor lamp (Southern N.E. Ultraviolet Co., Branford, CT, USA). Cells were irradiated at room temperature in an atmosphere of air in Costar or Falcon 48-well culture plates with lids. The lids ensured sterility during the illumination process and simultaneously absorbed any radiation below a wavelength of 290 nm, a filtering process which under natural conditions is carried out by stratospheric ozone. Irradiation was measured with an InstaSpecTM II photodiode array spectroradiometer calibrated with a 1 kW quartz halogen lamp (Oriental Corporation, Stratford, CT, USA). As well as UV-B (290-320 nm), the UV-B lamps emitted some visible (400-700 nm) and

some UV-A (320–400 nm) radiation. With two UV-B lamps, the photon fluence rate was $1.4 \mu\text{mol m}^{-2} \text{s}^{-1}$ UV-B (UV-A : UV-B, 1.5) (Appendix II). With one UV-B and one UV-A lamp, the photon fluence rate was $1.1 \mu\text{mol m}^{-2} \text{s}^{-1}$ UV-B (UV-A : UV-B, 9.7) (Appendix II). These values represent the photon fluence rates at the surface of the medium in the wells. A $500 \mu\text{l}$ /well aliquot of L-15/ex, which resulted in a 4.7 mm path length through the medium, had little discernible effect on these fluence rates. However, FBS was found to absorb some of the emitted UV radiation, diminishing the fluence rates by approximately 27 % for UV-B and 9 % for UV-A. The duration of irradiation was 2 hr for all experiments.

C. Solubilization of fluoranthene

Fluoranthene (InterScience Inc., Markham, ON, Canada) was dissolved in L-15/ex in order to simultaneously expose the cells to UV and fluoranthene. Two different solubilization methods were used. Firstly, fluoranthene was dissolved in 100 % DMSO to give a stock solution of 1 mg/ml. Before each experiment, fluoranthene was further diluted in DMSO to give 200 times the final concentration required by each design treatment. A constant volume of this working solution was added to L-15/ex to give the desired concentrations of fluoranthene. This medium, in which the final DMSO concentration is 0.5 % v/v, is referred to as L-15/ex/DMSO. In some cases FBS was added to the L-15/ex/DMSO to give 10 % FBS (v/v). This medium is designated L-15/ex/DMSO with FBS.

In addition, fluoranthene was dissolved without the use of a carrier solvent, using a modification of methods developed for the application of PAHs to microorganisms (Mihelcic and Luthy, 1988; Millette et al., 1995). One mg of fluoranthene was added to 1 liter of sterile L-15/ex in a volumetric flask which was wrapped in aluminum in order to protect the solution from light. The solution was stirred for 24 hr at 40°C , followed by 24 hr of constant stirring at room temperature. In order to remove any undissolved crystals, the solution was filtered through a type A/B extra thick borosilicate glass fiber filter with a pore size of $1 \mu\text{m}$ (Gelman Sciences Inc., Ann Arbor, MI, USA). The filtration apparatus was sterile and the solution was collected into a sterilized amber glass storage bottle (VWR Canlab, Mississauga, ON, Canada). The simplicity of L-15/ex meant that this solution could be injected directly onto an HPLC column. HPLC analysis of 3 independently prepared stock solutions showed a fluoranthene concentration of 60–70 ng/ml. The fluoranthene solutions were stored in the dark at room temperature and were stable for at least 6 months, as periodic HPLC analysis showed no change in concentration and no peak other than fluoranthene in the scanned range of 250–300 nm. The concentration of 60–70 ng/ml (297–346 nM) was approximately 30 % of the reported water solubility for fluoranthene and was the highest

concentration that could be applied to cell cultures. In some cases 10 % FBS was added to the solution of L-15/ex with fluoranthene.

D. HPLC analysis of fluoranthene solutions

HPLC was done with a Shimadzu SCL-10A liquid chromatograph with a SPD-M10A diode array detector and two LC-10AD pumps (Shimadzu, Columbia, MD, USA). Aliquots of 100 μ l from sample solutions were loaded onto a 25 cm LC-18 column (Supelco, Mississauga, ON, Canada). Fluoranthene was eluted with 85 % HPLC-grade acetonitrile (BDH Inc., Toronto, ON, Canada) and 15 % Milli-Q filtered distilled water at a flow rate of 1 ml/min. Fluoranthene was detected at 280 nm with a 20 nm band width. The peak areas of unknown samples were compared to that of an external fluoranthene standard. With this method, the detection limit was found to be 2 ng/ml (10 nM).

E. Fluoranthene distribution in cell cultures

The influence of solubilization method and of FBS on the compartmentalization of fluoranthene in cell cultures was studied. After CHSE-214 or RTgill-W1 cells had been grown to confluency in 12 well culture plates, the growth medium was removed. Each culture well was rinsed once with 1 ml of L-15/ex. Fluoranthene (60 ng/ml) in 1 ml of either L-15/ex, L-15/ex with FBS, L-15/ex/DMSO, or L-15/ex/DMSO with FBS was added to each well and incubated in the dark. Twenty four hours later the amount of fluoranthene was measured by HPLC in three compartments: the culture medium, the cells, and the polystyrene surface of the culture wells after the removal of the cells.

Due to the presence of cells and serum, an extraction protocol was necessary for the analysis of fluoranthene. The medium from 6-12 wells for each treatment was collected into glass tubes. Cells were removed from the culture surface by treatment with trypsin or cell dissociation solution (Sigma, St. Louis, MO, USA) and gentle scraping into L-15/ex. The samples were mixed 2:1 with hydrochloric acid (J.T. Baker Chemical Co., Phillipsburg, NJ, USA) and left overnight at room temperature. Aliquots of 2-3 ml hexane (Fisher Scientific, Nepean, ON, Canada) were added and after the phases had partitioned the mixtures were placed at -80 °C. The hexane phase, which did not freeze and remained on top, was pipetted into new glass tubes and evaporated by a gentle stream of nitrogen. The dried extracts were redissolved in 1 ml methanol and transferred to HPLC autosampler vials. With this extraction procedure, the recovery of fluoranthene was found to be 102 ± 9 % (n=5) from L-15/ex. In the presence of serum, the recovery was lower and more variable and ranged from 57 - 90 % with a mean of 67 ± 13 % (n=5).

After removal of cells, the culture surfaces were extracted for 100 min with 1 ml of HPLC-grade methanol (BDH Inc., Toronto, ON, Canada) per well. This volume extracted the sides of each well to the height originally occupied by the medium. The methanol solutions were then transferred to HPLC autosampler vials. With methanol, $98 \pm 10 \%$ ($n=5$) of the fluoranthene was recovered from the plates.

F. Cytotoxicity of fluoranthene and photomodified fluoranthene

Confluent cultures of RTgill-W1 in 48 well culture plates were exposed to fluoranthene in the dark to determine whether fluoranthene was cytotoxic without a UV radiation treatment. The confluent cultures were achieved by plating 50,000 cells per well and allowing them to grow for 3 days. Confluent cultures were used because, more so than logarithmically growing populations, they reflect the primary in vivo target of PAH phototoxicity, the gill epithelium (Oris and Giesy, 1985). Also, in preliminary experiments, confluent cultures were found to give more reproducible results than the log phase cultures. This likely can be attributed to the fact that the same cell number is more consistently obtained in different wells in confluent cultures and also to the fact that the culture is in a more uniform state as cells begin to arrest in G1 phase of the cell cycle. The cultures showed no loss of viability upon reaching confluency, which has been observed previously with another salmonid cell line that was kept viable at confluency for weeks (Lee and Bols, 1988). At confluency the growth medium was removed and each culture well rinsed once with 500 μ l of L-15/ex. After the rinse, control wells received 500 μ l of L-15/ex, while experimental wells received 500 μ l of L-15/ex containing 60 ng/ml fluoranthene. At various times afterwards for up to 101 hr in the dark, the exposures were terminated by removing the medium from the wells. At these times, the cytotoxicity assays, to be described later, were initiated by adding 150 μ l of L-15/ex with the appropriate fluorescent indicator dyes.

In order to determine whether photomodification of fluoranthene yielded cytotoxic products, confluent cultures also were exposed in the dark to fluoranthene solutions that previously had been UV irradiated. Aliquots of fluoranthene solution (60 ng/ml in L-15/ex) were placed in multiwell culture plates without cells and irradiated for 2 hr with a photon fluence rate of $1.1 \mu\text{mol m}^{-2} \text{s}^{-1}$ UV-B (UV-A : UV-B, 9.7). HPLC of this solution revealed fluoranthene at approximately 17 % of the original concentration and at least one product, whose identity is currently unknown. This photomodified fluoranthene solution was placed onto confluent cultures of RTgill-W1 cells in 48 well culture plates. These were incubated in the dark for up to 101 hr, with brief interruptions for occasional examination by phase-contrast microscopy. After 2, 24, 48, and 101 hr, cytotoxicity assays were performed as described below. A control plate, which had received L-15/ex with fluoranthene but no UV irradiation, was also examined.

G. Photocytotoxicity of fluoranthene

Confluent cultures of RTgill-W1 cells in 48 well culture plates were concurrently exposed to fluoranthene and UV radiation. Each well received a 500 μ l aliquot of L-15/ex, L-15/ex with FBS, L-15/ex/DMSO, or L-15/ex/DMSO with FBS containing fluoranthene over a concentration range from 0 to 60 ng/ml. Either immediately after the addition of fluoranthene or 24 hr later, the plates were irradiated for 2 hr as described under UV radiation exposure. Upon termination of the UV radiation treatment, the cytotoxicity assays were performed immediately or in some cases immediately and 24 hr later. For immediate measurement, the experimental medium was removed and replaced with 150 μ l of L-15/ex with the fluorescent indicator dyes. For later measurements, the indicator dyes were removed after the assay, and the culture wells received L-15 with FBS for 24 hr before cytotoxicity assays were repeated again on the same wells. In addition to these assays, observations by phase-contrast microscopy were carried out routinely in order to qualitatively detect signs of cytotoxicity.

H. Alamar Blue cytotoxicity assay

Alamar Blue solution was purchased from Immunocorp. Science Inc. (Montreal, PQ, Canada) and diluted into L-15/ex to 5 % v/v. Each culture well received 150 μ l of this solution, and 2 hr later the wells were read with a fluorometric multiwell plate reader, the CytoFluor 2350 (PerSeptive Biosystems, Burlington, ON, Canada) at respective excitation and emission wavelengths of 530 (\pm 30) and 595 (\pm 35) nm.

I. CFDA-AM cytotoxicity assay

The esterase substrate, 5-carboxyfluorescein diacetate acetoxymethyl ester (CFDA-AM), was purchased from Molecular Probes (Eugene, OR, USA) and dissolved in DMSO to give 4 mM CFDA-AM. This stock solution was diluted just prior to use into L-15/ex to give 4 μ M CFDA-AM. A 150 μ l aliquot of this solution was added to each well, and 2 hr later the wells were read on the CytoFluor 2350 at respective excitation and emission wavelengths of 485 (\pm 22) and 530 (\pm 30) nm.

The loss of fluorescent product from cells during the assay was examined for its impact on cell viability measurement. After exposure of confluent 48 well cultures to CFDA-AM for 2 hr, fluorescence readings were compared before and after a rinse with L-15/ex. Based on readings at different sensitivities, fluorescence was approximately 20 times lower after a rinse. However, this was true for both experimental and control wells, indicating that the change in % cell viability was

the same whether the measurement was of the total CFDA-AM product, or just the amount retained in the cells after a rinse.

K. Alamar Blue and CFDA-AM cytotoxicity assay

In addition, the possibility of using the two dyes together was explored. Alamar Blue and CFDA-AM were prepared together in L-15/ex to give final concentrations respectively of 5 % v/v and 4 μ M. This mixture was applied to wells containing RTgill-W1 cells over the range of 20,000 to 100,000 cells. After 3 hr, fluorescence was quantified with the CytoFluor as described above. The fluorescent readings increased linearly with cell number. This standard curve of cell number versus fluorescence units was not statistically different from standard curves of cell number versus fluorescence units for each dye used separately. This result led to the two dyes being used together in many experiments. As well as being performed immediately after UV radiation exposure, the assay with the two dyes was done in the same wells 24 hr later. In the intervening 24 hr between the assays, the cells were incubated in L-15 with FBS.

L. Data analysis

The fluorescent readings in experimental wells were expressed as a percentage of the readings in control wells. Prior to these calculations, fluorescence readings for wells without cells were subtracted from the experimental and control values with cells. EC₅₀ values were determined using the logistic function option in SigmaPlot (Jandel Scientific).

1.4. RESULTS

A. Utility of L-15/ex

UV-irradiated L-15/ex supported fish cell viability. In the experiments to follow, cells were UV irradiated for 2 hr in L-15/ex. As a control, cultures were incubated in the dark for 2 hr either in L-15/ex or in L-15/ex that had previously been irradiated for 2 hr. Neither cytotoxicity assay revealed any difference between the two cultures. In a few of the experiments to follow, cells were incubated for several days in L-15/ex that had previously been UV-irradiated. When cultures were exposed to UV-irradiated L-15/ex for 101 hr, cells remained attached to the growth surface and retained their normal epithelial-like shape. Relative to the values obtained during the first 2 hr of exposure, the CFDA-AM assay indicated no change in viability 101 hr later. However, the alamar Blue assay indicated a 15 % decline (Figure 1.1.). In summary, L-15/ex was a convenient and appropriate solution for studying the cytotoxicity arising from exposure to fluoranthene and UV radiation together.

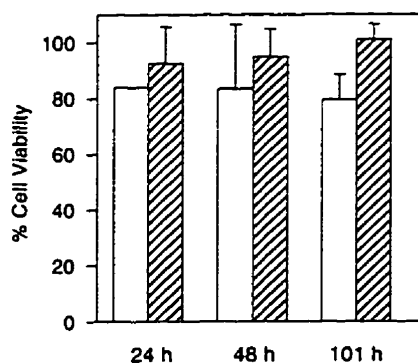


Figure 1.1. Utility of UV-irradiated L-15/ex to support fish cell viability. Confluent cultures of RTgill-W1 cells were exposed in the dark for several days to L-15/ex that previously had been irradiated at a photon fluence rate of $1.4 \mu\text{mol m}^{-2} \text{s}^{-1}$ UV-B (UV-A : UV-B, 1.5) for 2 hr. Viability was assayed with a mixture of alamar Blue (open bars) and CFDA-AM (dashed bars) and expressed as a percentage of the readings in control cultures that received UV-irradiated L-15/ex for 2 hr, which in turn were the same as cultures receiving L-15/ex for 2 hr. In each separate experiment, each treatment was performed on four culture wells and a mean calculated. Each bar represents the mean of the means for 2 independent experiments. The vertical lines indicate the standard deviation.

B. UV exposure

The UV treatments alone had little or no effect on the fish cells as measured from 0 to 2 and 24 to 26 hr after the end of irradiation (Figure 1.2.). When viewed 2 hr after irradiation, cells remained attached and retained their shape. As judged by alamar Blue and CFDA-AM assays, any decline in viability was less than 10 % during this period. At 24 to 26 hr after irradiation, cytotoxicity was detected only with a photon fluence rate of $1.4 \mu\text{mol m}^{-2} \text{s}^{-1}$ UV-B (UV-A : UV-B, 1.5). Relative to the dark control, viability was reduced by approximately 30 % and 25 % in respectively the alamar Blue and CFDA-AM assays (Figure 1.2., panel A).

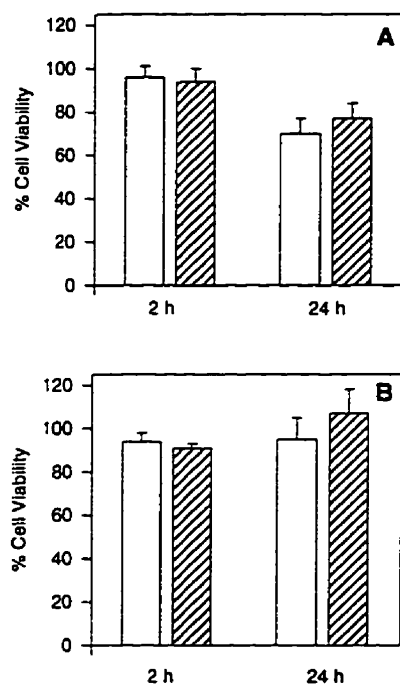


Figure 1.2. Effect of UV treatment on fish cell viability. Confluent cultures of RTgill-W1 cells were UV irradiated for 2 hr in L-15/ex at photon fluence rates of either $1.4 \mu\text{mol m}^{-2} \text{s}^{-1}$ UV-B (UV-A : UV-B, 1.5) (panel A) or $1.1 \mu\text{mol m}^{-2} \text{s}^{-1}$ UV-B (UV-A : UV-B, 9.7) (panel B). Immediately afterwards, viability was assayed with a mixture of alamar Blue (open bars) and CFDA-AM (dashed bars) and expressed as a percentage of the readings in control cultures that were kept in the dark. After these readings had been taken, the cultures received L-15 with FBS and were incubated for 24 hr before the cytotoxicity assays were again performed on the same cultures. In each separate experiment, each treatment was performed on four culture wells and a mean calculated. Each bar represents the mean of the means for 5 independent experiments. The vertical lines indicate the standard deviation.

C. Distribution of fluoranthene in cell cultures

The presence or absence of FBS dramatically influenced the distribution of fluoranthene in fish cell cultures. This is shown for CHSE-214 in Figure 1.3., and a similar distribution was obtained in a single experiment with RTgill-W1. Without FBS in the culture medium, the amount of fluoranthene still in solution 24 hr after the solution had been applied to cell cultures was only $8 \pm 5 \%$ ($n=5$) of the initial concentration. The majority ($79 \pm 14 \%$, $n=5$) was recovered from the polystyrene culture surface. With FBS in the culture medium, $70 \pm 17 \%$ ($n=5$) of the fluoranthene added initially was still in solution 24 hr later. Less than 10 % was recovered from the plastic surface. With or without FBS, the cells acquired a similar amount of fluoranthene. As a % of the initial value, this was $23 \pm 12 \%$ ($n=4$) and 15 % ($n=1$) for respectively CHSE-214 and RTgill-W1 in the presence of FBS and $14 \pm 11 \%$ ($n=4$) and 11 % ($n=1$) for respectively CHSE-214 and RTgill-W1 in the absence of FBS. These distributions were influenced little by the presence of DMSO.

D. Cytotoxicity of fluoranthene and photomodified fluoranthene

No signs of cytotoxicity were detected in cultures exposed in the dark to fluoranthene at 60 ng/ml, the highest concentration possible without a carrier solvent. This was true in L-15/ex with or without DMSO and for exposures of up to 101 hr, the longest used.

A 60 ng/ml solution of fluoranthene in L-15/ex that had been photomodified by UV irradiation for 2 hr also was not cytotoxic. RTgill-W1 cultures that were exposed to the photomodified solution for up to 101 hr in the dark showed similar readings in the alamar Blue or CFDA-AM assays as control cultures that were exposed in the dark to an unirradiated solution of 60 ng/ml fluoranthene in L-15/ex. As well, the cultures showed no signs of cytotoxicity as judged by phase contrast microscopy.

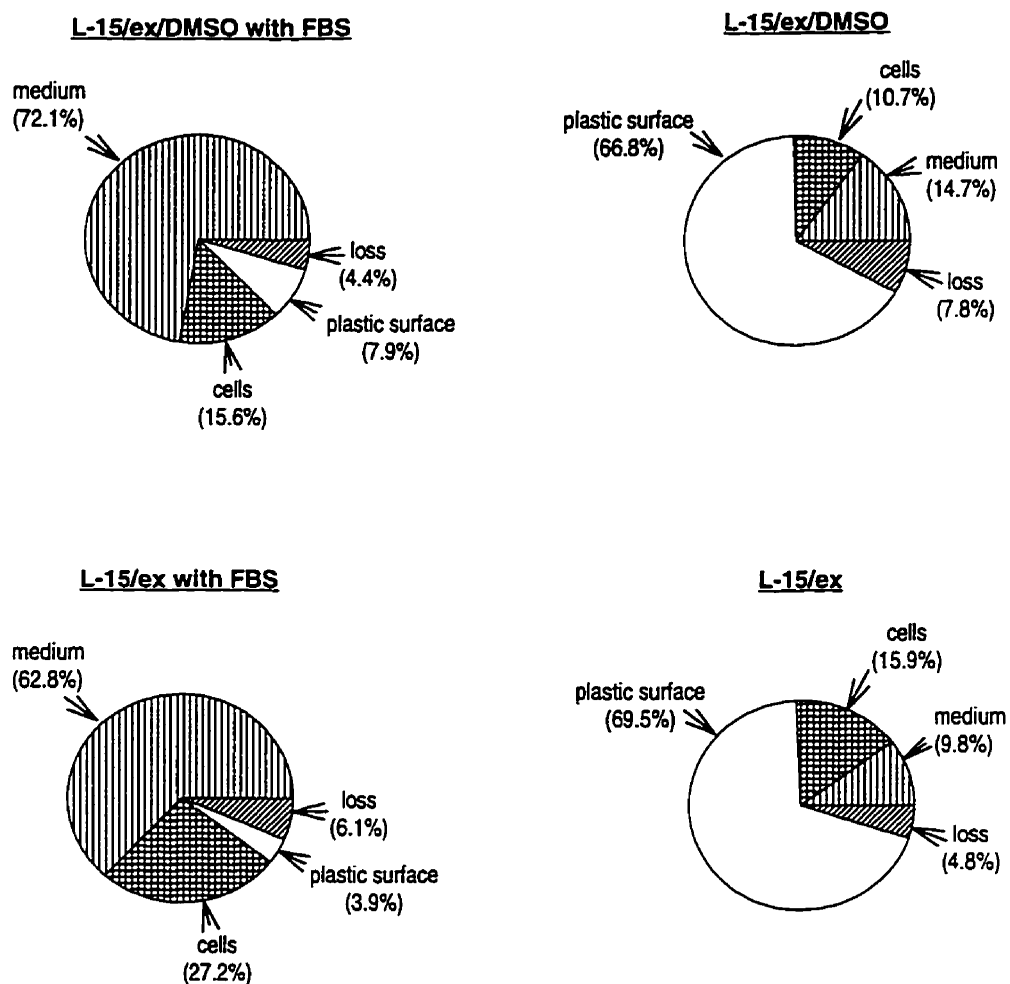


Figure 1.3. Distribution of fluoranthene 24 hr after its addition to confluent cell cultures. Fluoranthene at 60 ng/ml in either L-15/ex, L-15/ex with FBS, L-15/ex/DMSO, or L-15/ex/DMSO with FBS was added to CHSE-214 cells in 12 well polystyrene culture plates to give a total of 60 ng/well. Twenty four hours later, three compartments were analyzed for fluoranthene: the culture medium, the cells and the polystyrene wells after cells and medium had been removed. The graph illustrates the % recovered in each compartment and is one of five similar experiments.

E. Photocytotoxicity of fluoranthene

Concurrent fluoranthene exposure and UV irradiation were cytotoxic in cultures without FBS. During the first 2 hr after irradiation, the phase-contrast appearance of cells changed in those cultures in L-15/ex or L-15/ex/DMSO with fluoranthene concentrations of 10-20 ng/ml (49-99 nM) or greater. The cells appeared darker, the cell boundaries became distinct, and blebs were evident on some cells (Figure 1.4.). This was true with both cell lines and regardless of whether

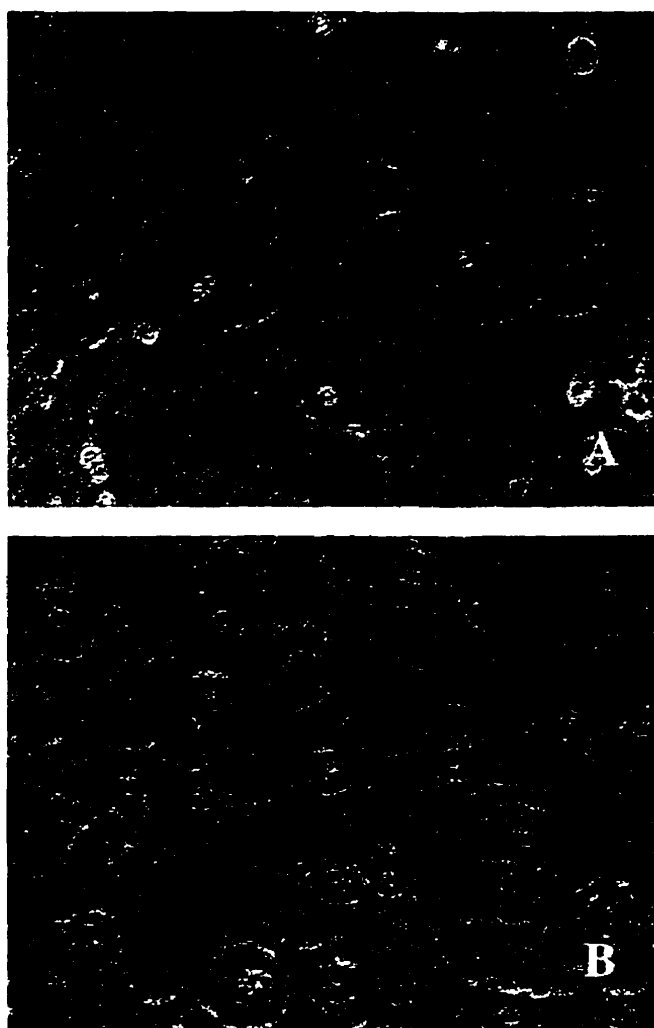


Figure 1.4. Phase-contrast appearance of RTgill-W1 cells before (panel A) and 2 hr after (panel B) being concurrently exposed to fluoranthene and UV radiation. A confluent culture in a well of a 48 well culture plate was exposed to 60 ng/ml fluoranthene in L-15/ex and irradiated at a photon fluence rate of $1.1 \mu\text{mol m}^{-2} \text{s}^{-1}$ UV-B (UV-A : UV-B, 9.7) for 2 hr. The photographs were taken at 320x.

the cultures had been exposed to fluoranthene and immediately irradiated, or had been exposed to fluoranthene for 24 hr before irradiation. Upon UV irradiation with either photon fluence rate, increasing doses of fluoranthene led to increasing loss of viability as measured with either indicator dye (Figures 1.5. and 1.6.). When the fluoranthene exposure was for the 2 hr during UV irradiation at a photon fluence rate of $1.4 \mu\text{mol m}^{-2} \text{s}^{-1}$ UV-B (UV-A : UV-B, 1.5), the EC₅₀ values ranged from 23.5 to 32.6 ng/ml (116 to 161 nM) with a mean of 143 ± 19 nM (n=3) for alamar Blue and from 28.5 to 43.9 ng/ml (141 to 217 nM) with a mean of 175 ± 39 nM (n=4) for CFDA-AM. For fluoranthene exposures of 26 hr, which consisted of a 24 hr exposure before irradiation plus the 2 hr during UV treatment, a similar dose-response curve was obtained. The EC₅₀ was 185 nM (37.4 ng/ml) in the alamar Blue assay and 212 nM (42.9 ng/ml) in the CFDA-AM assay. If DMSO was present, the shapes of the dose-response curves were slightly altered and the EC₅₀ values were consistently lower (Figure 1.5.). EC₅₀ values for fluoranthene in L-15/ex/DMSO ranged from 18.0 to 27.7 ng/ml (89 to 137 nM) with a mean of 113 ± 34 nM (n=2) for alamar Blue and from 23.9 to 28.1 ng/ml (118 to 139 nM) with a mean of 129 ± 11 nM (n=3) for CFDA-AM. In a single experiment with CHSE-214, the EC₅₀ values were within this range.

Fluoranthene exposure followed by UV treatment in the absence of fluoranthene also was cytotoxic, but UV treatment followed by fluoranthene exposure in the dark was not. When cultures were exposed to 60 ng/ml fluoranthene in L-15/ex or L-15/ex/DMSO for 24 hr, rinsed free of fluoranthene, and then UV irradiated for 2 hr at a photon fluence rate of $1.4 \mu\text{mol m}^{-2} \text{s}^{-1}$ UV-B (UV-A : UV-B, 1.5) in L-15/ex alone, cytotoxicity was detected. Viability was reduced by 94 ± 3 % (n=3) and 67 ± 8 % (n=3) of control cultures as judged respectively by the alamar Blue and CFDA-AM assays. When cultures in L-15/ex were UV irradiated for 2 hr and then exposed for 2 hr in the dark to 60 ng/ml fluoranthene in L-15/ex or L-15/ex/DMSO, no signs of cytotoxicity were seen.

The presence of FBS during UV irradiation prevented fluoranthene from being photocytotoxic. When cultures were irradiated in 60 ng/ml of fluoranthene in L-15/ex with FBS or in L-15/ex/DMSO with FBS, no cytotoxicity was detected. This was true even if the cultures had been exposed to fluoranthene for 24 hr prior to irradiation. Cytotoxicity also was not observed if cultures were exposed to fluoranthene for 24 hr in L-15/ex or L-15/ex/DMSO and then irradiated in L-15/ex with FBS.

The presence of FBS after concurrent fluoranthene exposure and UV irradiation did not prevent photocytotoxicity. When cultures were exposed to fluoranthene in L-15/ex and irradiated for 2 hr at $1.1 \mu\text{mol m}^{-2} \text{s}^{-1}$ UV-B (UV-A : UV-B, 9.7), cytotoxicity was detected immediately after irradiation and was more pronounced 26 hr later (Figure 1.6.). During the intervening period of 24 hr, the cultures were exposed in the dark to L-15 with 10 % FBS. EC₅₀ values decreased by

approximately 60 % for both cytotoxicity assays. These results suggest that the cellular damage progressed irreversibly after initiation by the photosensitizing effects of fluoranthene.

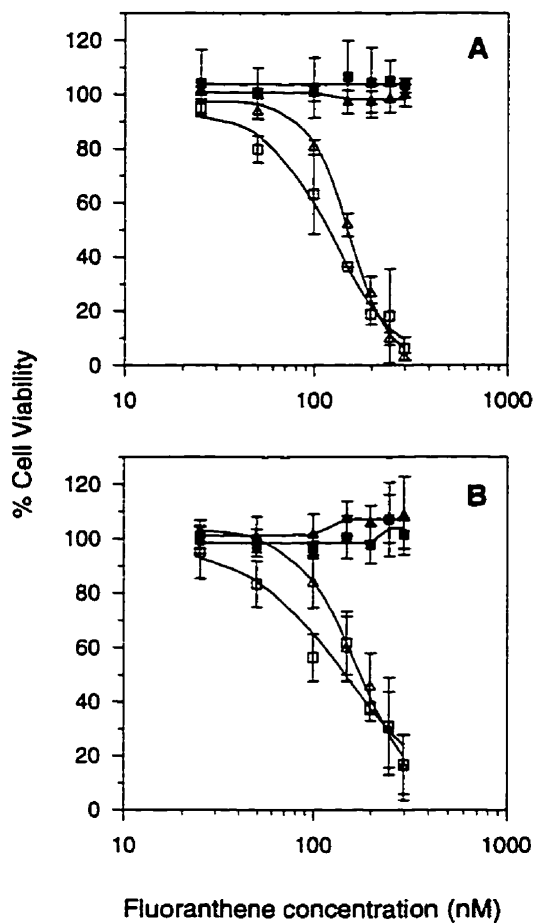


Figure 1.5. Viability of RTgill-W1 cells upon exposure to increasing concentrations of fluoranthene in the dark and during UV irradiation. Confluent cultures were exposed to fluoranthene and either kept in the dark in L-15/ex (▲) or L-15/ex/DMSO (■), or simultaneously irradiated for 2 hr at a photon fluence rate of $1.4 \mu\text{mol m}^{-2} \text{s}^{-1}$ UV-B (UV-A : UV-B, 1.5) in L-15/ex (△) or L-15/ex/DMSO (□). Immediately afterwards viability was assayed with a mixture of alamar Blue (panel A) and CFDA-AM (panel B) and expressed as a percentage of the readings in control cultures that received the appropriate dark or UV treatment but no fluoranthene. In each separate experiment, each treatment was performed on four culture wells and a mean calculated. The data points represent the mean of the means for 2 and 3 independent experiments that had been done respectively with DMSO (open and closed squares) and without DMSO (open and closed triangles). The vertical lines indicate the standard deviation.

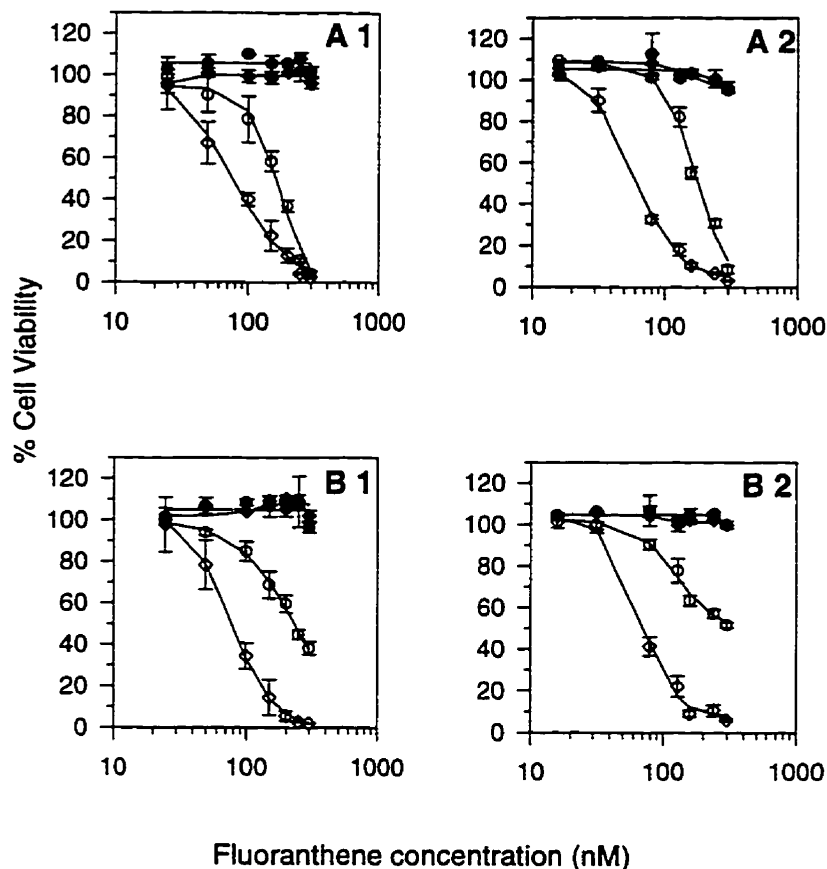


Figure 1.6. Viability of RTgill-W1 cells immediately and 24 hr after being UV irradiated in increasing concentrations of fluoranthene. Confluent cultures were exposed to fluoranthene in L-15/ex and either kept in the dark (closed symbols) or simultaneously irradiated at a photon fluence rate of $1.1 \mu\text{mol m}^{-2} \text{s}^{-1}$ UV-B (UV-A : UV-B, 9.7) (open symbols) for 2 hr. Immediately afterwards viability was assayed with a mixture of alamar Blue (panels A1 and A2; ● for the dark and ○ for the UV exposed cells) and CFDA-AM (panels B1 and B2; ● for the dark and ○ for the UV exposed cells). After these readings had been taken, the cultures received L-15 with FBS and were incubated for 24 hr before the cytotoxicity assays were again performed on the same cultures (panels A1 and A2 for alamar Blue; panels B1 and B2 for CFDA-AM; ◆ for the dark and ◇ for the UV exposed cells). The results were expressed as a percentage of the readings in control cultures that received the appropriate dark or UV treatment but no fluoranthene. One independent experiment is shown in panels A1 and B1; a second, in panels A2 and B2. In each the data points represent the mean of four culture wells. The vertical lines indicate the standard deviation.

1.5. DISCUSSION

A methodology has been established that allowed the photocytotoxicity of fluoranthene to cultured fish cells to be described and quantified. The photocytotoxicity appeared to be caused by damage to cellular membranes in general. Allison et al. (1966) distinguished between photocytotoxicity due to photosensitization of the cell membrane, which was manifested by the appearance of morphological changes soon after the radiation treatment, versus of the lysosomal membrane, which required the release of lysosomal enzymes in the cytoplasm and caused the cells to round up and die after approximately 24 hr. The responses of the fish cells occurred within 2 hr of UV irradiation, which might suggest that the cell membrane is the main site of damage. However, the cytotoxicity assays do not exclude other membrane targets. As the CFDA-AM assay has been carried out in this report, a decrease in fluorescent readings directly measures a decline in cellular esterase activity. This is attributed to the loss of the appropriate cellular milieu for the reaction. Support for this comes from the observation that cells disrupted by freeze and thaw show little esterase activity as measured with fluorescent substrates (Persidsky and Baillie, 1977). Therefore, a reduction in fluorescent readings indicates damage to either the cell membrane and/or internal membranes. Alternatively, the decrease is due to the specific inactivation of esterase activity. The latter hypothesis appears less likely because the lipophilic nature of fluoranthene make membranes more likely targets and because the results of the CFDA-AM assay parallel closely the more general responses of morphological change and of the alamar Blue assay. The slightly lower EC₅₀ with the alamar Blue assay hints at mitochondrial impairment occurring slightly before general membrane damage. However, because general membrane damage also would lead to mitochondrial impairment, under the current fluoranthene and UV exposure conditions, the two assays likely are measuring the same damage, with the alamar Blue assay being a slightly more sensitive indicator of this than the CFDA-AM assay.

This paper extends the utility of the fluorescent indicator dyes, alamar Blue and CFDA-AM, in cytotoxicity studies. Previously, alamar Blue was used to demonstrate daunorubicin cytotoxicity (Pagé et al., 1993), and the cytotoxicity of Cosmetics, Toiletry and Fragrance Association compounds was evaluated with CFDA-AM (O'Connor et al., 1991). The current paper shows the dyes to be useful for studying the photocytotoxicity of PAHs. In the past, the rapid loss of viability generated by PAH exposure and UV irradiation has been monitored by dye exclusion (Morimura et al., 1964; Allison et al., 1966) and by the phase-contrast appearance of cells (Van Gorp and Hankinson, 1983). The alamar Blue and CFDA-AM assays are superior because the response of the whole culture can be quantified rapidly and reliably with a fluorescent plate reader. As well, after a measurement on a culture well has been taken, growth medium can be returned and a measurement of the same well can be taken at a later time point. Potentially this could be done repeatedly. In addition, the current study shows that the two dyes can be used together. This

allows the assays to be done more rapidly and the results to be more comparable because the assays are done at the same time on the same cultures. Material costs are reduced because fewer multiwell cultures are used. One limitation of these assays is that they do not detect all the potential ways by which fluoranthene could be photocytotoxic. For example, the detection of sublethal damage that leads to the loss of replicative capacity would require a colony-forming assay, but this is not rapid, particularly for fish cells, and is difficult to do with most fish cell lines (Bols and Lee, 1994).

FBS profoundly influenced the distribution of fluoranthene in cell culture. Without FBS, most fluoranthene was adsorbed to the polystyrene culture surfaces; and with FBS, most fluoranthene was found in the culture medium. The adsorption of PAHs to culture plasticware has not been noted previously, but the adsorption of PAHs to surfaces of particles in the environment has been observed commonly (Law and Biscaya, 1994). Fluoranthene even has been shown to adsorb to Teflon and stainless steel (Schults et al., 1992). Tissue culture plasticware has been found to adsorb other hydrophobic compounds. When the adsorption of steroids to polystyrene plates was compared from different culture media, up to 40 % of the added steroid was adsorbed, but the least adsorption was from medium with FBS (Longman and Buehring, 1986). FBS also maintained fluoranthene in the culture medium. This confirmed a frequent experimental practice of using serum to solubilize PAHs. For cell culture experiments, serum has been used to dissolve PAHs either directly (Malling and Chu, 1970; Kocan et al., 1983) or in conjunction with acetone (Morimura et al., 1964; Lankas et al., 1980). Human plasma has been used to extract PAHs, including fluoranthene, from soot (Falk et al., 1958) and calf serum has been used to solubilize PAHs from glass surfaces (Morimura et al., 1964).

The amount of fluoranthene in the cells was similar with or without FBS. However, the methodology might not have been adequate to detect small differences. With FBS, 10-30 % of the added fluoranthene was found in the cell monolayer, whereas without FBS, the cell monolayer contained 10-20 % of the added fluoranthene. A potential source of variability was the removal of cells from the growth surface by either trypsin and/or scraping. This step could have resulted in a variable loss of fluoranthene from the cells or release of fluoranthene from the culture surface in the case of scraping.

Fluoranthene was not photocytotoxic if FBS was present during UV irradiation. Photocytotoxicity arises from photosensitized reactions, which generate singlet oxygen and other reactive oxygen species. These can damage membranes and cause cell death (Valenzo, 1987). FBS could have protected cells by removing the toxic lipid peroxides that would be generated by these species from the photoexcitation of fluoranthene within membranes and by providing to the plasma membrane vitamin E that would impair the development of lipid peroxides and quench singlet oxygen. Some of these protective actions by serum have been observed in other contexts (Hemler et al., 1979; Riley & Carlson, 1987; Halliwell & Gutteridge, 1985). As well, any

hydrogen peroxide that might be generated through the photoexcitation of fluoranthene outside the cell compartment would be quenched generally through interactions with serum proteins or removed specifically with serum catalase. Finally, some of the protective action might be due to FBS reducing the photon fluence rate reaching the cells.

Phototoxicity also can be due to cytotoxic products arising from photomodification of the original sensitizing compound (Ren et al., 1994). However, when fluoranthene was irradiated prior to being applied to the fish cell cultures, no cytotoxicity was observed. This would rule out the formation of stable, cytotoxic photooxidized products in the medium. However, their formation within the cells cannot be ruled out.

In the absence of FBS, the photocytotoxicity of fluoranthene was similar whether the fluoranthene exposure had been for 24 hr before the UV treatment or just for the 2 hr of UV irradiation. In the first case UV irradiation is initiated with the fluoranthene mainly adsorbed to the polystyrene. In the second case UV irradiation is initiated with the fluoranthene initially in solution. The fact that the EC_{50} s for photocytotoxicity were similar suggests that the total fluoranthene concentration in the culture well is critical and not the relative distribution between the medium and the polystyrene. Presumably in both situations the cells attain a similar critical concentration of fluoranthene, although this must occur very rapidly in the case where fluoranthene is added concurrently with the UV treatment. The fluoranthene outside the cell contributes indirectly to the photocytotoxicity by maintaining the critical cellular levels, but potentially could contribute directly by being a source of cytotoxic singlet oxygen and other reactive oxygen species (Valenzo, 1987). However, this direct contribution is likely minor compared to the photosensitization of fluoranthene occurring within the cells. If the total concentration per well is the critical parameter, then the relative photocytotoxicity of different PAHs can be compared by determining the dose of PAH in the culture well that reduces viability by 50 % under a standard UV treatment.

DMSO slightly enhanced the photocytotoxicity of fluoranthene in both toxicity assays, but had no influence on the distribution of fluoranthene in cell cultures. This enhancement could have been brought about by DMSO facilitating the entry of fluoranthene into membranes, and as a result, making the cells more sensitive at lower concentrations. As well, DMSO might have increased the susceptibility of cells by causing sublethal damage. Such an explanation has been put forth by Parkinson and Agius (1987) to explain the response of tilapia brain cell cultures to 1,1,1-trichloro-2,2-bis-(p-chlorophenyl) ethane (DDT) in DMSO versus acetone. The fact that the two assays are influenced by DMSO in a similar manner again suggests that both assays are measuring a common cytotoxic locus. Others have observed problems with carriers in PAH photosensitization studies. Malling and Chu (1970) found that benzo[a]pyrene was photocytotoxic when dissolved in dimethylformamide but not in bovine serum or DMSO. Eliminating carrier solvents in studies with PAHs in vitro appears to be the best solution to the problem. The current

paper offers a solubilization strategy, although it might not be appropriate for long term studies in which a more complete growth medium is required.

Fluoranthene appears to be photocytotoxic to animal cells in general. This was true in the current study with fish cell lines and had been observed previously with cell lines from humans (Morimura et al., 1964) and rodents (Van Gurp and Hankinson, 1983). The UV radiation treatments that rendered fluoranthene cytotoxic were different and in some cases hard to compare. However, the photon fluence rates that were used with the fish cells could potentially be achieved in clear water to depths of at least 10 meters. As well, photocytotoxicity could be demonstrated without the use of a carrier solvent and at fluoranthene concentrations that have been found at some contaminated sites. In aquatic ecosystems, PAHs are present mostly bound to particulate matter, but in addition, they are found dissolved in the water column. For rivers in industrialized areas, PAH concentrations have been estimated at 1-5 ng/ml (Neff, 1985), but at a contaminated lake site, concentrations as high as 5,000 ng/ml have been reported for total PAHs (Munkittrick et al., 1995). For individual PAHs, concentrations will depend on their behavior in mixture and will mostly be limited by their theoretical water solubility which for most PAHs is well below 300 ng/ml (Neff, 1985; Mackay et al., 1992). Therefore, the photocytotoxicity of fluoranthene has potential environmental impact. The methodological developments of this report should allow other environmentally important PAHs to be tested rapidly and inexpensively for their potential photocytotoxicity.

1.6. ACKNOWLEDGMENTS

We would like to thank U. Klee for his suggestions concerning the fluoranthene extraction procedure and B. McConkey for his advice on HPLC analysis. This research was supported by a Strategic Grant from the Natural Sciences and Engineering Research Council of Canada and by the Canadian Network of Toxicology Centers.

1.7. REFERENCES

- Allison, A. C., Magnus, I. A. and Young, M. R. (1966) Role of lysosomes and of cell membranes in photosensitization. *Nature* **209**, 874-878.
- Bols, N. C., Barlian, A., Chirino-Trejo, S. J., Caldwell, S. J., Goegan, P. and Lee, L. E. J. (1994) Development of a cell line from primary cultures of rainbow trout, *Oncorhynchus mykiss* (Walbaum), gills. *Journal of Fish Diseases* **17**, 601-611.
- Bols, N. C. and Lee, L. E. J. (1994) Cell lines: availability, propagation and isolation. In: *Biochemistry and molecular biology of fishes*. P.W. Hochachka and T. P. Mommsen (Eds) Elsevier Science, Amsterdam, Vol. 3, 145-159.
- Bowling, J. W., Lerversee, G. J., Landrum, P. F. and Giesy, J. P. (1983) Acute mortality of anthracene-contaminated fish exposed to sunlight. *Aquatic Toxicology* **3**, 79-90.
- Epstein, J. H. (1989) Photomedicine. In: *The Science of Photobiology*. K. C. Smith. (Ed), Plenum Press, New York, NY, 155-193.
- Falk, H. L., Miller, A., and Kotin, P. (1958) The elution of 3,4-benzpyrene and related other polycyclic aromatic hydrocarbons from soot by plasma proteins. *Science* **127**, 474-475.
- Foote, C. S. (1976) Photosensitized Oxidation and Singlet Oxygen: Consequences in biological systems. In: *Free Radicals in Biology*. W. A. Pryor (Ed), Academic Press, New York, NY, Vol. II, 85-113.
- Goegan, P., Johnson, G. and Vincent, R. (1995) Effects of serum protein and colloid on the alamar Blue assay in cell cultures. *Toxicology in Vitro* **9**, 257-266.
- Halliwell, B. and Gutteridge, J. M. C. (1985) Lipid peroxidation: a radical chain reaction. In: *Free radicals in biology and medicine*. Clarendon Press, Oxford, 139-189.
- Hemler, M. E., Cook, H. W. and Lands, W. E. M. (1979) Prostaglandin biosynthesis can be triggered by lipid peroxides. *Archives of Biochemistry and Biophysics* **193**, 340-345.
- Huang, X..D., Dixon, D. G. and Greenberg, B. M. (1993) Impacts of UV radiation and photomodification on the toxicity of PAHs to the higher plant *Lemna Gibba* (Duckweed). *Environmental Toxicology and Chemistry* **12**, 1067-1077.
- Kagan, J., Kagan, E. D., Kagan, I. A., Kagan, P. A., and Quigley, S. (1985) The phototoxicity of non-carcinogenic polycyclic aromatic hydrocarbons in aquatic organisms. *Chemosphere* **14**, 1829-1834.
- Kocan, R. M., Chi, E. Y., Eriksen, N., Benditt, E. P., Landolt, M. L. (1983) Sequestration and release of polycyclic aromatic hydrocarbons by vertebrate cells in vitro. *Environmental Mutagenesis* **5**, 643-656.
- Landrum, P. F., Giesy, J. P., and Allred, P. M. (1985) Photoinduced toxicity of polycyclic aromatic hydrocarbons to aquatic organisms. In: *Oil and Freshwater: Chemistry, Biology,*

- Technology. J. H. Vandermeulen and S. Hrudey (Eds), Pergamon Press, New York, NY, 304-318.
- Lankas, G. R., Haugen, D. A., and Elkind, M. M. (1980) Enhanced near-ultraviolet light sensitivity induced by coal combustor effluents in cultured mammalian cells. *Journal of Toxicology and Environmental Health* **6**, 723-729.
- Lannan, C. N., Winton, J. R. and Fryer, J. L. (1984) Fish cell lines: establishment and characterization of nine cell lines from salmonids. *In Vitro* **20**, 671-676.
- Law, R. L. and Biscaya, J. L. (1994) Polycyclic aromatic hydrocarbons (PAH) - Problems and progress in sampling, analysis and interpretation. *Marine Pollution Bulletin* **29**, 235-241.
- Lee, L. E. J., Martinez, A. and Bols, N. C. (1988) Culture conditions for arresting and stimulating the proliferation of a rainbow trout fibroblast cell line, RTG-2. *In Vitro Cellular & Developmental Biology* **24**, 795-802.
- Lee, L. E. J., Clemons, J. H., Bechtel, D. G., Caldwell, S. J., Han, K-B., Pasitschniak-Arts, M., Mosser, D. D. and Bols, N. C. (1993) Development and characterization of a rainbow trout liver cell line expressing cytochrome P450-dependent monooxygenase activity. *Cell Biology and Toxicology* **9**, 279-294.
- Leibovitz, A. (1963) The growth and maintenance of tissue-cell cultures in free gas exchange with the atmosphere. *American Journal of Hygiene* **78**, 173-180.
- Leibovitz, A. (1977) Preparation of medium L-15. *Tissue Culture Association Manual* **3**, 557-559.
- Lewis, M. R. (1935) The photosensitivity of chick-embryo cells growing in media containing certain carcinogenic substances. *American Journal of Cancer* **25**, 305-309.
- Longman, S. M. and Buehring, G. C. (1986) A method for measuring steroid adsorption to tissue culture plasticware. *Journal of Tissue Culture Methods* **10**, 253-255.
- Lorenzen, A., James, C. A. and Kennedy, S. W. (1993) Effects of UV irradiation of cell culture medium on PCB-mediated porphyrin accumulation and EROD induction in chick embryo hepatocytes. *Toxicology in Vitro* **7**, 159-166.
- Mackay, D., Shiu, W. Y., and Ma, K. C. (1992) Illustrated handbook of physical-chemical properties and environmental fate for organic chemicals. Lewis Publishers, Chelsea, MI, Vol. 2, 57-367.
- MacRobert, A. J., Bown, S. G. and Phillips, D. (1989) What are the ideal photoproperties for a sensitizer? In: *Photosensitizing Compounds: their Chemistry, Biology and Clinical Use*. Ciba Foundation Symposium 146, Wiley-Interscience publication, Chichester, 4-16.
- Malling, H. V. and Chu, E. H. Y. (1970) Carcinogenic and noncarcinogenic polycyclic hydrocarbons in *Neurospora crassa* and Chinese Hamster Cells: their photodynamic effects. *Cancer Research* **30**, 1236-1240.

- Mihelcic, J. R. and Luthy, R. G. (1988) Degradation of polycyclic aromatic hydrocarbon compounds under various redox conditions in soil-water systems. *Applied and Environmental Microbiology* **54**, 1182-1187.
- Millette, D., Barker, J. F., Comeau, Y., Butler, B. J., Frind, E.O., Clement, B. and Samson, R. (1995) Substrate interaction during aerobic biodegradation of creosote-related compounds: a factorial batch experiment. *Environmental Science and Technology* **29**, 1944-1952.
- Morimura, Y., Kotin, P. and Falk, H. L. (1964) Photodynamic toxicity of polycyclic aromatic hydrocarbons in tissue culture. *Cancer Research* **24**, 1249-1259.
- Munkittrick, K. R., Blunt, B. R., Leggett, M., Huestis, S. and McCarthy, L. M. (1995) Development of a sediment bioassay to determine bioavailability of PAHs to fish. *Journal of Aquatic Ecosystem Health* **4**, 169-181.
- Neff, J. M. (1985) Polycyclic aromatic hydrocarbons. In: *Fundamentals of aquatic toxicology*. G. M. Rand and S. R. Petrocelli. (Eds), Hemisphere Publishing Corporation, 416-454.
- O'Connor, S., McNamara, L., Swerdin, M. and Van Buskirk, R. G. (1991) Multifluorescent assays reveal mechanisms underlying cytotoxicity- phase I CFTA compounds. *In Vitro Toxicology* **4**, 197-206.
- Oris, J. T. and Giesy, J. P. JR. (1985) The photoenhanced toxicity of anthracene to juvenile sunfish (*Lepomis* spp.). *Aquatic Toxicology* **6**, 133-146.
- Oris, J. T. and Giesy, J. P. JR. (1986) Photoinduced toxicity of anthracene to juvenile bluegill sunfish (*Lepomis Macrochirus* Rafinesque): Photoperiod effects and predictive hazard evaluation. *Environmental Toxicology and Chemistry* **5**, 761-768.
- Pagé, B., Pagé, M. and Noël, C. (1993) A new fluorometric assay for cytotoxicity measurements *in vitro*. *International Journal of Oncology* **3**, 473-476.
- Parkinson, C. and Agius, C. (1987) The effects of solvents on the toxicity of DDT to fish cells. *Archives of Toxicology, Supplement* **11**, 240-242.
- Persidsky, M. D. and Baillie, G. S. (1977) Fluorometric test of cell membrane integrity. *Cryobiology* **14**, 322-331.
- Ren, L., Huang, X..D., McConkey, B. J., Dixon, D. G., and Greenberg, B. M. (1994) Photoinduced toxicity of three polycyclic aromatic hydrocarbons (fluoranthene, pyrene, and naphthalene) to the duckweed *Lemna gibba* L. G-3. *Ecotoxicology and Environmental Safety* **28**, 160-171.
- Riley, J. C. M. and Carlson, J. C. (1987) Involvement of phospholipase A activity in the plasma membrane of the rat corpus luteum during luteolysis. *Endocrinology* **121**, 776-781.
- Schirmer, K., Ganassin, R. C., Brubacher, J. L. and Bols, N. C. (1994) A DNA fluorometric assay for measuring fish cell proliferation in microplates with different well sizes. *Journal of Tissue Culture Methods* **16**, 133-142.

- Schults, D. W., Ferraro, S. P., Roberts, F. A., and Poindexter, C. K. (1992) Comparison of methods for collecting interstitial water for trace organic compounds and metal analysis. *Water Research* **26**, 989-995.
- Spikes, J. D. (1989) Photosensitization. In: *The Science of Photobiology*. K. C. Smith. (Ed), Plenum Press, New York, NY, 79-110.
- Stoien, J. D. and Wang, R. J. (1974) Effect of near-ultraviolet and visible light on mammalian cells in culture. II Formation of toxic photoproducts in tissue culture medium by blacklight. *Proceedings of the National Academy of Sciences of the U.S.A.* **71**, 3961-3965.
- Utsumi, H. and Elkind, M.M. (1979) Photodynamic cytotoxicity of mammalian cells exposed to sunlight-simulating near ultraviolet light in the presence of the carcinogen 7,12 dimethylbenz[a]anthracene. *Photochemistry and Photobiology* **30**, 271-278.
- Valenzo, D. P. (1987) Photomodification of biological membranes with emphasis on singlet oxygen mechanisms. *Photochemistry and Photobiology* **46**, 147-160.
- Van Gorp, J. R. and Hankinson, O. (1983) Single-step phototoxic selection procedure for isolating cells that possess aryl hydrocarbon hydroxylase. *Cancer Research* **43**, 6031-6038.
- Wang, R. J. (1976) Effect of room fluorescent light on the deterioration of tissue culture medium. *In Vitro* **12**, 1547-1552.

CHAPTER 2

ABILITY OF 16 PRIORITY PAHs TO BE DIRECTLY CYTOTOXIC TO A CELL LINE FROM THE RAINBOW TROUT GILL ⁽¹⁾

2.1. ABSTRACT

Sixteen polycyclic aromatic hydrocarbons (PAHs) were screened for their ability to be directly cytotoxic to a cell line from the rainbow trout gill, RTgill-W1. Exposure times of 2 hours or less were sufficient for direct cytotoxicity to be detected, which appeared to be caused by a common mechanism, the general perturbation of membranes. This was judged by the similarity of results obtained for three fluorescent indicator dyes, alamar Blue™, 5-carboxyfluorescein diacetate acetoxymethyl ester (CFDA-AM), and neutral red. Among the 16 PAHs tested, just two- and three-ring PAHs were cytotoxic. These were naphthalene \cong acenaphthylene \cong acenaphthene > fluorene \cong phenanthrene. The relative potency of these five PAHs suggested that water solubility is important but another contributing factor is lipophilicity. Thus, for PAHs to be directly cytotoxic, they must accumulate in membranes and the failure of larger PAHs to be cytotoxic likely was caused by their failure to accumulate in membranes sufficiently. Only naphthalene was effective at concentrations well below its water solubility limit. Therefore, direct cytotoxicity is likely to be most environmentally relevant only with naphthalene.

2.2. INTRODUCTION

As well as causing genotoxicity (Benedict et al., 1972; Smolarek et al. 1987; Varanasi et al., 1989), many polycyclic aromatic hydrocarbons (PAHs) cause cytotoxicity to animal cells in culture after they have been activated metabolically. This has been studied most intensively with benzo[a]pyrene. Benzo[a]pyrene cytotoxicity has been observed in primary cultures from rodent embryos (Diamond and Gelboin, 1969) and liver (McQueen and Williams, 1982), and with cell lines from mammals (Gelboin et al., 1969; Babich et al., 1988), amphibia (Diamond and Clark, 1970), reptilia (Diamond and Clark, 1970) and fish (Diamond and Clark, 1970; Babich and Borenfreund, 1988; Lee et al., 1993). The cytotoxicity has been measured variously as growth

⁽¹⁾ This paper is for submission to Toxicology. Co-authors are D.G. Dixon, B.M. Greenberg, and N.C. Bols.

inhibition (Diamond and Clark, 1970; Diamond and Gelboin, 1969; Lee et al., 1993), enzyme leakage (McQueen and Williams, 1982), and neutral red retention (Babich et al., 1988), and develops after a 2-3 day exposure to benzo[a]pyrene in complete growth medium. Several observations indicate that the cytotoxicity of benzo[a]pyrene is dependent on the xenobiotic metabolism of the cytochrome P450 system. Cytotoxicity is reduced by α -naphthoflavone (Diamond and Gelboin, 1969; Babich et al., 1988), which inhibits the catalytic activity of cytochrome P4501A, and enhanced by exposure of the cells to hepatic S-9 microsomal fraction (Babich and Borenfreund, 1987) or to cytochrome P4501A inducing agents (Babich et al., 1988). Little or no cytotoxicity is observed in cell cultures with little or no cytochrome P450 dependent monooxygenase activity (Gelboin et al., 1969; Babich and Borenfreund, 1987; Babich et al., 1988; Lee et al., 1993). Other PAHs cause cytotoxicity in a manner similar to benzo[a]pyrene but several of them, including anthracene and fluorene, do not (Babich et al., 1988).

A more quick and direct mode of cytotoxicity has been observed with the smallest PAH, naphthalene. Harmon and Sanborn (1982) studied the effect of naphthalene on cellular respiration and morphology in monkey (Vero) and human (Hep-2) cell lines and in primary cultures of turkey embryos. A 2 hr naphthalene exposure strongly inhibited oxygen consumption in all three culture types. As well, pronounced morphological changes were observed at naphthalene concentrations near or above the EC_{50} value for oxygen consumption. The mechanism of cytotoxicity was studied with isolated mitochondria and appeared to involve the inhibition of mitochondrial respiration at the level of ubiquinone (Struble and Harmon, 1983; Beach and Harmon, 1992). Except for acenaphthene (Beach and Harmon, 1992), the ability of other PAHs to be directly and quickly cytotoxic is largely unexplored.

Methodologies for conveniently quantifying the photocytotoxicity of fluoranthene to fish cells have been developed (Chapter 1) and have features that should make them suitable for screening PAHs for their ability to be directly cytotoxic. For photocytotoxicity, two fluorescent indicator dyes, 5-carboxyfluorescein diacetate acetoxymethyl ester (CFDA-AM) and alamar Blue, were applied to multiwell cultures of the rainbow trout gill cell line, RTgill-W1, and the results quantified rapidly with a fluorescent multiwell plate reader. The alamar Blue detects changes in the cellular function that is the focus of naphthalene cytotoxicity, the mitochondrial electron transport chain. The CFDA-AM measures the more general response of cell membrane integrity. The time frame is also appropriate. The photocytotoxicity is detected within 2 hr from the termination of a 2 hr concurrent exposure to fluoranthene and UV light. Finally, RTgill-W1 should be suitable for detecting direct cytotoxicity because the results should not be confounded by PAH metabolism. As well as the short exposure time, PAH metabolism should be absent because 7-ethoxyresorufin-*O*-deethylase (EROD) activity, which is a measure of cytochrome P4501A, is undetectable in this cell line (Bols, unpublished data).

In this paper we have used alamar Blue, CFDA-AM, and a fluorescent indicator dye that measures lysosomal membrane integrity, neutral red, to screen 16 priority PAHs for their ability to be directly cytotoxic to RTgill-W1 cells. The results are discussed with respect to the water solubility of individual PAHs in order to evaluate the environmental relevance.

2.3. MATERIALS AND METHODS

A. *Cell culture and cytotoxicity testing*

The rainbow trout gill cell line, RTgill-W1, was developed in this laboratory (Bols et al., 1994). Cells were cultured in 75 cm² culture flasks at 22°C in Leibovitz's L-15 medium supplemented with 10 % fetal bovine serum (FBS). The source of the tissue culture supplies and a description of the subcultivation procedure have previously been presented in detail (Bols and Lee, 1994; Schirmer et al., 1994).

Confluent monolayers of RTgill-W1 cells in two 48 well tissue culture plates were used to study the direct cytotoxic effects of each PAH. Confluent cultures were achieved by plating 50,000 cells per well and allowing them to grow for 3 days. At confluency, the culture medium was removed and each well rinsed once with 500 µl of L-15/ex. L-15/ex, a modification of Leibovitz's L-15 medium, was developed specifically for presenting to the cells PAHs in the dark or with a concurrent UV radiation exposure (Chapter 1). A description of the constituents of L-15/ex and preparation procedures have been outlined previously (Appendix IV; Chapter 1). After the rinse, all wells received 500 µl of L-15/ex. The cells were then dosed with 2.5 µl aliquots of PAH dissolved in DMSO, using a Nichiryo Model 800 digital positive displacement micropipetter (Fisher Scientific, Toronto, ON, Canada). The duration of exposure in the dark was 2 hr for all experiments.

B. *Cytotoxicity assays*

Upon termination of exposure, cytotoxicity assays were performed immediately and 24 hr later. Three fluorescent indicator dyes were used. These were alamar Blue (Immuncorp. Science Inc., Montreal, PQ, Canada), an indicator of cellular metabolic activity; 5-carboxyfluorescein diacetate acetoxymethyl ester (CFDA-AM, Molecular Probes, Eugene, OR, USA), an esterase substrate that indirectly measures plasma membrane integrity; and neutral red (94%, Sigma Chemical Co., St. Louis, MO, USA), an indicator of lysosomal membrane integrity.

Alamar Blue and CFDA-AM: The alamar Blue and CFDA-AM indicator dyes were used in combination as described in Chapter 1 with minor modifications. Alamar Blue and CFDA-AM were prepared together in L-15/ex to give a final concentration respectively of 5% v/v and 4 µM (Appendix IV). For immediate measurements, aliquots of 100 µl/well of this solution were added to one of the culture plates. After 30 min, or in some cases after 2 hr, fluorescence was quantified with the CytoFluor 2350 (PerSeptive Biosystems, Burlington, ON, Canada) at respective excitation and emission wavelengths of 530 (± 30) and 595 (± 35) nm for alamar Blue, and 485 (± 22) and

530 (\pm 30) nm for CFDA-AM. For measurements 24 hr later, the dye solution was removed from the wells and replaced with L-15 with 10 % FBS before cytotoxicity assays were repeated again on the same wells.

Neutral red: The neutral red (3-amino-7-dimethylamino-2-methylphenanzine hydrochloride, 94 %; Sigma Chemical Co., St. Louis, MO, USA) indicator dye was prepared as a stock solution of 5 mg neutral red in 1 ml of ddH₂O (Appendix IV). This solution was protected from light and stored at room temperature. Under these storage conditions, neutral red had previously been shown to be stable for at least three months (Löwik et al., 1993). The neutral red working solution was prepared prior to each cytotoxicity test by diluting the stock solution 1:100 in L-15/ex to yield 50 μ g neutral red in 1 ml of L-15/ex. This working solution was filter-sterilized with a 0.2 μ m sterile acrodisc (Gelman Sciences Inc., Ann Arbor, MI, USA) to remove fine precipitates of the dye.

For immediate measurements, aliquots of 100 μ l of this working solution were added to the second culture plate. After an incubation period of 1 hr, which allowed the dye to be taken up by cells with intact lysosomes, the dye solution was removed and wells were rinsed with 100 μ l of a mild fixative, containing 0.5% v/v formaldehyde and 1% w/v CaCl₂ in ddH₂O. This rinsing step removed any excess neutral red that had not been localized in lysosomes during the incubation period. In order to solubilize lysosomal neutral red, an aliquot of 100 μ l of an extraction solution (1% v/v acetic acid and 50% v/v ethanol in ddH₂O) was then added to each well. The plates were placed on an orbital shaker and shaken at ~ 40 rpm before fluorescence was measured 10 min later. Fluorescence was quantified with the CytoFluor 2350 at respective excitation and emission wavelengths of 530 (\pm 30) and 645 (\pm 50) nm.

In contrast to the alamar Blue and CFDA-AM cytotoxicity assays, cells that had been exposed to neutral red could not be used for repeated measurements. This resulted from the fixation and extraction steps during the neutral red cytotoxicity assay which eradicated cell viability. Therefore, the neutral red measurements that were taken 24 hr after irradiation were performed in plates that had previously been exposed to the alamar Blue and CFDA-AM indicator dyes. Upon completion of the fluorescent measurements, alamar Blue and CFDA-AM were removed from wells and replaced with 100 μ l/well neutral red working solution. The neutral red cytotoxicity assay was then performed as described above. A prior experiment, in which extra plates were prepared to measure the toxicity after 24 hr in separate plates, had shown that results were similar whether the neutral red assay was performed on separate plates or subsequent to the alamar Blue/CFDA-AM assays on the same cultures.

C. Solubilization of PAHs and HPLC analysis

PAHs were purchased in crystallized form as follows: naphthalene (99%), acenaphthylene (99%), anthracene (99%), chrysene (95%), and benzo[a]pyrene (98%) were from Sigma Chemical Co. (St. Louis, MO, USA); acenaphthene (99%), fluorene (98%), phenanthrene (98%), fluoranthene (98%), pyrene (99%), benzo[a]anthracene (99%), benzo[b]fluoranthene (99%), benzo[k]fluoranthene (98%), dibenzo[a,h]anthracene (97%), and benzo[g,h,i]perylene (98%) were from Aldrich Chemical Co. (Milwaukee, WI, USA); and indeno[1,2,3-cd]pyrene (99%) was from Supelco (Mississauga, ON, Canada).

PAHs were dissolved in 100 % dimethyl sulphoxide (DMSO, BDH Inc., Toronto, ON, Canada) to yield stock solutions of 0.5 to 1 mg/ml. For some PAHs, particularly the higher molecular weight compounds, solubilization was slow and required shaking over night. The PAH stock solutions were serially diluted in DMSO to give 200 times the final concentration required by each design treatment. These working solutions were stored at room temperature, protected from light in 1.5 or 5 ml amber screw cap vials (Kimble, VWR Canlab, Mississauga, ON, Canada). A 2.5 μ l aliquot of these working solutions was added to 500 μ l of L-15/ex in wells of 48 well tissue culture plates to give the desired PAH concentrations.

The concentrations of PAHs in the working solutions were confirmed by HPLC. Samples were prepared by adding 2.5 μ l working solution to a 500 μ l aliquot of 50 % HPLC-grade acetonitrile (BDH Inc., Toronto, ON, Canada) and 50 % Milli-Q filtered distilled water in 1.5 ml amber screw cap vials. HPLC was done with a System Gold liquid chromatograph with a System Gold 168 diode array detector and a Model 126 liquid chromatograph pump (Beckman Instruments Inc., Mississauga, ON, Canada). Aliquots of 100 μ l from sample solutions were loaded manually onto a 25 cm LC-18 column (Supelco, Mississauga, ON, Canada). PAHs were eluted with 75 % HPLC-grade acetonitrile and 25 % Milli-Q filtered distilled water at a flow rate of 1 ml/min. Detection of PAHs was done at 254 nm with a 30 nm band width. The peak areas of unknown samples were compared to those of individual standards or a PAH calibration mix (Supelco, Bellefonte, PA, USA).

D. Data analysis

The fluorescence readings in wells that contained PAHs in DMSO were expressed as a percentage of the readings in control wells that contained DMSO only. Prior to these calculations, fluorescence readings for wells without cells were subtracted from the experimental and control values with cells. Dose-response data followed a sigmoid relationship and were analyzed by nonlinear regression using the curve-fitting routine of SigmaPlot (Jandel Scientific). Data were

fitted to the logistic function for continuous response data as described by Kennedy et al. (1993) for analyzing enzyme activities, with minor modifications. The logistic function was

$$(1) \quad y(d) = Y_{\min} + (Y_{\max} - Y_{\min})\{1 + \exp[-g(\ln(d) - \ln(EC_{50}))]\}^{-1}$$

where $y(d)$ is the % cell viability at the PAH concentration d , Y_{\min} is the minimum % cell viability, Y_{\max} is the maximum % cell viability, g is a slope parameter, and EC_{50} is the PAH concentration that produces 50 % cell viability. Because experimental results were expressed relative to a control on a 0 - 100 % basis, Y_{\max} was 100 % while Y_{\min} was 0 %, which simplified the equation to:

$$(2) \quad y(d) = 100 (\%) \{1 + \exp[-g(\ln(d) - \ln(EC_{50}))]\}^{-1} .$$

All statistical tests were performed using SYSTAT™ software (SPSS Inc., 1996).

2.4. RESULTS











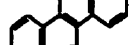


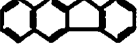
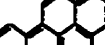

Three fluorescent indicator dyes were used to screen sixteen PAHs for their ability to cause cytotoxic responses in RTgill-W1 cells within 2 hr of a 2 hr application. Alamar Blue, CFDA-AM, and neutral red were the indicator dyes and gave similar results. Five PAHs were cytotoxic, whereas the other eleven were not.

A. Cytotoxic PAHs

Naphthalene, acenaphthylene, acenaphthene, fluorene, and phenanthrene were directly cytotoxic. However, these compounds differed in their ability to be cytotoxic at concentrations below their maximum solubility in water (Table 2.1.). Differences in solubility made obtaining full dose-response curves difficult for some of these PAHs (see below). However, when estimated EC_{50} s for either of the three cytotoxicity assays were used to rank these compounds, the sequence of cytotoxicity was naphthalene ($48 \pm 6 \mu\text{M}$, $n=9$) \cong acenaphthylene ($43 \pm 7 \mu\text{M}$, $n=6$) \cong acenaphthene ($73 \pm 12 \mu\text{M}$, $n=5$) $>$ fluorene ($144 \pm 39 \mu\text{M}$, $n=3$) \cong phenanthrene ($177 \pm 63 \mu\text{M}$, $n=6$), as determined by analysis of variance, followed by Tukey's post hoc test ($\alpha = 0.05$).

Naphthalene: This was the only PAH that was cytotoxic at concentrations well below its maximum solubility in water, which is $240 \mu\text{M}$ (Table 2.1.). The shapes of the dose-response curves and the EC_{50} values were similar for each of the fluorescent indicator dyes and did not change in the 24 hr that followed the 2 hr of exposure (Figure 2.1.). Immediately after exposure, EC_{50} values were $54 \pm 1 \mu\text{M}$ ($n=2$) for alamar Blue, $55 \pm 3 \mu\text{M}$ ($n=2$) for CFDA-AM, and $48 \pm 1 \mu\text{M}$ ($n=2$) for neutral Red. Twenty four hours later, the EC_{50} values were $51 \pm 9 \mu\text{M}$ ($n=2$) for alamar Blue, $49 \pm 1 \mu\text{M}$ ($n=2$) for CFDA-AM, and $57 \mu\text{M}$ ($n=1$) for neutral red. Analysis of variance revealed no significant differences between these EC_{50} values ($\alpha=0.05$). The results of the fluorescent assays were also confirmed by the phase-contrast appearance of the cells (Figure 2.2.). At concentrations close to the observed EC_{50} values, cells were characterized by distinct, dark nuclei. Cells were round and balloon-shaped, a morphology that is typically observed for necrosis (Cobb et al., 1996). These morphological changes were observed within 20 minutes after dosing and remained the same for up to 24 hr, although some cells detached from the growth surface over the 24 hr period.

Table 2.1. Summary of physical-chemical data of the 16 priority PAHs and their ability to elicit direct cytotoxicity in RTgill-W1 cells

PAH	Molecular Structure	Molecular Weight (g/mol)	Water Solubility ⁽¹⁾ (μM)	Highest concentration tested (μM)	Cyto-toxicity? YES/NO
Naphthalene		128.17	240	107	YES
Acenaphthylene		152.20	26	53	YES
Acenaphthene		154.21	23	35	YES
Fluorene		166.22	12	128	YES
Phenanthrene		178.23	7.20	200	YES
Anthracene		178.23	0.409	1.00	NO
Fluoranthene		202.26	1.28	4.95	NO
Pyrene		202.26	0.667	2.91	NO
Benzo[a]anthracene		228.29	0.048	0.137	NO
Chrysene		228.29	0.013	0.325	NO
Benzo[b]fluoranthene		252.32	0.006	1.63	NO
Benzo[k]fluoranthene		252.32	0.003	0.624	NO
Benzo[a]pyrene		252.32	0.016	0.180	NO
Dibenzo[a,h]anthracene		278.35	0.001 800	2.389	NO
Benzo[g,h,i]perylene		276.34	0.020	0.264	NO
Indeno[1,2,3-cd]pyrene		276.34	0.000 700	2.10	NO

(1) Source: Mackay et al., 1992

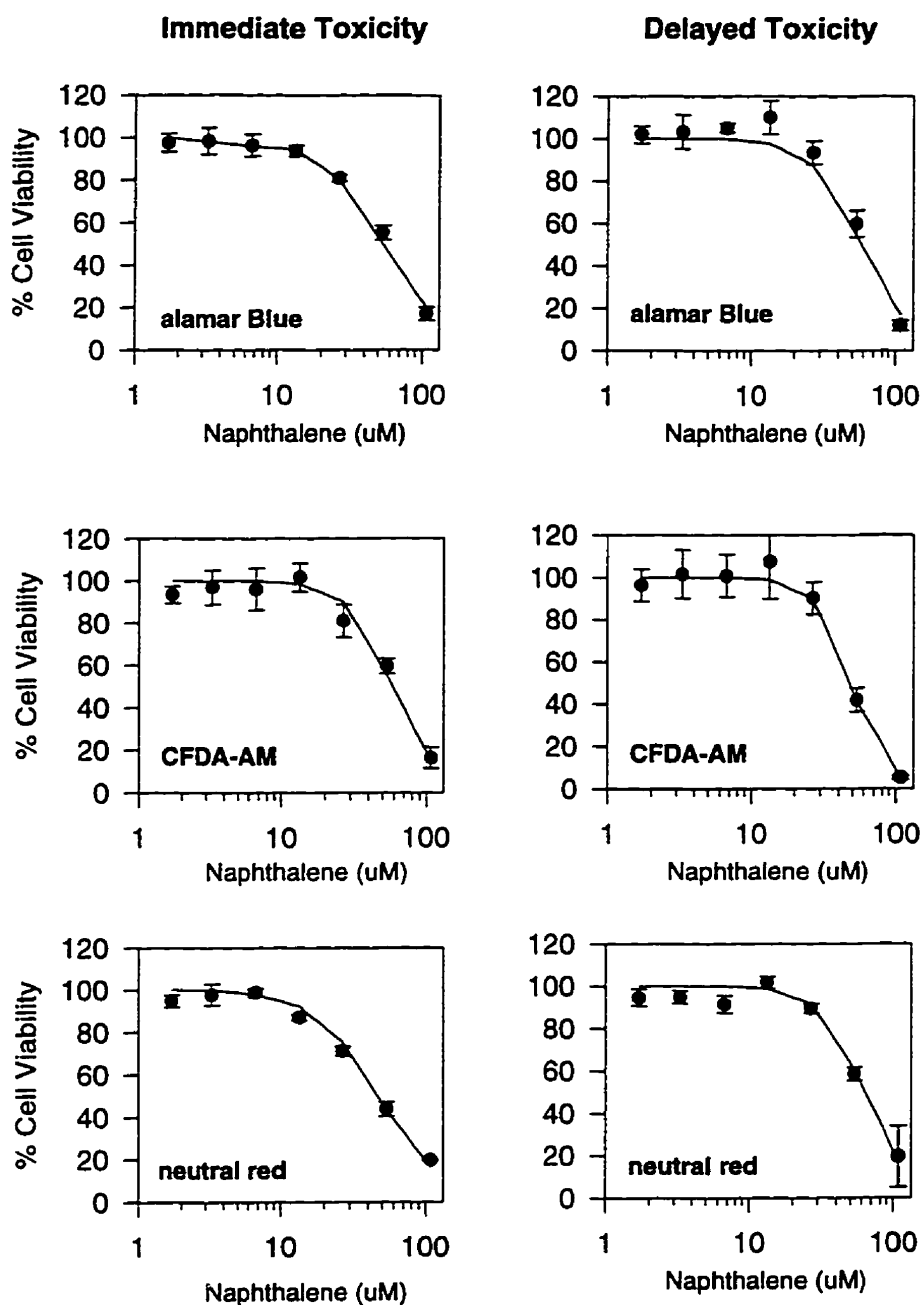


Figure 2.1. Viability of RTgill-W1 cells immediately and 24 hr after being exposed to increasing concentrations of naphthalene. Confluent cultures were exposed to naphthalene in L-15/ex and kept in the dark for 2 hr. Immediately afterwards and 24 hr later, cell viability was assayed with a mixture of alamar Blue (top panels) and CFDA-AM (middle panels), and with neutral red (bottom panels). The results were expressed as a percentage of the readings in control cultures that received no naphthalene. One representative experiment is shown. Each data point is the mean of four culture wells with the vertical lines indicating the standard deviation.

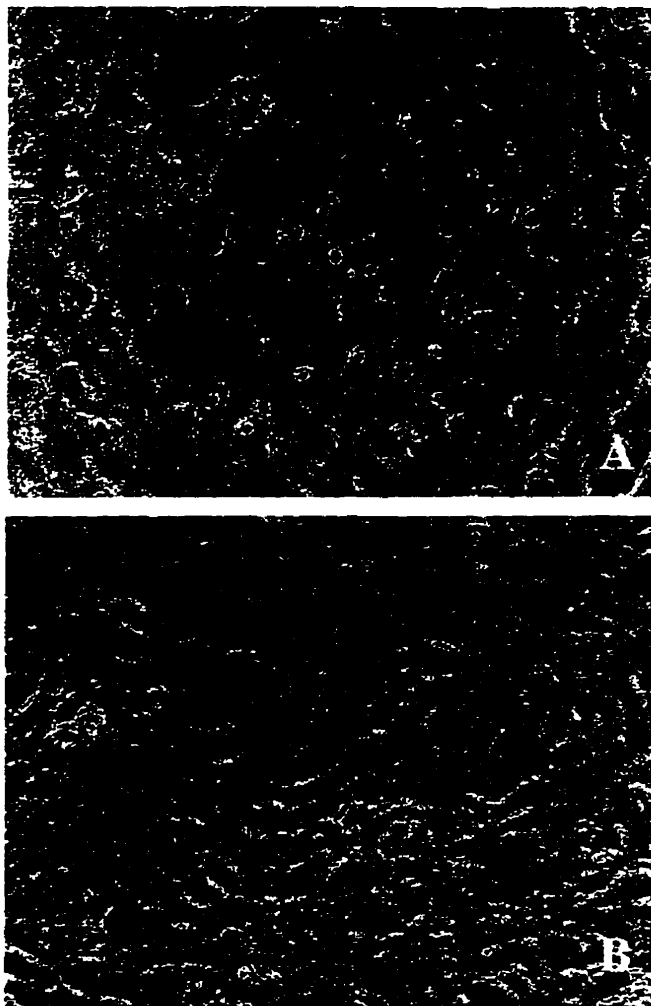


Figure 2.2. Phase-contrast appearance of RTgill-W1 cells 2 hr after being exposed to 54 μM naphthalene (panel A) and compared to the control containing no naphthalene (panel B). Confluent cultures in wells of a 48 well culture plate were exposed to 54 μM naphthalene or the appropriate DMSO control in L-15/ex and kept in the dark for 2 hr. The photographs were taken at 160x.

Acenaphthylene and Acenaphthene: These two PAHs were most cytotoxic at concentrations above their water solubility limits, which are 26 μM for acenaphthylene and 23 μM for acenaphthene. However, as for naphthalene, dose-response curves were obtained that were similar in shape for each of the fluorescent indicator dyes and did not change in the 24 hr that followed the 2 hr of exposure (Figure 2.4.). Likewise, morphological changes were seen and paralleled those observed for naphthalene. When dose-response curves were used to estimate the percent cell viability at water solubility, cytotoxicity was found for both acenaphthylene and acenaphthene but was significant in only a few cases (Figure 2.3., panels A and B).

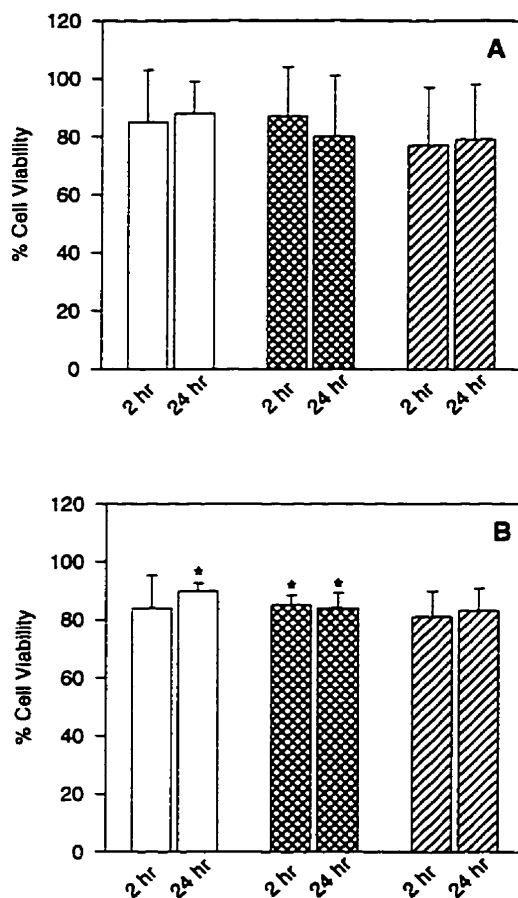


Figure 2.3. Cell viability of RTgill-W1 immediately and 24 hr after exposure to 26 μM acenaphthylene (panel A) and 23 μM acenaphthene (panel B). Dose-response curves that were obtained as described in Figure 2.1. were used to calculate the percent cell viability for each of the compounds at their respective water solubility limits. The results for alamar Blue, CFDA-AM and neutral red are indicated, respectively, by open, crossed, and dashed bars. Each bar represents the mean of 4 independent experiments for acenaphthylene and 3 for acenaphthene. Vertical lines indicate the standard deviation. One sample t-tests that revealed a significant difference from 100 % cell viability are indicated by asterisks ($\alpha=0.05$).

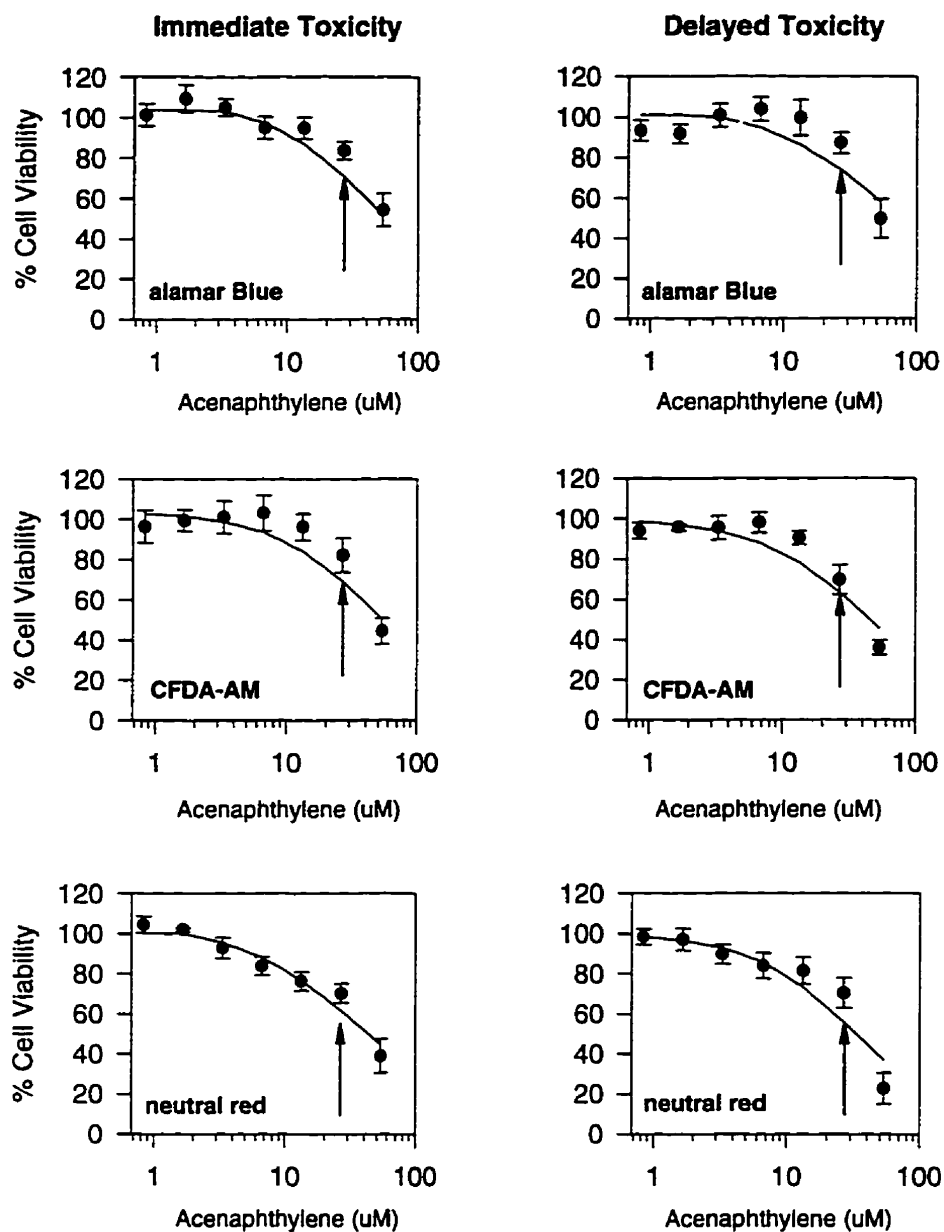


Figure 2.4. Viability of RTgill-W1 cells immediately and 24 hr after being exposed to increasing concentrations of acenaphthylene. Exposure of cell cultures to acenaphthylene and subsequent cell viability assays were performed as described in Figure 2.1.. One representative experiment is shown. Each data point is the mean of four culture wells with the vertical lines indicating the standard deviation. The arrows indicate the concentration at which acenaphthylene is maximally soluble in water (26 μM). Similar results were obtained for acenaphthene.

Fluorene: Little cytotoxicity was observed with this PAH at its water solubility limit, 12 μM (Figure 2.5., panel A). However, when higher concentrations were tested, dose-response curves were obtained with all three cytotoxicity assays but they were more variable than for other PAHs. This was likely due to the formation of large fluorene crystals which were visible by phase-contrast microscopy at concentrations as low as 28 μM and even more so at 57 and 113 μM , with the latter being the highest concentration tested (Figure 2.6.). Although the crystals made observing cell morphology more difficult, the cells appeared round and frequently detached from the growth surface.

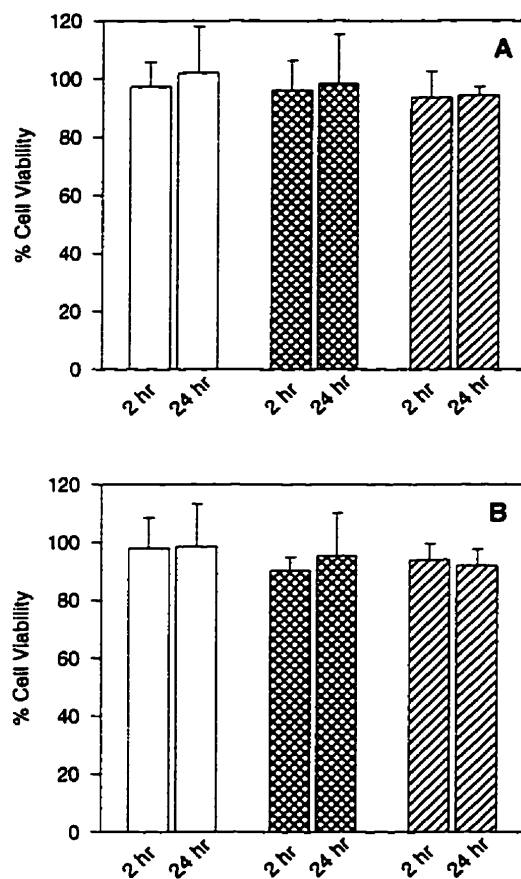


Figure 2.5. Cell viability of RTgill-W1 immediately and 24 hr after exposure to 12 μM fluorene (panel A) and 7 μM phenanthrene (panel B). Dose-response curves that were obtained as described in Figure 2.1. were used to calculate the percent cell viability for each of the compounds at their respective water solubility limits. The results for alamar Blue, CFDA-AM and neutral red are indicated by, respectively, open, crossed, and dashed bars. Each bar represents the mean of 2 independent experiments for phenanthrene. For fluorene, 2 independent experiments are shown for neutral red, whereas three independent experiments are shown for alamar Blue and CFDA-AM. Vertical lines indicate the standard deviation. One sample t-tests revealed no significant differences from 100 % cell viability ($\alpha=0.05$).

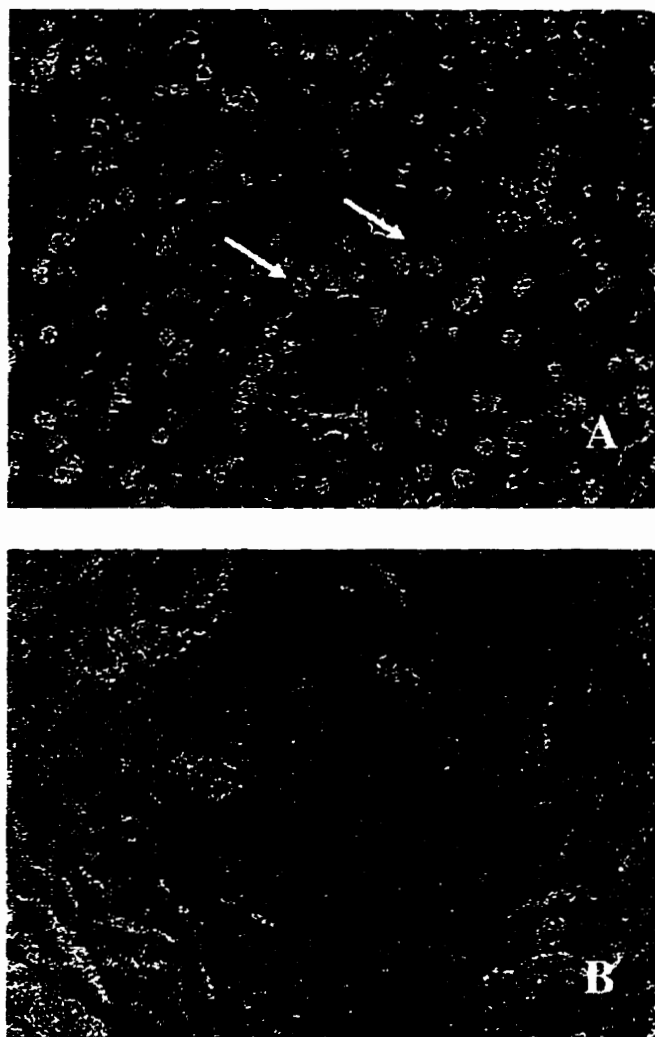


Figure 2.6. Phase-contrast appearance of RTgill-W1 cells 2 hr after being exposed to 113 μM fluorene (panel A) and compared to the control containing no fluorene (panel B). Confluent cultures in wells of a 48 well culture plate were exposed to 113 μM fluorene or the appropriate DMSO control in L-15/ex and kept in the dark for 2 hr. Crystal formation in the fluorene-containing wells is indicated by the arrows. The photographs were taken at 160x.

Phenanthrene: Although directly cytotoxic, phenanthrene was only slightly cytotoxic at 7 μM , its water solubility limit (Figure 2.5., panel B). Nevertheless, dose-response curves were obtained by applying high phenanthrene concentrations. These curves were similar for each of the fluorescent indicator dyes and for the two time points at which cytotoxicity was measured (Figure 2.7.). As well, at the concentrations that were cytotoxic with the indicator dyes, morphological changes were seen that were similar to those observed for naphthalene.

B. Non-cytotoxic PAHs

Neither the alamar Blue, CFDA-AM, nor neutral red assays detected cytotoxicity for the following PAHs: anthracene, fluoranthene, pyrene, benzo[a]anthracene, chrysene, benzo[b]fluoranthene, benzo[k]fluoranthene, benzo[a]pyrene, dibenzo[a,h]anthracene, benzo[g,h,i]perylene, and indeno[1,2,3-cd]pyrene. This was true even when PAHs were tested at concentrations several orders of magnitude above their water solubility limits (Table 2.1., Figure 2.8.).

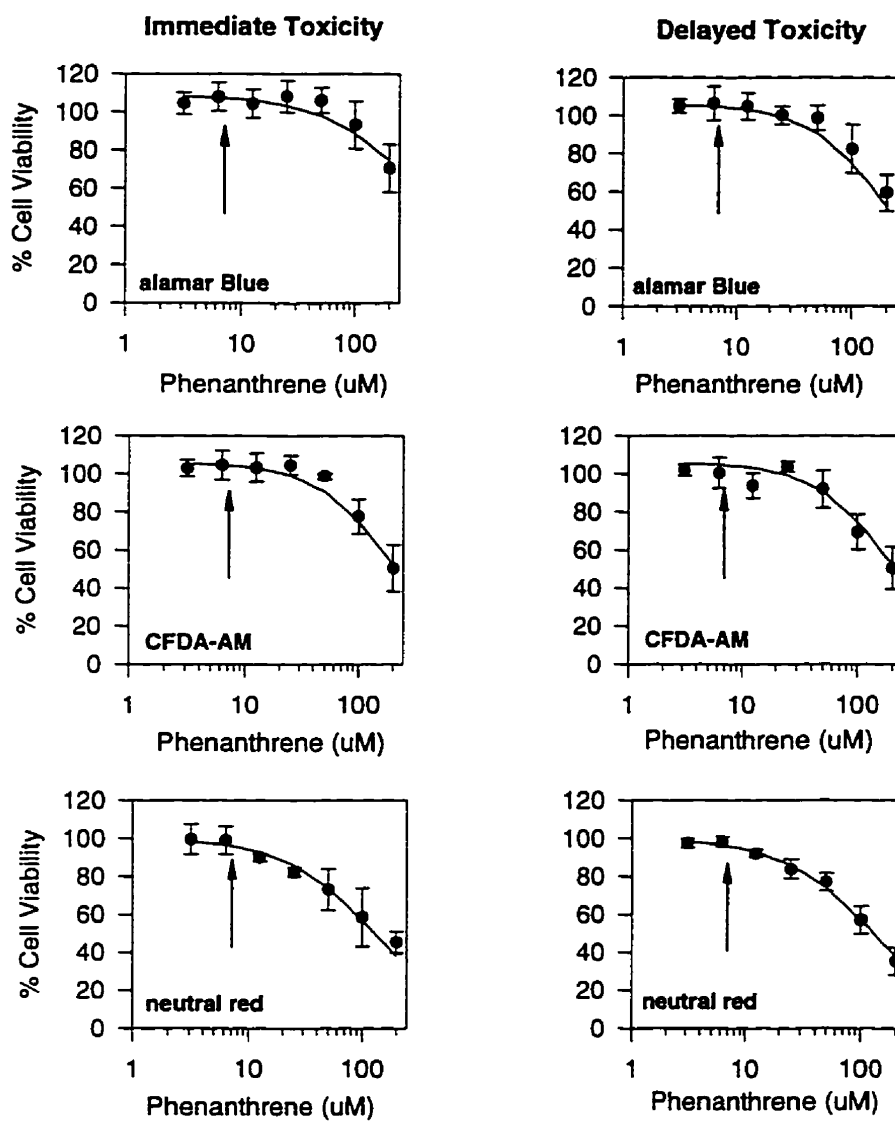


Figure 2.7. Viability of RTgill-W1 cells immediately and 24 hr after being exposed to increasing concentrations of phenanthrene. Exposure of cell cultures to phenanthrene and subsequent cell viability assays were performed as described in Figure 2.1.. One representative experiment is shown. Each data point is the mean of four culture wells with the vertical lines indicating the standard deviation. The arrows indicate the concentration at which phenanthrene is maximally soluble in water (7 μM).

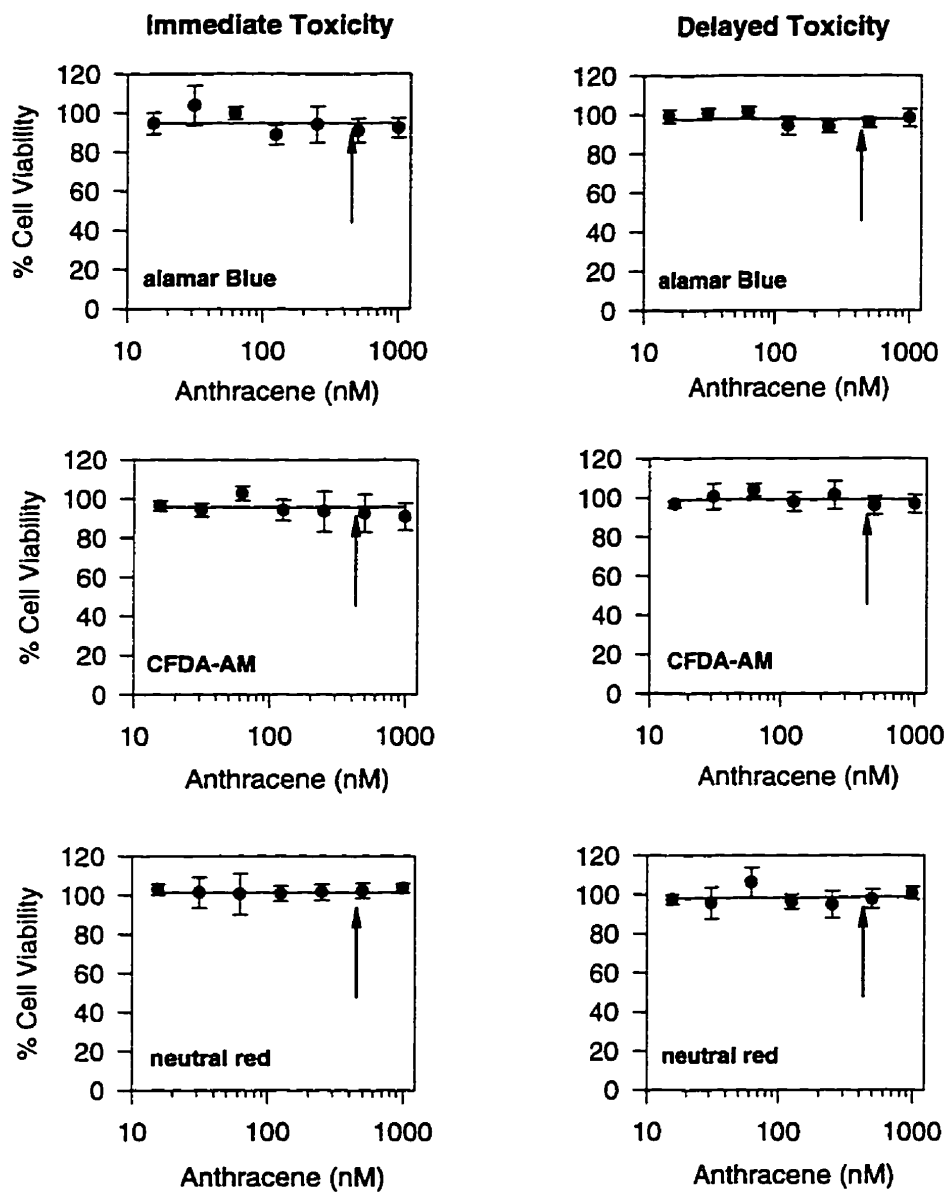


Figure 2.8. Viability of RTgill-W1 cells immediately and 24 hr after being exposed to increasing concentrations of anthracene. Exposure of cell cultures to anthracene and subsequent cell viability assays were performed as described in Figure 2.1.. One representative experiment is shown. Each data point is the mean of four culture wells with the vertical lines indicating the standard deviation. The arrows indicate the water solubility limit of anthracene (409 nM).

2.5. DISCUSSION

The current research showed that a few PAHs elicited cytotoxic responses rapidly. This is referred to as a direct cytotoxic mode of action and is distinguished by the time frame of its development from a cytotoxic response that requires metabolic activation of the PAH. Exposure times of several hours or less have been sufficient for direct cytotoxicity to be detected, whereas much longer exposure times have been needed for PAH metabolism to cause cytotoxicity. Direct cytotoxicity had been observed previously with naphthalene through the monitoring of oxygen consumption (Harmon and Sanborn, 1982) and has now been found with naphthalene, acenaphthylene, acenaphthene, fluorene and phenanthrene by measuring changes in cellular functions with the fluorescent indicator dyes, alamar Blue, CFDA-AM, and neutral red.

The fact that the different cytotoxicity assays gave similar results suggested a common mechanism for the directly cytotoxic mode of action. The work of others on the toxicity of PAHs suggests several possibilities. Using isolated mitochondria (Beach and Harmon, 1992; Harmon, 1988; Harmon and Sanborn, 1982; Strubel and Harmon, 1983), as well as cells (Harmon and Sanborn, 1982), Harmon and his coworkers found that naphthalene and acenaphthylene specifically inhibited mitochondrial respiration, and did so at the level of ubiquinone (coenzyme Q₁₀). Another school of thought, which has been developed for anesthetic compounds, is that inhibitory actions are due to general changes in membrane integrity (Seeman, 1972). On the other hand, using liposomes, Sikkema et al. (1994) found that cyclic hydrocarbons caused effects both on membrane integrity and on a specific membrane enzyme. In the current study the perturbation of membranes generally appears to be the cause of cytotoxicity because all three fluorescent assays are indirectly measuring the maintenance of membrane integrity. The CFDA-AM assay needs an intact plasma membrane in order to maintain a cytoplasmic milieu that supports esterase activity and the formation of a fluorescent product. The alamar Blue assay requires intact mitochondrial membranes in order that the electron transport chain functions and reduces the dye to a more fluorescent form. The neutral red assay is a measure of lysosomal membrane integrity because this membrane is required for the uptake and retention of the fluorescent dye. However, a specific action on mitochondria that developed within minutes could lead several hours later to the three assays giving similar results as the functional integrity of plasma and lysosomal membranes will ultimately be dependent on ATP. Therefore, a specific mechanism appears unlikely but cannot be ruled out.

The ability of PAHs to be directly cytotoxic appeared to be related to their water solubility and to their lipophilicity. Among the 16 PAHs tested, just two- and three-ring PAHs, which have the highest water solubility (Mackay et al., 1992), were cytotoxic. The exception, anthracene, also supported the correlation. Although of the same size and with the same number of rings as the

cytotoxic phenanthrene, anthracene is much less water soluble because its three benzene rings are arranged in a linear rather than in an angular fashion (Harvey, 1991). The relative potency of the five PAHs that were cytotoxic suggested that water solubility is again important, but an additional factor to be considered is lipophilicity, which can be expressed as the water/octanol partition coefficient ($P_{O/w}$) or as the membrane-aqueous phase partition coefficient (Sikkema et al., 1994). Phenanthrene and fluorene were the least water soluble and the least cytotoxic. Among the remaining three PAHs, naphthalene was approximately 10 fold more water soluble than acenaphthylene and acenaphthene but the three PAHs were equally cytotoxic as judged by EC_{50} s. Acenaphthylene and acenaphthene are approximately 6 and 10 fold more lipophilic than naphthalene, as judged by their $P_{O/w}$ values (Mackay et al., 1992). The interpretation for these observations is that in order for the PAHs to be directly cytotoxic, they must accumulate in membranes. If this interpretation is correct, the larger PAHs failed to be directly cytotoxic because they failed to accumulate in membranes sufficiently to generally disrupt membrane functions.

The failure of the cells to recover or to be further damaged in the 24 hr following removal of the cytotoxic PAHs points to a toxicity mechanism that is distinct from the mechanism underlying the photocytotoxicity of fluoranthene (Chapter 1). Previously, using the alamar Blue and CFDA-AM cytotoxicity assays, we had observed that cytotoxicity was more pronounced 24 hr after the termination of a concurrent fluoranthene and UV exposure than after 2 hr. In the case of fluoranthene photocytotoxicity, the membrane impairment appears to be due to the generation of reactive oxygen species (ROS) within the membrane (Chapter 1). In the case of direct cytotoxicity, the membrane impairment appears to be due to a different mechanism, likely the physical disruption of membrane integrity by the presence of the PAH. Support for this comes from work with liposomes by Sikkema et al. (1994) who found that the accumulation of cyclic hydrocarbons caused swelling of the membrane bilayer and an increase in membrane fluidity. If direct cytotoxicity requires maintenance of the PAH in the cell membranes, removal of the PAH-containing medium should limit further damage but not necessarily lead to recovery as the lipophilicity of the PAH would favor retention of the accumulated PAH in membranes.

The potential of a directly cytotoxic mode of action to be environmentally relevant appears to exist only for naphthalene. Naphthalene was the only PAH to be cytotoxic below its water solubility, and naphthalene concentrations similar to the EC_{50} values observed in this study have been measured in aquatic environments at point sources of PAH contamination, such as wood treatment or storage sites (Environment Canada, 1993). Furthermore, EC_{50} values obtained with the RTgill-W1 cell line are in the range of those found for lethality to fish in laboratory tests (Neff, 1985). Although fish lethality was measured after 24 to 96 hr of exposure, the damage to

fish gill epithelial cells soon after contact with naphthalene, as would be expected from the current study, likely occurred before damage to other tissues and organs. Support for this also comes from a study by Lee et al. (1972) who detected within 25 to 60 min of fish being exposed to naphthalene an increase in the naphthalene concentration of gills. Thus, naphthalene is an important compound to be considered in the environmental risk assessment of PAHs and its directly cytotoxic action should be part of any evaluation.

Despite the importance of naphthalene, the contribution of other PAHs to a directly cytotoxic mode of action might still have to be considered in the environment. Naphthalene is commonly present at contaminated sites along with other PAHs, whose concentrations are usually well below saturation (Mackay et al., 1992; Neff, 1985). If the directly cytotoxic mode of action is due to the general accumulation of PAHs in membranes and is independent of PAH structure, these other PAHs would be expected to contribute to the cytotoxic response, even though individually their concentrations would be too low to cause cytotoxicity. Within membranes, the different PAHs could interact in either an additive or non additive manner to elicit cytotoxicity. In other experimental systems, the toxicity of several aromatic hydrocarbons has been observed to be additive whether the compounds have been thought to be toxic through a general membrane-perturbing effect (Broderius and Kahl, 1985; Deneer et al., 1988; Muñoz and Tarazona, 1993) or a specific action on mitochondrial function (Beach and Harmon, 1992).

The *in vitro* evaluation of the cytotoxicity of PAHs is problematic. One general difficulty is their low water solubility and the necessity to apply them to cell cultures at concentrations above their water solubility. At supersaturated concentrations, PAHs tend to form microcrystals, and these could influence uptake, and in turn, cytotoxicity of PAH solutions (Klamer et al., 1997; Kocan et al. 1981; Lakowicz et al., 1980). Although only fluorene crystals were visible in our study, the formation of crystals that were too small to be visualized by phase-contrast microscopy cannot be ruled out for other PAHs. The appearance of fluorene crystals coincided with variable toxicity and morphological changes that appeared to be slightly different from those found for other cytotoxic PAHs in the absence of visible crystals. However, for acenaphthylene, acenaphthene and phenanthrene, continuous dose-response curves could be obtained consistently and morphological changes were similar to those found for naphthalene. This indicates that these PAHs are available to cells at concentrations that exceed their water solubility limits and that the toxic mechanisms remains either unchanged or changes in a way that was not detected with the fluorescent indicator dyes. Another general difficulty is that PAHs have the potential to elicit cytotoxicity by multiple modes of action and detecting responses will depend on exposure times and endpoints. Although in the current study a general cytotoxic mechanism appeared to be at work, the use of screening protocols with multiple endpoints, and perhaps more complex endpoints, is probably still desirable in order to detect any specific actions. An example of a

complex cytotoxic action of PAHs that occurs without metabolic activation is the inhibition of cell to cell communication (Upham et al., 1994). This effect on intercellular communication was observed at much higher PAH concentrations than those used in the current study, and unlike the results with the fluorescent dyes, was lost upon removal of the PAH. However, both studies found that the three-ringed PAHs were more likely to be inhibitory than four- and five-ringed PAHs.

2.6. ACKNOWLEDGMENTS

This research was supported by a Strategic Grant from the Natural Sciences and Engineering Research Council of Canada and by the Canadian Network of Toxicology Centers. K.S. received financial support through an Ontario Graduate Scholarship for international students.

2.7. REFERENCES

- Babich, H. and Borenfreund, E. (1987) Polycyclic aromatic hydrocarbon in vitro cytotoxicity to bluegill BF-2 cells: mediation by S-9 microsomal fraction and temperature. *Toxicology Letters* **36**, 107-116.
- Babich, H., Sardana, M.K. and Borenfreund, E. (1988) Acute cytotoxicities of polynuclear aromatic hydrocarbons determined in vitro with the human liver tumor cell line, HepG2. *Cell Biology and Toxicology* **4**, 295-309.
- Beach, A.C. and Harmon, H.J. (1992) Additive effects and potential inhibitory mechanism of some common aromatic pollutants on in vitro mitochondrial respiration. *Journal of Biochemical Toxicology* **7**, 155-161.
- Benedict, W.F., Gielen, J.E. and Nebert, D.W. (1972) Polycyclic hydrocarbon-produced toxicity, transformation, and chromosomal aberrations as a function of aryl hydrocarbon hydroxylase activity in cell cultures. *International Journal of Cancer* **9**, 435-451.
- Bols, N.C., Barlian, A., Chirino-Trejo, S.J., Caldwell, S.J., Goegan, P. and Lee, L.E.J. (1994) Development of a cell line from the primary cultures of rainbow trout, *Oncorhynchus mykiss* (Walbaum), gills. *Journal of Fish Diseases* **17**, 601-611.
- Bols, N.C. and Lee, L.E.J. (1994) Cell lines: availability, propagation and isolation. In: *Biochemistry and molecular biology of fishes*. P.W. Hochachka and T.P. Mommsen (Eds), Elsevier Science, Amsterdam, Vol. 3, 145-159.
- Broderius, S. and Kahl, M. (1985) Acute toxicity of organic chemical mixtures to the fathead minnow. *Aquatic Toxicology* **6**, 307-322.
- Cobb, J.P., Hotchkiss, R.S., Karl, I.E. and Buchman, T.G. (1996) Mechanisms of cell injury and death. *British Journal of Anaesthesia* **77**, 3-10.
- Diamond, L. and Clark, H.F. (1970) Comparative studies on the interaction of benzo[a]pyrene with cells derived from poikilothermic and homeothermic vertebrates. I. Metabolism of benzo[a]pyrene. *Journal of the National Cancer Institute* **45**, 1005-1012.
- Diamond, L. and Gelboin, H.V. (1969) Alpha-naphthoflavone: an inhibitor of hydrocarbon cytotoxicity and microsomal hydroxylase. *Science* **166**, 1023-1026.
- Deneer, J.W., Sinnige, T.L., Seinen, W. and Hermens, J.L.M. (1988) The joint acute toxicity to *Daphnia magna* of industrial organic chemicals at low concentrations. *Aquatic Toxicology* **12**, 33-38.
- Environment Canada (1993) Creosote-impregnated waste materials. Environmental Protection Act, Report En40-215/13-E, Ottawa, ON, Canada.

- Gelboin, H.V., Huberman, E. and Sachs, L. (1969) Enzymatic hydroxylation of benzopyrene and its relationship to cytotoxicity. *Proclamation of the National Academy of Science* **64**, 1188-1194.
- Harmon, H.J. (1988) Effect of naphthalene on cytochrome oxidase activity. *Bulletin of Environmental Contamination and Toxicology* **40**, 105-109.
- Harmon, H.J. and Sanborn, M.R. (1982) Effect of naphthalene on the respiration in heart mitochondria and intact cultured cells. *Environmental Research* **29**: 160-173.
- Harvey, R.G. (1991) Polycyclic aromatic hydrocarbons: chemistry and carcinogenicity. Cambridge University Press, Cambridge, Chapter 1.
- Klamer, H.J.C., Villerius, L.A., Roelsma, J., de Maagd, P.G.-J. and Opperhuizen, A. (1997) Genotoxicity testing using the Mutatox™ assay: evaluation of benzo[a]pyrene as a positive control. *Environmental Toxicology and Chemistry* **16**, 857-861.
- Kocan, R.M., Landolt, M.L., Bond, J. and Benditt, E.P. (1981) In vitro effects of some mutagens/carcinogens on cultured fish cells. *Archives of Environmental Contamination and Toxicology* **10**, 663-671.
- Lankowicz, J.R., Bevan, D.R. and Riemer, S.C. (1980) Transport of a carcinogen, benzo[a]pyrene, from particulates to lipid bilayers. *Biochimica et Biophysica Acta* **629**, 243-258.
- Lee, L.E.J., Clemons, J.H., Bechtel, D.G., Caldwell, S.J., Han, K-B., Pasitschniak-Arts, M., Mosser, D.D. and Bols, N.C. (1993) Development and characterization of a rainbow trout liver cell line expressing cytochrome P450-dependent monooxygenase activity. *Cell Biology and Toxicology* **9**, 279-294.
- Lee, R.F., Sauerheber, S. and Dobbs, G.H. (1972) Uptake, metabolism and discharge of polycyclic aromatic hydrocarbons by marine fish. *Marine Biology* **17**, 201-208.
- Löwik, C.W.G.M., Alblas, M.J., van de Ruit, M., Papapoulos, S.E. and van der Pluijm, G. (1993) Quantification of adherent and nonadherent cells cultured in 96-well plates using the supravital stain Neutral Red. *Analytical Biochemistry* **213**, 426-433.
- Mackay, D., Shiu, W.Y. and Ma, K.C. (1992) Illustrated handbook of physical-chemical properties and environmental fate for organic chemicals (2). Lewis Publishers, Chelsea, MI.
- McQueen, C.A. and Williams, G.M. (1982) Cytotoxicity of xenobiotics in adult rat hepatocytes in primary culture. *Fundamental and Applied Toxicology* **2**, 139-144.
- Muñoz, M.J. and Tarazona, J.V. (1993) Synergistic effect to two- and four component combinations of the polycyclic aromatic hydrocarbons: Phenanthrene, anthracene, naphthalene and acenaphthene on *Daphnia magna*. *Bulletin of Environmental Contamination and Toxicology* **50**, 363-368.

- Neff, J.M. (1985) Polycyclic aromatic hydrocarbons. In: *Fundamentals of aquatic toxicology*. G.M. Rand and S.R. Petrocelli (Eds), Hemisphere Publishing Corporation, Washington D.C., Chapter 14.
- Schirmer, K., Ganassin, R.C., Brubacher, J.L. and Bols, N.C. (1994) A DNA fluorometric assay for measuring fish cell proliferation in microplates with different well sizes. *Journal of Tissue Culture Methods* **16**, 133-142.
- Seeman, P. (1972) The membrane actions of anesthetics and tranquilizers. *Pharmacological Reviews* **24**, 583-655.
- Sikkema, J., de Bont, J.A.M. and Poolman, B. (1994) Interactions of cyclic hydrocarbons with biological membranes. *Journal of Biological Chemistry* **269**, 8022-8028.
- Smolarek, T.A., Morgan, S.L., Moynihan, C.G., Lee, H., Harvey, R.G. and Baird W.M. (1987) Metabolism and DNA adduct formation of benzo[a]pyrene and 7,12-dimethylbenz[a]anthracene in fish cell lines in culture. *Carcinogenesis* **8**, 1501-1509.
- Struble, V.G. and Harmon, H.J. (1983) Molecular basis for inhibition of mitochondrial respiration by naphthalene. *Bulletin of Environmental Contamination and Toxicology* **31**, 644-648.
- Upham, B.L., Masten, S.J., Lockwood, B.R. and Trosko, J.E. (1994) Nongenotoxic effects of polycyclic aromatic hydrocarbons and their ozonation by-products on the intercellular communication of rat liver epithelial cells. *Fundamental and Applied Toxicology* **23**, 470-475.
- Varanasi, U., Nishimoto, M., Baird, W.M. and Smolarek, T.A. (1989) Metabolic activation of PAHs in subcellular fractions and cell cultures from aquatic and terrestrial species. In: *Metabolism of polycyclic aromatic hydrocarbons in the aquatic environment*. U. Varanasi (Ed), CRC Press, Boca Raton, FL, Chapter 6.

CHAPTER 3

ABILITY OF 16 PRIORITY PAHs TO BE PHOTOCYTOTOXIC TO A CELL LINE FROM THE RAINBOW TROUT GILL ⁽¹⁾

3.1. ABSTRACT

Sixteen polycyclic aromatic hydrocarbons (PAHs) were screened for their ability to be photocytotoxic to a cell line from the rainbow trout gill, RTgill-W1. PAHs could be divided into one of 3 groups: incapable of being photocytotoxic, able to be photocytotoxic but also to be directly cytotoxic, or capable of only being photocytotoxic. Photocytotoxicity was distinct from direct cytotoxicity in that EC₅₀ values were lower with the neutral red assay immediately after the PAH/UV treatment than with alamar Blue or CFDA-AM, indicating a more specific action on lysosomes. As well, in photocytotoxicity but not in direct cytotoxicity, the three assays showed increased impairment 24 hr after the treatment. This is consistent with the contention that reactive oxygen species are involved in photocytotoxicity. Most PAHs were found to be strictly photocytotoxic; however, only six compounds were photocytotoxic at concentrations theoretically achievable in water. When photocytotoxic PAHs were ranked relative to fluoranthene to establish fluoranthene equivalent factors (FEFs), benzo[a]pyrene and benzo[g,h,i]perylene were found to be most potent. However, when the water solubility of each compound was taken into account in order to calculate the potential environmental photocytotoxic potency (PEPP), fluoranthene and pyrene appeared to have the most potential to impact fish through photocytotoxicity.

3.2. INTRODUCTION

The toxicity that arises from simultaneous exposure to polycyclic aromatic hydrocarbons (PAHs) and UV radiation has been studied in a number of aquatic organisms, including fish (Bowling et al., 1983; Kagan et al. 1987; Kagan et al., 1985; Oris and Giesy, 1985, 1986). In fish, the dorsal epidermis and the gill epithelium have been identified as target tissues of the photoinduced toxicity caused by anthracene and fluoranthene (Oris and Giesy, 1985, Weinstein et al., 1997), and the disruption of cell membranes has been proposed as the major cause (McCloskey

⁽¹⁾ This paper is for submission to Toxicology. Co-authors are A.G.J. Chan, B.M. Greenberg, D.G. Dixon and N.C. Bols

and Oris, 1993; Oris and Giesy, 1985). However, because determining the potential of other PAHs to be phototoxic is done more easily with fish cells in culture, we previously developed a methodology that allows environmentally important PAHs to be tested rapidly and inexpensively, using confluent cell cultures from the rainbow trout gill as a model system (Chapter 1).

Upon absorbing UV radiation, PAHs undergo photochemical reactions that involve the formation of singlet oxygen, free radicals and, potentially, photomodified PAH products (Arfsten, 1996; Foote, 1976; Girotti, 1983, Huang et al., 1995). The damaging or killing of cells that results from these photochemical reactions is defined as photocytotoxicity (Chapter 1; MacRobert et al., 1989). This is in contrast to PAHs eliciting a cytotoxic response rapidly in the absence of UV radiation which is referred to as direct cytotoxicity (Chapter 2).

Both photocytotoxicity and cytotoxicity can be monitored efficiently for various cellular endpoints using fluorescent indicator dyes that can be read with a fluorescent plate reader. Indicator dyes that have previously been used with fish cells are alamar Blue (metabolic activity), 5-carboxyfluorescein diacetate acetoxymethyl ester (CFDA-AM) (cell membrane integrity) and neutral red (lysosomal membrane integrity) for quantifying the cytotoxicity of PAHs (Chapter 2) and alamar Blue and CFDA-AM for measuring photocytotoxicity (Chapter 1). Thus, the neutral red assay has yet to be applied in studies on the photocytotoxicity of PAHs.

In this paper, we have used previously developed methodologies to demonstrate the potential of 16 priority PAHs to be photocytotoxic to the rainbow trout gill cell line, RTgill-W1. Our goals were three-fold. Firstly, we wanted to identify PAHs that are toxic in the presence of UV radiation, and secondly, compare how photocytotoxic PAHs affect different cellular endpoints either immediately after UV irradiation or 24 hr later. This involved exposing cells to individual PAHs and UV radiation, and applying the three fluorescent indicator dyes, alamar Blue, CFDA-AM and neutral red. Thirdly, we determined the photocytotoxic potencies of PAHs relative to fluoranthene. This required the calculation of EC_{50} values and resulted in the proposal of fluoranthene equivalent factors (FEFs) for photocytotoxicity. In addition, a second ranking value was calculated in order to indicate relative to fluoranthene the potential environmental photocytotoxic potency (PEPP) of each PAH.

3.3. MATERIALS AND METHODS

A. *Cell culture, cytotoxicity tests and assays*

The rainbow trout gill cell line, RTgill-W1, was developed in this laboratory (Bols et al., 1994). Cells were cultured in 75 cm² culture flasks at 22°C in Leibovitz's L-15 medium supplemented with 10 % fetal bovine serum (FBS). The source of the tissue culture supplies and a description of the subcultivation procedure have previously been presented in detail (Bols and Lee, 1994; Schirmer et al., 1994).

Confluent monolayers of RTgill-W1 cells in 48 well tissue culture plates were used to study the photoinduced cytotoxic effects of PAHs. Confluent cultures were achieved and cells dosed with the PAHs as described in Chapter 2. Immediately after the dosing, UV irradiation was performed as described below. As well as preparing plates for UV irradiation, control plates were prepared for exposure of cells in the dark. Fluoranthene was included as a positive control in most experiments because of its ability to be photocytotoxic to RTgill-W1 cells (Appendix III; Chapter 1).

Upon termination of the UV radiation exposure, cytotoxicity assays were performed immediately and 24 hr later. Three cytotoxicity assays were used that are based on the fluorescent indicator dyes, alamar Blue, CFDA-AM and neutral red. A detailed description of the preparation and application of these dyes is given in Appendix IV and Chapter 2. All cell cultures received L-15 with 10 % FBS in the 24 hr between the assays.

B. *UV radiation exposure*

After the cells had been dosed and before the cytotoxicity assays were carried out, UV radiation was applied to the cell monolayers. UV irradiation was done with one UV-A and one UV-B photoreactor lamp (Southern N.E. Ultraviolet Co., Branford, CT, USA). Cells were irradiated at room temperature in an atmosphere of air and in the presence of tissue culture plate lids as described previously (Chapter 1). Irradiation was measured frequently with an InstaSpecTMII photodiode array spectroradiometer calibrated with a 1 kW quartz halogen lamp (Oriel corporation, Stratford, CT, USA). With one UV-A and one UV-B lamp, and varying distances between the radiation source and the tissue culture plates, the photon fluence rate was adjusted to 10 $\mu\text{mol m}^{-2} \text{s}^{-1}$ ($\pm 10 \%$) for UV-A and 1 $\mu\text{mol m}^{-2} \text{s}^{-1}$ ($\pm 6 \%$) for UV-B (Appendix II). These values represent the photon fluence rates at the surface of the medium in the wells. A 500 μl /well aliquot of L-15/ex had previously been shown to have little discernible effect on these fluence rates (Chapter 1). The duration of irradiation was 2 hr for all experiments.

The absorption by each PAH of the UV radiation emitted by the UV photoreactor lamps was calculated by multiplying the values of the UV emission- and PAH absorption-spectra at each wavelength and integrating the area under the resulting curve (Appendices I and II; Krylov et al., 1997). This integrated absorption value, which is designated J, was normalized for the largest absorption value, which was obtained for benzo[a]pyrene (Table 3.1.).

Table 3.1. Summary of photo-physical properties of PAHs

PAH	$J_{(norm)}^{(1)}$	$\Phi^{(2)}$
Naphthalene	0.023	0.80 ^(b)
Acenaphthylene	0.242	d.n.a. ^(c)
Acenaphthene	0.047	0.58 ^(b)
Fluorene	0.045	0.31 ^(a)
Phenanthrene	0.049	0.80 ^(a)
Anthracene	0.334	0.60 ^(a)
Fluoranthene	0.476	0.60 ^(a)
Pyrene	0.579	0.27 ^(a)
Benzo[a]anthracene	0.390	0.80 ^(a)
Chrysene	0.191	0.67 ^(a)
Benzo[b]fluoranthene	0.717	d.n.a. ^(c)
Benzo[k]fluoranthene	0.687	d.n.a. ^(c)
Benzo[a]pyrene	1.000	0.40 ^(a)
Dibenzo[a,h]anthracene	0.654	0.98 ^(b)
Benzo[g,h,i]perylene	0.788	0.60 ^(a)
Indeno[1,2,3-cd]pyrene	0.874	d.n.a. ^(c)

(1) $J_{(norm)}$ = Absorption of UV radiation by the PAH, normalized for benzo[a]pyrene

(2) Φ = quantum yield of triplet-state formation; values were obtained from available literature:

(a) Krylov et al., 1997

(b) Birks, 1970, pg. 251-253

(c) d.n.a. = data not available

C. Preparation of PAH solutions and HPLC analysis

PAHs were purchased in crystallized form and dissolved in 100 % dimethyl sulphoxide (DMSO, BDH Inc., Toronto, ON, Canada) as described previously (Chapter 2). The PAH stock solutions were serially diluted in DMSO to give 200 times the final concentration required by each design treatment. These working solutions were stored at room temperature, protected from light in 1.5 or 5 ml amber screw cap vials (Kimble, VWR Canlab, Mississauga, ON, Canada). A 2.5 μ l aliquot of these working solutions was added to 500 μ l of L-15/ex in wells of 48 well tissue culture plates prior to a UV radiation treatment to give the desired PAH concentrations. DMSO has

previously been shown to have a slightly sensitizing effect on cells in the presence of a UV radiation treatment (Chapter 1). However, for screening purposes, DMSO qualifies as a suitable solvent. In contrast to the previously introduced method of solubilizing fluoranthene in the absence of a carrier, DMSO required smaller volumes and allowed the preparation of a wider dose range for each of the PAHs tested.

The concentrations of PAHs in the working solutions were confirmed by HPLC as described in Chapter 2. Briefly, samples were prepared by adding 2.5 μ l working solution to a 500 μ l aliquot of 50 % HPLC-grade acetonitrile (BDH Inc., Toronto, ON, Canada) and 50 % Milli-Q filtered distilled water in 1.5 ml amber screw cap vials. HPLC was done with a System Gold liquid chromatograph with a System Gold 168 diode array detector and a Model 126 liquid chromatograph pump (Beckman Instruments Inc., Mississauga, ON, Canada). Aliquots of 100 μ l from sample solutions were loaded manually onto a 25 cm LC-18 column (Supelco, Mississauga, ON, Canada) and eluted/detected as described (Chapter 2).

D. Data analysis

The fluorescence readings in wells that contained PAHs in DMSO were expressed as a percentage of the readings in control wells that contained DMSO only. Prior to these calculations, fluorescence readings for wells without cells were subtracted from the experimental and control values with cells. Dose-response data followed a sigmoid relationship and were analyzed by nonlinear regression using the curve-fitting routine of SigmaPlot (Jandel Scientific). Data were fitted to the logistic function as described previously (Chapter 2). The logistic function was

$$(1) \quad y(d) = 100 (\%) \{1 + \exp[-g(\ln(d) - \ln(EC_{50}))]\}^{-1},$$

where $y(d)$ is the % cell viability at the PAH concentration d , g is a slope parameter, and EC_{50} is the PAH concentration that produces 50 % cell viability.

All statistical tests were performed using SYSTAT™ software (SPSS Inc., 1996).

3.4. RESULTS

The response of RTgill-W1 cells to PAH/UV treatments allowed the sixteen priority PAHs to be divided into three basic groups. Under the conditions of the assays, PAHs were either incapable of being photocytotoxic, able to be both photocytotoxic and directly cytotoxic, or capable of only being photocytotoxic.

A. *Non-photocytotoxic PAHs*

Three PAHs showed no photocytotoxicity. For naphthalene and fluorene, this was judged from the similarities of dose-response curves that were obtained after exposure for 2 hr in the dark or after 2 hr of UV irradiation (Figure 3.1.). For chrysene dose-response curves were not obtained for either treatment, even when chrysene was tested at concentrations that exceeded its water solubility limit by approximately 25 times (Figure 3.2.).

B. *Photocytotoxic and cytotoxic PAHs*

Acenaphthylene, acenaphthene and phenanthrene, which were previously found to be cytotoxic (Chapter 2), also showed some photocytotoxicity. This was judged from dose-response curves that were shifted towards lower PAH concentrations in the presence of UV radiation (Figure 3.3.). Unlike cytotoxicity, photocytotoxicity was measurable immediately after UV exposure only with the neutral red assay. In the measurements that were taken 24 hr later, photocytotoxicity was detected with the alamar Blue and CFDA-AM indicator dyes and dose-response curves were similar to those obtained with the neutral red assay either immediately or 24 hr after UV irradiation (Figure 3.3.). When EC_{50} s for either of the three cytotoxicity assays were compared by analysis of variance, followed by Tukey's post hoc test ($\alpha = 0.05$), the rank order for photocytotoxicity was similar to that for cytotoxicity with acenaphthylene \cong acenaphthene $>$ phenanthrene.

C. *Strictly photocytotoxic PAHs*

The majority of the PAHs was found to be only photocytotoxic (Tables 3.2. and 3.3.). These PAHs could be divided into two groups.

The first group consisted of PAHs that were photocytotoxic only at relatively high concentrations (Figure 3.4). As estimated from dose-response data, benzo[k]fluoranthene and indeno[1,2,3-cd]pyrene elicited no toxicity at concentrations at which these compounds are

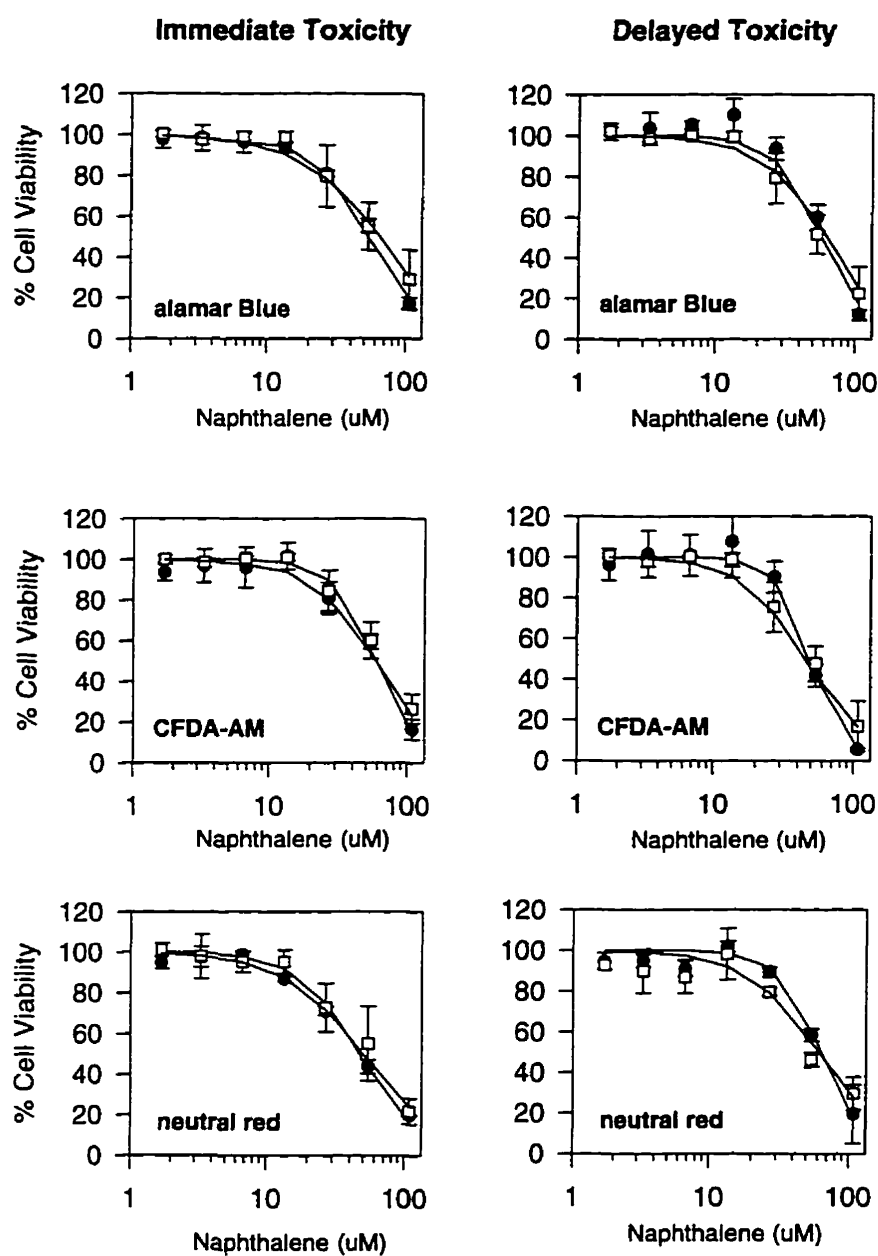


Figure 3.1. Viability of RTgill-W1 cells after being exposed to increasing concentrations of naphthalene in the presence or absence of UV radiation. Confluent cultures were exposed to naphthalene in L-15/ex and either kept in the dark (●) or simultaneously UV irradiated for 2 hr (□). Immediately afterwards and 24 hr later, cell viability was assayed with a mixture of alamar Blue (top panels) and CFDA-AM (middle panels), as well as with neutral red (bottom panels). The results were expressed as a percentage of the readings in control cultures that received the appropriate dark or UV treatment but no naphthalene. One representative experiment is shown. Each data point is the mean of four culture wells with the vertical lines indicating the standard deviation. Similar relative dose-response curves were obtained for fluorene.

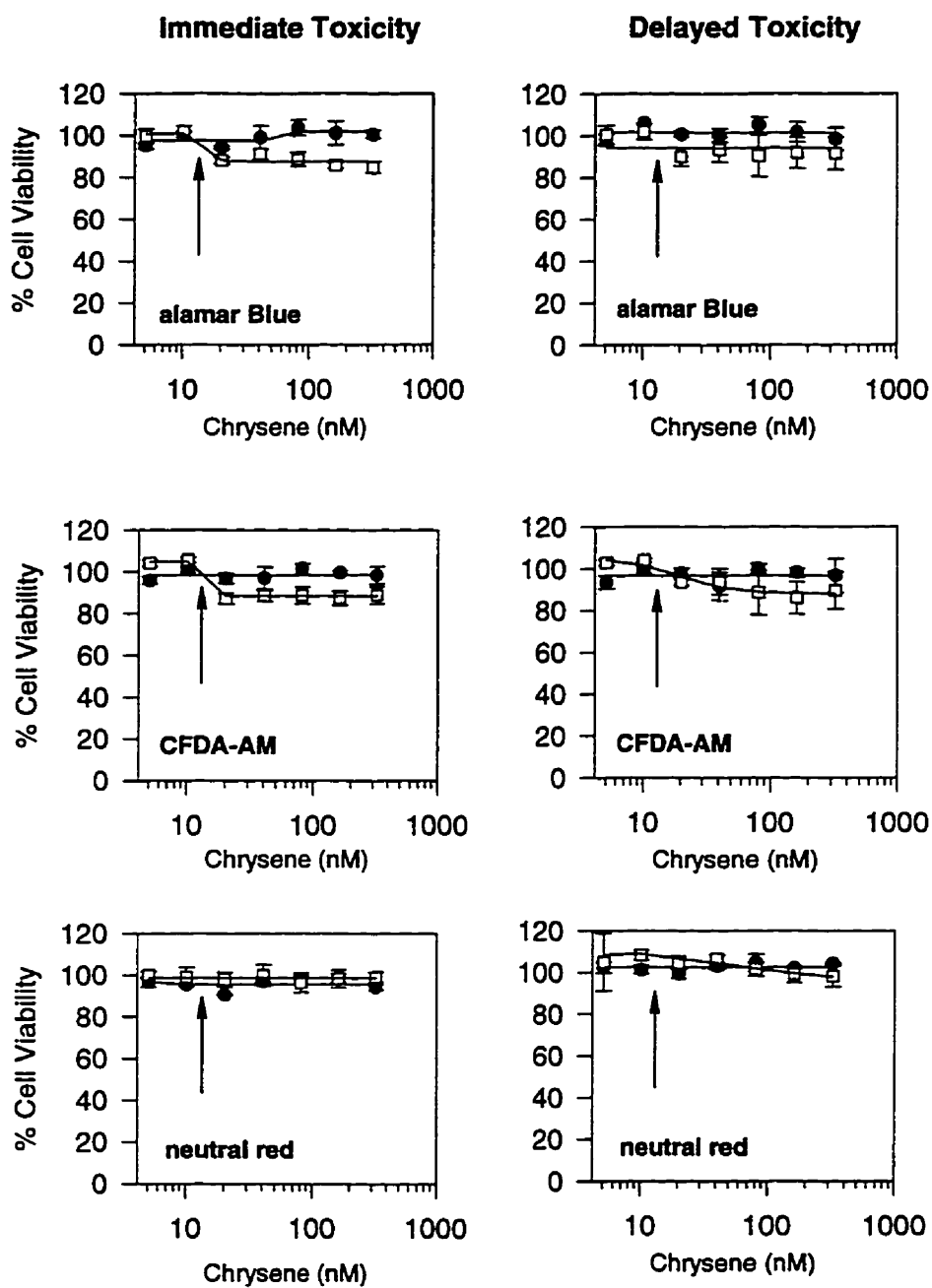


Figure 3.2. Viability of RTgill-W1 cells immediately and 24 hr after being exposed to increasing concentrations of chrysenes in the presence (□) or absence (●) of UV radiation. Exposure of cell cultures to chrysenes and subsequent cell viability assays were performed as described in Figure 3.1.. One representative experiment is shown. Each data point is the mean of four culture wells with the vertical lines indicating the standard deviation. The arrows indicate the concentration at which chrysenes is maximally soluble in water (13nM).

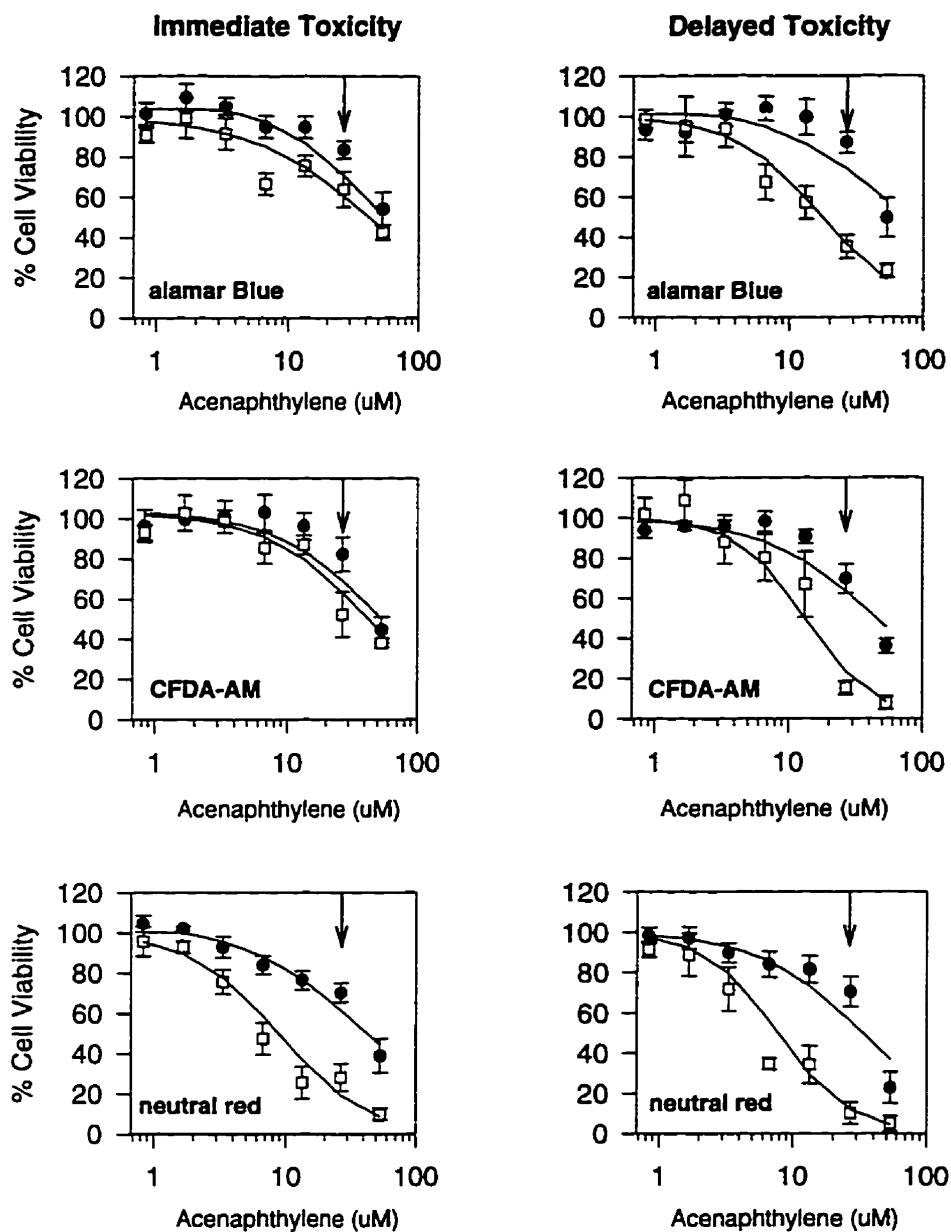


Figure 3.3. Viability of RTgill-W1 cells immediately and 24 hr after being exposed to increasing concentrations of acenaphthylene in the presence (□) or absence (●) of UV radiation. Exposure of cell cultures to acenaphthylene and subsequent cell viability assays were performed as described in Figure 3.1.. One representative experiment is shown. Each data point is the mean of four culture wells with the vertical lines indicating the standard deviation. The arrows indicate the concentration at which acenaphthylene is maximally soluble in water (26 μ M). Similar relative dose-response curves were obtained for acenaphthene and phenanthrene.

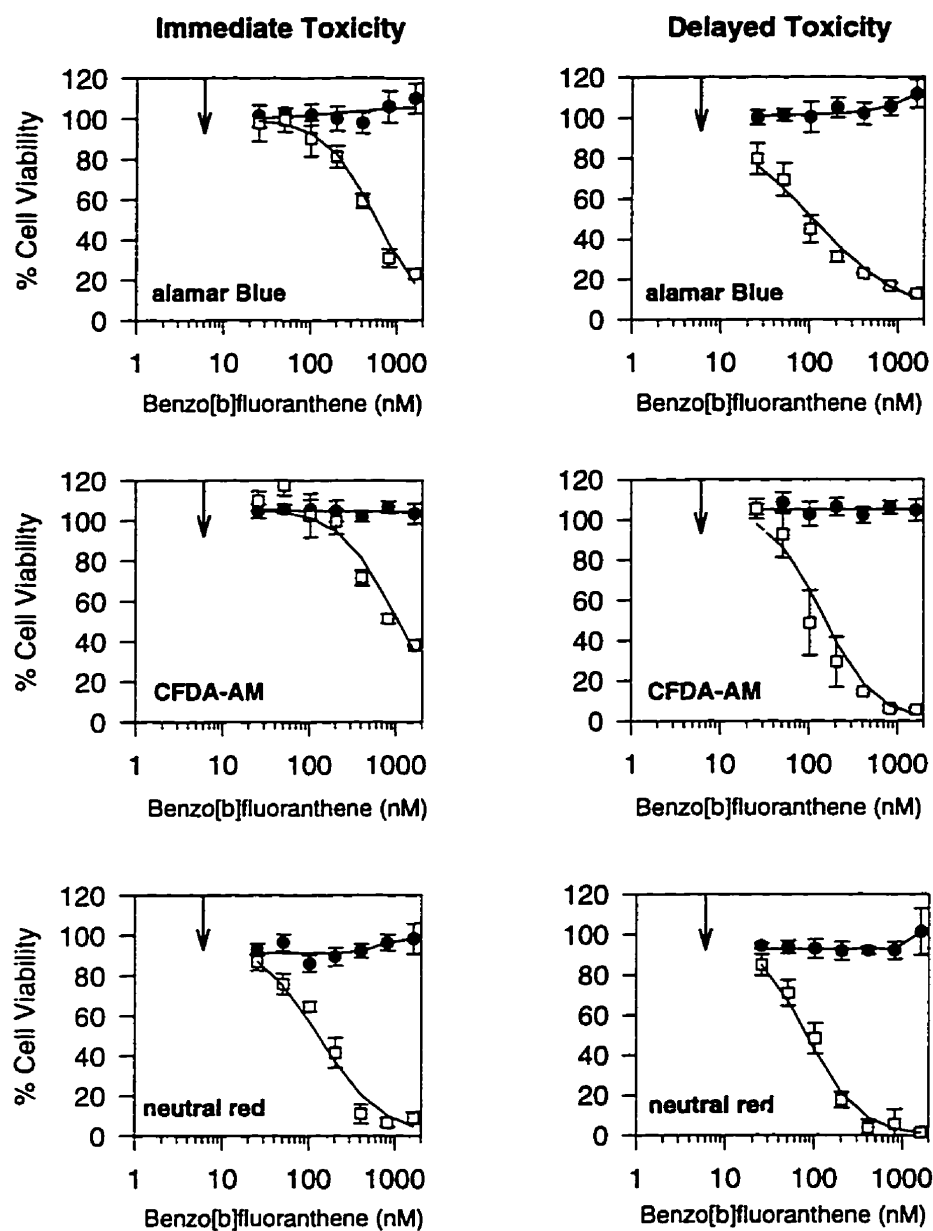


Figure 3.4. Viability of RTgill-W1 cells immediately and 24 hr after being exposed to increasing concentrations of benzo[b]fluoranthene in the presence (□) or absence (●) of UV radiation. Exposure of cell cultures to benzo[b]fluoranthene and subsequent cell viability assays were performed as described in Figure 3.1.. One representative experiment is shown. Each data point is the mean of four culture wells with the vertical lines indicating the standard deviation. The arrows indicate the concentration at which benzo[b]fluoranthene is maximally soluble in water (6 nM).

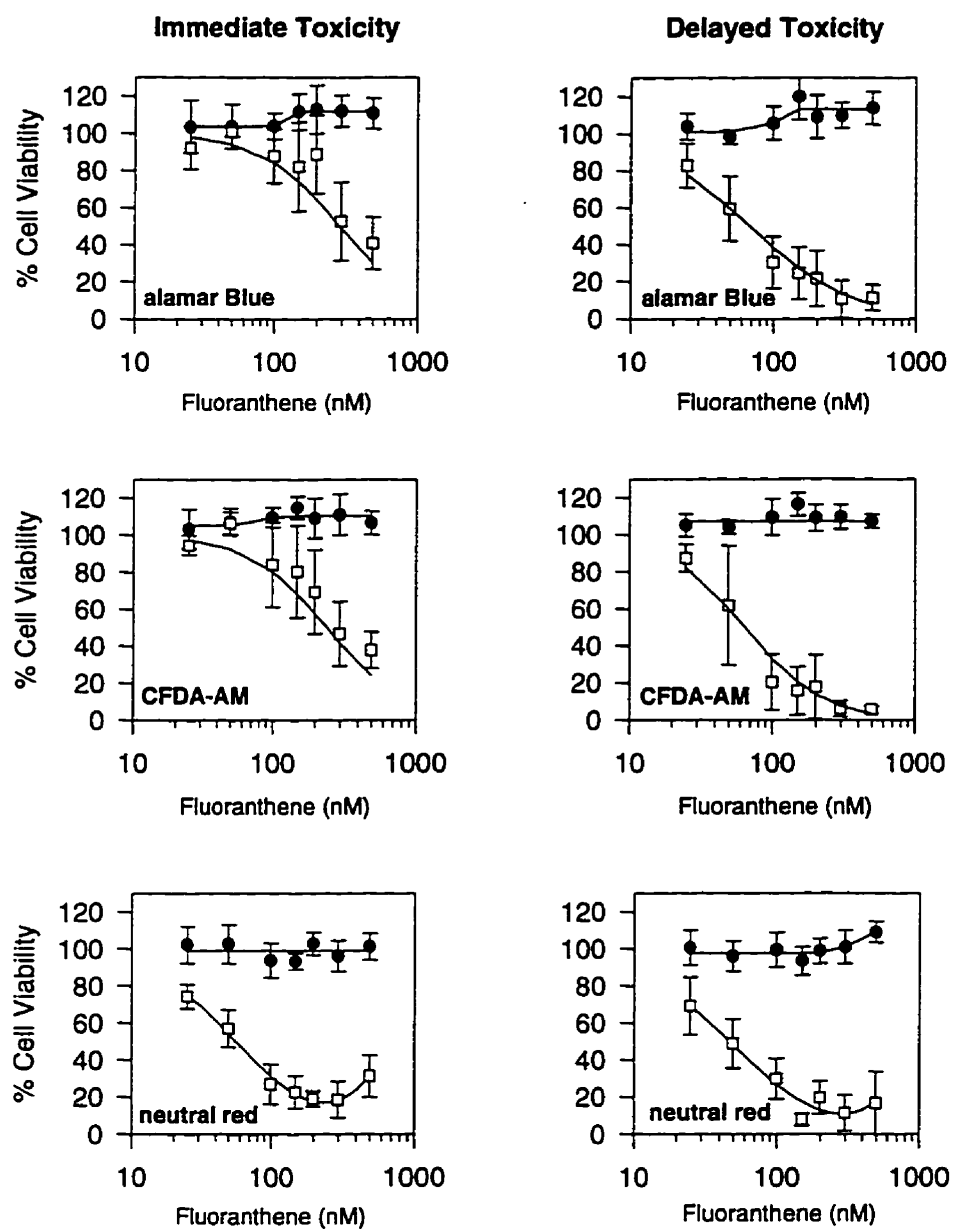


Figure 3.5. Viability of RTgill-W1 cells immediately and 24 hr after being exposed to increasing concentrations of fluoranthene in the presence (□) or absence (●) of UV radiation. Exposure of cell cultures to fluoranthene and subsequent cell viability assays were performed as described in Figure 3.1.. The data points represent the mean of 5 independent experiments in which fluoranthene served as a positive control. The vertical lines indicate the standard deviation.

maximally soluble in water. For benzo[b]fluoranthene and dibenzo[a,h]anthracene, cell viability was decreased by less than 10 % at their respective water solubility limits in the assays that were performed 24 hr after UV irradiation. EC_{50} values, which were lowest in the assays 24 hr after UV exposure, ranged from approximately 14-23 times above water solubility for benzo[b]fluoranthene, 50-72 times for benzo[k]fluoranthene, and 57-89 and 144-163 times above water solubility for, respectively, dibenzo[a,h]anthracene and indeno[1,2,3-cd]pyrene. At these high concentrations, PAHs are likely present in the culture medium in microcrystalline form, which potentially affects their UV absorption and uptake characteristics (Lakowicz et al., 1980; Weinberger and Cline Love, 1984). Therefore, the toxicity that was observed for benzo[k]fluoranthene, benzo[b]fluoranthene, dibenzo[a,h]anthracene and indeno[1,2,3-cd]pyrene likely was governed by factors more complex than those present for the second group of photocytotoxic PAHs.

This second group consisted of PAHs that were photocytotoxic at concentrations below the concentrations which these compounds could theoretically achieve in water (Figure 3.5.; Table 3.2.). In the presence of UV radiation, fluoranthene, pyrene, anthracene, benzo[a]pyrene, benzo[a]anthracene, and benzo[g,h,i]perylene caused the cellular activities of all three assays to be impaired immediately after UV exposure. However, the degree of impairment differed between the assays. As judged from the EC_{50} values, neutral red was found to be the most sensitive measure of photocytotoxicity immediately after concurrent UV irradiation and exposure to any one of the six PAHs (Table 3.2.). For an individual PAH, the EC_{50} s obtained in the alamar Blue and the CFDA-AM assays were very similar. In the assays that were performed 24 hr later, all three fluorescent indicator dyes gave similar EC_{50} values (Table 3.2.). Furthermore, when EC_{50} values for the immediate and 24 hr assays were compared for each of the three dyes, it was found that in all cases alamar Blue and CFDA-AM EC_{50} s decreased significantly over the 24 hr period, whereas neutral red EC_{50} s did not, with one exception: benzo[a]pyrene. Finally, slightly U-or L-shaped dose-response curves were obtained in the neutral red assay with fluoranthene, pyrene, benzo[g,h,i]perylene (Figures 3.5. and 3.6.), and in a few cases for benzo[a]pyrene (data not shown).

D. Photocytotoxicity rankings relative to fluoranthene

For the PAHs that were identified as photocytotoxic to RTgill-W1 cells, relative photocytotoxic potencies were calculated in two ways. Fluoranthene was chosen as a reference compound because it is an ubiquitous environmental contaminant (Ankley et al., 1994) and because it was phototoxic in this and a previous study with fish cells at concentrations well below its water solubility limit (Chapter 1). Calculations were based on the mean of the mean EC_{50} values for the three assays at 24 hr after UV irradiation. These

values were used because they were similar for all three indicator dyes and comparable to the EC_{50} values obtained for the neutral red assay 2 hr after UV irradiation, which was the most sensitive indicator of immediate photocytotoxicity (Table 3.2.). A fluoranthene equivalent factor (FEF) ranked a PAH according to its relative toxicity at concentrations equimolar to fluoranthene and was calculated by dividing the EC_{50} for fluoranthene by the EC_{50} for the PAH. In addition to FEFs, another ranking value was calculated in order to indicate relative to fluoranthene the potential environmental photocytotoxic potency (PEPP) of a PAH. A PEPP incorporated the photocytotoxicity of a PAH together with its highest possible concentration in aquatic environments and was calculated by dividing the water solubility to EC_{50} ratio for a PAH by the water solubility to EC_{50} ratio for fluoranthene. As the UV exposures and toxicity assays were carried out in this report, benzo[a]pyrene was the most photocytotoxic PAH (Table 3.3., FEF) but fluoranthene was the PAH most likely to occur in the environment at concentrations at which photocytotoxicity could occur (Table 3.3., PEPP).

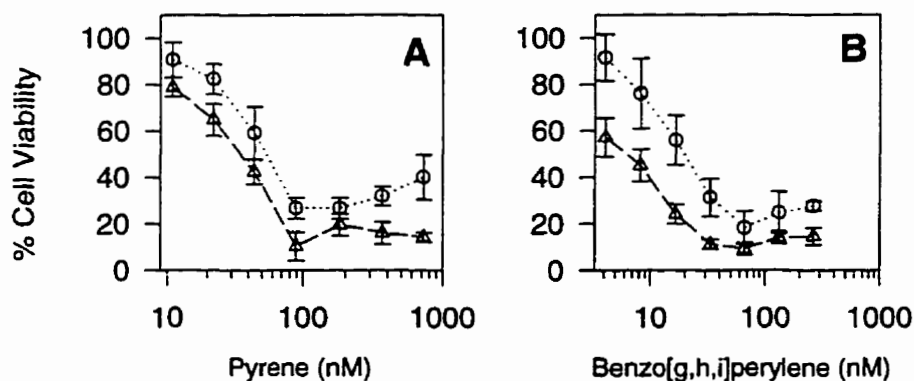


Figure 3.6. Viability of RTgill-W1 cells immediately (O) and 24 hr (Δ) after being simultaneously exposed for 2 hr to UV radiation and increasing concentrations of pyrene (panel A) and benzo[g,h,i]perylene (panel B), and as measured with the neutral red assay. Exposures of cell cultures to pyrene and benzo[g,h,i]perylene, followed by the neutral red assay were performed as described in Figure 3.1.. One representative experiment is shown for each compound. Each data point is the mean of four culture wells with the vertical lines indicating the standard deviation.

Table 3.2. EC₅₀ values for PAHs that were photocytotoxic but not directly cytotoxic to RTgill-W1 cells at concentrations below water solubility



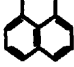
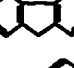
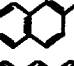
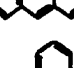
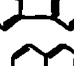
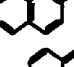
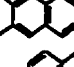
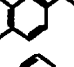
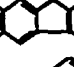
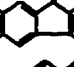
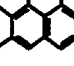
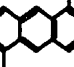


PAH	EC _{50s} (nM) 2 hr after UV irradiation			EC _{50s} (nM) 24 hr after UV irradiation		
	alamar Blue	CFDA-AM	neutral red	alamar Blue	CFDA-AM	neutral red
benzo[a]pyrene	56 ± 23 n=5	66 ± 24 n=5	30 ± 11* n=5	10 ± 5* n=4	12 ± 6* n=4	10 ± 4* n=2
benzo[g,h,i]perylene	253 ± 35 n=3	201 ± 34 n=3	37 ± 20** n=4	14 ± 8* n=4	11 ± 4* n=4	10 ± 8 n=3
benzo[a]anthracene	69 ± 21 n=4	87 ± 35 n=4	58 ± 23 n=3	30 ± 24* n=4	23 ± 16* n=4	30 ± 23 n=2
anthracene	201 ± 72 n=5	238 ± 110 n=4	67 ± 22** n=4	58 ± 23* n=5	45 ± 24* n=5	45 ± 4 n=3
pyrene	184 ± 31 n=2	204 ± 6 n=2	71 ± 13** n=2	61 ± 25* n=3	44 ± 15* n=3	60 ± 39 n=2
fluoranthene	255 ± 55 n=9	225 ± 44 n=13	84 ± 33** n=10	102 ± 45* n=18	92 ± 40* n=17	84 ± 39 n=17

* EC₅₀ value obtained for neutral red was significantly lower than EC₅₀ value for CFDA-AM 2 hr after UV irradiation (Tukey's test; $\alpha = 0.025$)

** EC₅₀ value obtained for neutral red was significantly lower than EC₅₀ values for CFDA-AM and alamar Blue 2 hr after UV irradiation (Tukey's test; $\alpha = 0.025$)

◆ EC₅₀ values obtained 24 hr after UV irradiation were significantly lower than EC₅₀ values for the same cellular endpoint 2 hr after UV irradiation (Student's t-test; $\alpha = 0.05$)

Table 3.3. EC₅₀ values for the photocytotoxicity of PAHs and their potencies relative to fluoranthene

PAH	Molecular Structure	W.S. (nM) ⁽¹⁾	EC ₅₀ (nM) ⁽²⁾	W.S./EC ₅₀ ⁽⁵⁾	PEPP ⁽³⁾	FEF ⁽⁴⁾
Naphthalene		240 x 10 ³	none	n.a. ⁽⁵⁾	n.a.	n.a.
Acenaphthylene		26 x 10 ³	24 x 10 ³ ⁽⁶⁾	1.1	0.078	0.003 800
Acenaphthene		23 x 10 ³	26 x 10 ³ ⁽⁶⁾	0.880	0.063	0.003 600
Fluorene		12 x 10 ³	none	n.a.	n.a.	n.a.
Phenanthrene		7 000	54 x 10 ³ ⁽⁶⁾	0.130	0.009	0.001 700
Anthracene		409	49	8.3	0.593	1.898
Fluoranthene		1 285	93	14	1.000	1.000
Pyrene		667	55	12	0.857	1.691
Benzo[a]anthracene		48	28	1.7	0.121	3.321
Chrysene		13	none	n.a.	n.a.	n.a.
Benzo[b]fluoranthene		6.0	111	0.054	0.004	0.838
Benzo[k]fluoranthene		3.0	184	0.016	0.001	0.505
Benzo[a]pyrene		16	11	1.5	0.107	8.454
Dibenzo[a,h]anthracene		1.8	132	0.014	0.001	0.704
Benzo[g,h,i]perylene		20	12	1.7	0.121	7.750
Indeno[1,2,3-cd]pyrene		0.7	176	0.004	0.000 280	0.528

(1) W.S. = Water solubility; Source: Mackay et al., 1992

(2) EC₅₀ values were calculated as the mean of the mean EC₅₀ values obtained for each fluorescent indicator dye 24 hr after UV irradiation.

(3) PEPP = potential environmental photocytotoxic potency ($(W.S./EC_{50(PAH)}) / (W.S./EC_{50(Fluoranthene)})$).

(4) FEF = Fluoranthene equivalent factor ($EC_{50(Fluoranthene)} / EC_{50(PAH)}$).

(5) n.a. = not applicable

(6) Toxicity is partly due to cytotoxicity.

3.5. DISCUSSION

Most of the priority PAHs were photocytotoxic, and the ability to be photocytotoxic appeared to depend on the proper combination of photochemical and solubility properties. Photocytotoxicity appeared to correlate with the PAHs' photochemical properties that others have identified as favoring the formation of the triplet excited state and singlet oxygen (Foote, 1976; MacRobert et al., 1989). One photochemical property is the absorption of UV radiation which varies among PAHs and can be quantified by the overlap of the absorption spectrum of each compound and the spectrum of the UV radiation source (Huang et al., 1997; Krylov et al., 1997). Secondly, PAHs differ in their ability to undergo the conversion from the singlet excited state to the longer-lived triplet excited state. This photochemical property is commonly expressed as the triplet state quantum yield (Φ) (MacRobert et al., 1989), and values for Φ can be obtained from the literature (Birks, 1970; Krylov et al., 1997). Naphthalene and fluorene showed the least overlap of their respective absorption spectra with that of the UV-radiation source and were not photocytotoxic. Benzo[a]pyrene showed the greatest overlap and was most photocytotoxic as judged from the EC_{50} values. Acenaphthene and phenanthrene showed an overlap similar to that of fluorene but their triplet state quantum yields are much higher than that of fluorene. Chrysene showed a different behavior. Although intermediate between phenanthrene and anthracene in absorption and triplet state quantum yield, it is not photocytotoxic. Therefore, an additional factor to be considered is the ability of PAHs to accumulate at critical cellular sites, which we have argued previously are cell membranes (Chapters 1 and 2). Thus, additional properties influencing the ability of a PAH to be photocytotoxic are water solubility and lipophilicity (Chapter 2). Consequently, it is likely that chrysene did not accumulate in cells sufficiently to elicit a photocytotoxic response.

Although the occurrence of additional mechanisms working at different levels and having different degrees of specificity is possible, the general mechanism behind the photocytotoxicity of the PAHs appears to be the impairment of membranes generally. This is because the three assays of cellular viability indirectly measure the maintenance of membrane integrity and gave broadly similar results. In this way the photocytotoxicity of PAHs is similar to the direct cytotoxicity of PAHs (Chapter 2). Yet, one important observation shows that the origins of the impairment are different between the two modes of toxicity. Most of the PAHs that are photocytotoxic are not directly cytotoxic. However, in the presence of UV radiation, these photocytotoxic PAHs have properties that would be expected to lead to the formation of reactive oxygen species (ROS). ROS can damage membranes, and therefore, are the likely cause of membrane impairment in photocytotoxicity (Valenzo, 1987).

In addition to a general mechanism of damage, a more specific action on lysosomes appears to contribute to photocytotoxicity. This is suggested by the neutral red assay, which measures the

uptake and retention of the dye in lysosomes (Babich and Borenfreund, 1992). With acenaphthylene, acenaphthene and phenanthrene, only the neutral red assay detected photocytotoxicity immediately after the PAH/UV treatments. When all three assays of cellular viability were performed immediately after concurrent PAH and UV treatments, the EC_{50} s were lower with the neutral red assay than with the other two assays. This means that at some PAH concentrations significant lysosomal damage was occurring while mitochondrial activity and plasma membrane integrity was being maintained as normal. The greater sensitivity of lysosomes was likely due to the specific accumulation of PAHs in this organelle. Preferential PAH accumulation in lysosomes has been found to occur in animal cells generally (Allison and Mallucci, 1964; Kocan et al., 1983) and would cause lysosomal damage to occur at lower nominal concentrations.

The specific action on the lysosome was not apparent twenty four hours after termination of the PAH/UV treatment. At this time the neutral red assay gave very similar results to the CFDA-AM and alamar Blue assays. This means that after the PAH/UV treatments had ended, impairment of mitochondrial activity and plasma membrane integrity continued more rapidly than damage to lysosomes. Two very different scenarios can be advanced to explain this. One possibility is that early damage to lysosomes caused the release of lysosomal enzymes which during the next 24 hr caused further damage to mitochondria and plasma membranes more so than impairment to lysosomes. This is reminiscent of a proposal by Allison et al. (1966). An alternative mechanism is that lysosomes can slow down the formation of ROS better than other cellular sites. Once initiated, the generation of ROS proceeds in a cascade fashion unless disrupted by protective cellular actions, such as vitamin E (Halliwell and Gutteridge, 1985). ROS formation might overwhelm any local protective actions in mitochondria and plasma membranes and cause damage to continue at these sites after termination of the PAH/UV treatments, while in the lysosome damage due to ROS would be slowed down or halted. In support of this idea, rat liver lysosomal membranes have been shown to have much higher vitamin E (α -tocopherol) levels than mitochondrial membranes and microsomes (Rupar et al., 1992).

Several PAHs among the photocytotoxic PAHs appeared to differ in the manner or extent to which they acted at the lysosome. This was seen by comparing the results from neutral red assays that had been done immediately after the termination of the concurrent exposure to UV/PAH and 24 hr later. Fluoranthene and B[a]P most clearly showed contrasting behavior. With fluoranthene, the neutral red assay showed little change between the two time periods, although alamar Blue and CFDA-AM assays indicated more damage at 24 hr than at 2 hr. By contrast, with B[a]P, the neutral red assay indicated more damage at 24 hr than at 2 hr, as did the other two assays. In mollusc, the isomeric PAHs phenanthrene and anthracene have been observed to act differently in their interaction with lysosomes (Nott and Moore, 1987). Perhaps, specific features of the

lysosomal membrane could account for some PAHs having a unique action on the lysosome in addition to a more general one.

In the neutral red assay, an additional difference was observed between the photocytotoxic PAHs and might be accounted for by the differential formation of excimers. At high concentrations of some PAHs, increasing photocytotoxicity was not observed with increasing concentration of PAH, resulting in a dose-response curve with a U-or L-shape. This was observed for pyrene, benzo[g,h,i]perylene, fluoranthene and, less frequently and to a smaller extent, for benzo[a]pyrene. Previously, U-shaped dose-response curves were observed for the phototoxicity of pyrene to the fathead minnow, and excimer formation was thought to be the cause (Kagan et al., 1987). At high concentrations several PAHs form excimers, which are complexes of an electronically excited and a ground state molecule (Birks, 1970, Turro, 1978). Excimers have reduced phototoxic potential because they have less capacity to facilitate photochemical reactions (Kagan et al., 1987). For instance, excimers simultaneously involve two PAH molecules and the energy of the excimer singlet excited state is lower than that of the monomeric PAH molecule in the same state (Turro, 1978). As well, both the quantum yield and the lifetime of excimer triplet excited states are diminished (Birk, 1970). The occurrence of U-shaped dose-response curves only in the neutral red assay, which preferentially measures lysosomal impairment, might be due to PAH concentrations being higher, and in turn, excimer formation being greater in the lysosome. The failure of other photocytotoxic PAHs to show U-shaped dose-response curves in the neutral red assay has several different explanations. For anthracene, this result would be expected because with this PAH others were unable to detect excimer formation in the presence of oxygen (Birks, 1970; Weinberger and Cline Love, 1984). As well, both anthracene and benzo[a]anthracene are among the PAHs with the shortest half-life in the presence of oxygen and UV radiation (Huang et al., 1997; Mackay et al., 1992). Therefore, their concentrations in lysosomes likely were too low to lead to excimers. For the PAHs that showed photocytotoxicity only at concentrations above their water solubility, a change in their dose-response curves at high concentrations was difficult to observe because the curves were incomplete and/or showed rather shallow negative slopes. However, due to the high concentrations necessary to elicit any toxic response with these compounds, the formation of molecule aggregates cannot be ruled out.

The three assays of cellular viability emphasized differences between photocytotoxicity and direct cytotoxicity. In direct cytotoxicity but not photocytotoxicity, the neutral red assay always gave the same result as the other two assays. This suggests that specific lysosomal effects are not part of the directly cytotoxic mechanism. In direct cytotoxicity but not photocytotoxicity, the three assays showed the same level of impairment 24 hr after the PAH treatments as immediately afterwards (Chapter 2). This observation is consistent with the contention that ROS are involved in photocytotoxicity but not in direct cytotoxicity.

Of the sixteen priority PAHs, thirteen were photocytotoxic, but only two appear to have the potential to impact on fish in the environment through photocytotoxicity. The most restrictive factor is availability in the water column, which is influenced by water solubility. Water solubility reduces the consideration from thirteen to eight PAHs: acenaphthylene, acenaphthene, anthracene, fluoranthene, pyrene, benzo[a]anthracene, benzo[a]pyrene and benzo[g,h,i]perylene. These are the PAHs that showed significant photocytotoxicity at concentrations at or below their water solubility. Among these, the EC_{50} s of the PAHs varied greatly with respect to their water solubility limit, and only fluoranthene and pyrene had EC_{50} s much lower than their water solubility. The other six had EC_{50} values that were too close to their maximum water solubility to likely have an environmental impact, except at exceptional point sources. For example, benzo[a]pyrene was most photocytotoxic (FEF=8.454) but its EC_{50} value was close to its maximum solubility in water. This was in contrast to fluoranthene whose EC_{50} value was approximately 14 fold below its water solubility limit, making fluoranthene 10 times more likely to occur at photocytotoxic concentrations in the aquatic environment than benzo[a]pyrene (PEPP=0.107). An additional factor that limits availability in aquatic environments is stability. For example, anthracene has a half-life of only a few hours to days in UV-irradiated environments compared to weeks for fluoranthene (Mackay et al., 1992). Thus, although anthracene (FEF=1.898) was found to have approximately twice the photocytotoxic potency of fluoranthene in our study (FEF=1.000), it appears less likely to play a role as a photosensitizer in the environment.

An additional factor to consider in assessing the potential of PAHs to be photocytotoxic to fish is their ability to persist in the main target tissue, the gill. This has never been measured directly but two interrelated factors that might influence persistence are metabolism and accumulation of the PAH in fish. Metabolism would reduce the likelihood of persistence. On the other hand, accumulation of PAHs in fat depots would provide an endogenous PAH source that could supply the gill through a very small fraction of the PAH partitioning from fat into blood. Generally, PAHs are metabolized rapidly and fail to accumulate substantially in fish, but this generalization is based mostly on research with just B[a]P (Varanasi et al., 1989). How other PAHs would behave is unclear, but because mixed function oxygenases (MFOs) are critical to PAH metabolism, the inability to induce these enzymes likely would make metabolism slower and accumulation more likely. Fluoranthene and pyrene were noninducers or extremely poor inducers of MFOs in rainbow trout in vivo (Gerhart and Carlson, 1978) and in vitro (Bols, unpublished data), and thus, could persist in fish. Therefore, in the environment, fluoranthene and pyrene appear to be the PAHs with the most potential to impact on fish through photocytotoxicity.

3.6. ACKNOWLEDGMENTS

This research was supported by a Strategic Grant from the Natural Sciences and Engineering Research Council of Canada and by the Canadian Network of Toxicology Centers. K.S. received financial support through an Ontario Graduate Scholarship for international students.

3.7. REFERENCES

- Allison, A. C., Magnus, I. A. and Young, M. R. (1966) Role of lysosomes and of cell membranes in photosensitization. *Nature* **209**, 874-878.
- Allison, A.C. and Mallucci, L. (1964) Uptake of hydrocarbon carcinogens by lysosomes. *Nature* **203**, 1024-1027.
- Ankley, G. T., Collyard, S. A., Monson, P. D. and A., K. P. (1994) Influence of ultraviolet light on the toxicity of sediments contaminated with polycyclic aromatic hydrocarbons. *Environmental Toxicology and Chemistry* **13**, 1791-1796.
- Arfsten, D. P., Schaeffer, D. J. and Mulveny, D. C. (1996) The effects of near ultraviolet radiation on the toxic effects of polycyclic aromatic hydrocarbons on animals and plants: a review. *Ecotoxicology and Environmental Safety* **33**, 1-24.
- Babich, H. and Borenfreund, E. (1992) Neutral Red assay for toxicology in vitro. In: *In vitro methods of toxicology*, R.R. Watson (Ed), CRC Press, Boca Raton, 17, 237-251.
- Birks, J.B. (1970) *Photophysics of Aromatic Molecules*. Wiley, New York, NY, 251-253, 637; and Chapter 7.
- Bols, N.C., Barlian, A., Chirino-Trejo, S.J., Caldwell, S.J., Goegan, P. and Lee, L.E.J. (1994) Development of a cell line from primary cultures of rainbow trout, *Oncorhynchus mykiss* (Walbaum), gills. *Journal of Fish Diseases* **17**, 601-611.
- Bols, N.C. and Lee, L.E.J. (1994) Cell lines: availability, propagation and isolation. In: *Biochemistry and molecular biology of fishes*. P.W. Hochachka and T.P. Mommsen (Eds), Elsevier Science, Amsterdam, Vol. 3, 145-159.
- Bowling, J. W., Leversee, G. J., Landrum, P. F. and Giesy, J. P. (1983) Acute mortality of anthracene-contaminated fish exposed to sunlight. *Aquatic Toxicology* **3**, 79-90.
- Foote, C.S. (1976) Photosensitized Oxidation and Singlet Oxygen: Consequences in biological systems. In: *Free Radicals in Biology*. W.A. Pryor (Ed), Academic Press, New Yourk, NY, Vol. II, 85-133.
- Gerhart, EH and R.M. Carlson (1978) Hepatic mixed-function oxidase activity in rainbow trout exposed to several polycyclic aromatic compounds. *Environmental Research* **17**, 284-295.
- Girotti, A. W. (1983) Mechanisms of photosensitization. *Photochemistry and Photobiology* **38**, 745-751.
- Halliwell, B. and Gutteridge, J.M.C. (1985) Lipid peroxidation: a radical chain reaction. In: *Free radicals in biology and medicine*. Clarendon Press, Oxford, Chapter 4.
- Huang, X.D., Krylov, S.N., Ren, L., McConkey, B.J., Dixon, D.G. and Greenberg, B.M. (1997) Mechanistic QSAR model for the photoinduced toxicity of polycyclic aromatic hydrocarbons: II. An empirical model for the toxicity of 16 PAHs to the Duckweed *Lemna gibba* L. G-3. *Environmental Toxicology and Chemistry*, in press.

- Huang, X.D., Dixon, D.G. and Greenberg, B.M. (1995) Increased polycyclic aromatic hydrocarbon toxicity following their photomodification in natural sunlight: Impacts on the Duckweed *Lemna gibba* L. G-3. *Ecotoxicology and Environmental Safety* **32**, 194-200.
- Kagan, J., Kagan, E. D., Kagan, I. A., Kagan, P. A. and Quigley, S. (1985) The phototoxicity of non-carcinogenic polycyclic aromatic hydrocarbons in aquatic organisms. *Chemosphere* **14**, 1829-1834.
- Kagan, J., Sinnott, D. and Kagan, E. D. (1987) The toxicity of pyrene in the fish *Pimephales promelas*: synergism by piperonyl butoxide and by ultraviolet light. *Chemosphere* **16**, 2291-2298.
- Kocan, R. M., Chi, E. Y., Eriksen, N., Benditt, E. P. and Landolt, M. L. (1983) Sequestration and release of polycyclic aromatic hydrocarbons by vertebrate cells in vitro. *Environmental Mutagenesis* **5**, 643-656.
- Krylov, S.N., Huang, X-D., Zeiler, L.F., Dixon, D.G. and Greenberg, B.M. (1997) Mechanistic QSAR model for the photoinduced toxicity of polycyclic aromatic hydrocarbons: I. Physical model based on chemical kinetics in a two compartment system. *Environmental Toxicology and Chemistry*, in press.
- Lakowicz, J.R., Bevan, D.R. and Riemer, S.C. (1980) Transport of a carcinogen, benzo[a]pyrene, from particulates to lipid bilayers. *Biochimica et Biophysica Acta* **629**, 243-258.
- Mackay, D., Shiu, W.Y. and Ma, K.C. (1992) Illustrated handbook of physical-chemical properties and environmental fate for organic chemicals (2). Lewis Publishers, Chelsea, MI.
- MacRobert, A.J., Bown, S.G. and Phillips, D. (1989) What are the ideal photoproperties for a sensitizer? In: *Photosensitizing Compounds: their Chemistry, Biology and Clinical Use*, Ciba Foundation Symposium 146, Wiley-Interscience publication, Chichester, 4-16.
- McCloskey, J. T. and Oris, J. T. (1993) Effect of anthracene and solar ultraviolet radiation exposure on gill ATPase and selected hematologic measurements in the bluegill sunfish (*Lepomis macrochirus*). *Aquatic Toxicology* **24**, 207-218.
- Nott, J.A. and Moore, M.N. (1987) Effects of polycyclic aromatic hydrocarbons on molluscan lysosomes and endoplasmic reticulum. *Histochemical Journal* **19**: 357-368.
- Oris, J. T. and Giesy, J. P. (1986) Photoinduced toxicity of anthracene to juvenile bluegill sunfish (*Lepomis Macrochirus Rafinesque*): photoperiod effects and predictive hazard evaluation. *Environmental Toxicology and Chemistry* **5**, 761-768.
- Oris, J. T. and Giesy, J. P. (1985) The photoenhanced toxicity of anthracene to juvenile sunfish (*Lepomis* spp.). *Aquatic Toxicology* **6**, 133-146.
- Rupar, C.A., Albo, S. and Whitehall, J.D. (1992) Rat liver lysosome membranes are enriched in alpha-tocopherol. *Biochemistry and Cell Biology* **70**, 486-488.

- Schirmer, K., Ganassin, R.C., Brubacher, J.L. and Bols, N.C. (1994) A DNA fluorometric assay for measuring fish cell proliferation in microplates with different well sizes. *Journal of Tissue Culture Methods* **16**, 133-142.
- Turro, N.J. (1978) *Modern Molecular Photochemistry*. The Benjamin/Cummings Publishing Co., Menlo Park, CA, 135-146.
- Valenzo, D.P. (1987) Photomodification of biological membranes with emphasis on singlet oxygen mechanisms. *Photochemistry and Photobiology* **46**, 147-160.
- Varanasi, U., Stein, J.E. and Nisimoto M. (1989) Biotransformation and disposition of polycyclic aromatic hydrocarbons (PAH) in fish. In: *Metabolism of polycyclic aromatic hydrocarbons in the aquatic environment*. CRC Press, Boca Raton, FL, Chapter 4.
- Weinberger, R. and Cline Love, L. J. (1984) Luminescence properties of polycyclic aromatic hydrocarbons in colloidal or microcrystalline suspensions. *Spectrochimica Acta* **40A**, 49-55.
- Weinstein, J.E., Oris, J.T. and Taylor, D.H. (1997) An ultrastructural examination of the mode of UV-induced toxic action of fluoranthene in fathead minnows, *Pimephales promelas*. *Aquatic Toxicology*, in press.

CHAPTER 4

AN EVALUATION OF THE CYTOTOXICITY AND PHOTOCYTOTOXICITY OF INTACT AND PHOTOMODIFIED CREOSOTE THROUGH THE USE OF A RAINBOW TROUT GILL CELL LINE, RTgill-W1, AND TWO FLUORESCENT INDICATOR DYES, ALAMAR BLUE AND 5- CARBOXYFLUORESCIN DIACETATE ACETOXYMETHYL ESTER ⁽¹⁾

4.1. ABSTRACT

The influence of ultra violet (UV) irradiation on creosote toxicity was investigated with the rainbow trout gill cell line, RTgill-W1, and two indicator dyes: alamar Blue and 5-carboxyfluorescein diacetate acetoxymethyl ester (CFDA-AM). Respectively, these monitor metabolic activity and membrane integrity. After solubilization and chemical analysis, creosote was presented to cells in the dark to measure cytotoxicity or concurrently with UV irradiation to evaluate photocytotoxicity. As well, creosote was photomodified by two hours of UV irradiation prior to presentation to cells in the dark or together with UV. Cytotoxicity was detected only at high nominal creosote concentrations, but photocytotoxicity occurred at creosote concentrations 35 fold lower. All the aromatic hydrocarbons in creosote appeared to contribute to cytotoxicity, but photocytotoxicity was due only to the fluoranthene, pyrene, anthracene and benzo[a]anthracene of creosote. Photomodified creosote was much more cytotoxic than intact creosote and this difference was most pronounced in the alamar Blue assay. Likely, this was due to photomodification products that impaired the mitochondrial electron transport chain. Photomodified creosote was slightly less photocytotoxic than intact creosote. Overall these results indicate that UV irradiation potentially enhances the toxicity of creosote to fish in several different but significant ways.

4.2. INTRODUCTION

Despite the fact that the toxicity of selected polycyclic aromatic hydrocarbons (PAHs) in the presence of UV radiation had first been shown with cells in culture in 1935 (Lewis), UV radiation

⁽¹⁾ This paper is for submission to Environmental Toxicology and Chemistry. Co-authors are J.S. Herbrick, B.M. Greenberg, D.G. Dixon and N.C. Bols.

exposures have only recently been considered in the environmental risk analysis of PAHs. The pioneering work of Bowling and Giesy (1983) on the acute toxicity of UV-irradiated, anthracene-exposed sunfish was followed by the screening of PAHs in invertebrates (Ankley et al., 1997, Ankley et al., 1995; Newsted and Giesy, 1987) and plants (Huang et al., 1993; Huang et al., 1995; Ren et al., 1994). However, due to the costs involved, studies on the photoinduced toxicity of PAHs to fish are limited to only a few PAHs (Kagan et al., 1985; Oris and Giesy, 1986; 1987) and none on complex PAH mixtures.

Recently, a methodology was developed that allowed the testing and ranking of 16 priority PAHs rapidly and inexpensively for their direct and photoinduced toxicity to a cell line from the rainbow trout, RTgill-W1 (Chapter 1 to 3). This cell line was derived from a target tissue of photoinduced toxicity, the fish gill epithelium (Oris and Giesy, 1985; McCloskey, 1993; Weinstein et al., 1997) and thus can serve as a model system for the photoinduced toxic effects in fish. In this culture system, the rapid killing of cells by PAHs in the absence of UV radiation was designated direct cytotoxicity (Chapter 2), and was in contrast to the damaging or killing of cells due to photochemical reactions that followed the absorption of UV radiation by the PAH, which was termed photocytotoxicity (Chapters 1 and 3). The establishment of toxic potencies showed naphthalene to be most environmentally relevant for its direct cytotoxicity (Chapter 2), whereas fluoranthene and pyrene appeared to have the most potential to impact fish through photocytotoxicity (Chapter 3). These potencies should also be useful in predicting and/or explaining the cytotoxicity and photocytotoxicity of PAHs in mixture.

Although most previous studies on the UV-mediated toxic effects of PAHs have dealt with intact compounds, Greenberg and his group have shown that the UV-irradiation of PAH solutions prior to exposure to plants and bacteria also leads to a significant increase in toxicity (Huang et al., 1993, Huang et al., 1995; Mallakin et al., 1997; McConkey et al., 1997; Ren et al., 1994; Ren et al., 1996). This toxicity is apparently caused by PAH photomodification products which most commonly arise in large numbers from the direct chemical reaction of UV-irradiated PAHs with oxygen. Potentially, these photooxidation products can be toxic by themselves (McConkey et al., 1997) or by a concurrent UV radiation exposure (Huang et al., 1993; Mallakin et al., 1997). The toxicity of photooxidized PAH products has not yet been shown in fish or cultured fish cells but our previously developed RTgill-W1 bioassay has features that should make it suitable for not only detecting the cytotoxicity caused by these compounds but also for elucidating their potential different modes of toxic action. This is based on the use of the fluorescent indicator dyes, alamar Blue and 5-carboxyfluorescein diacetate acetoxymethyl ester (CFDA-AM), which measure, respectively, the metabolic activity and the membrane integrity of a cell. Thus, compounds that preferentially act on the electron transport chain will be detected specifically with alamar Blue, whereas the more general damage to membrane integrity will be measured with CFDA-AM.

The goal in this chapter is to apply the RTgill-W1 cell bioassay to a complex chemical mixture, creosote. Creosote was chosen because it is a widely used wood preservative and it can contain up to 85 % PAHs (Mueller et al., 1989). The study comprised three major steps. One was the solubilization of creosote in a modified cell culture medium without the use of a carrier solvent and the chemical analysis of the 16 priority PAHs and some additional hydrocarbons in the final creosote stock solution. This analysis allowed predictions of the cytotoxicity and photocytotoxicity of creosote, using previously established toxic equivalent factors, which summarized the relationships between the physical-chemical properties of PAHs and their toxicity (Chapters 2 and 3). The second step of this study was the application of the creosote solution to RTgill-W1 cells in the absence or presence of UV radiation and the measurement of the direct cytotoxicity and the photocytotoxicity of creosote using the fluorescent indicator dyes, alamar Blue and CFDA-AM. This procedure allowed the biological response of cells to creosote to be evaluated and compared to the predictions derived from the chemical analysis. Finally, the direct cytotoxicity and the photocytotoxicity of creosote that had been modified by a 2 hr UV irradiation in the absence of cells was studied.

4.3. MATERIALS AND METHODS

A. *Cell line and culture media*

The rainbow trout gill cell line, RTgill-W1, was developed in this laboratory (Bols et al., 1994). Cells were cultured in 75 cm² culture flasks at 22°C in Leibovitz's L-15 medium supplemented with 10 % fetal bovine serum (FBS). The source of the tissue culture supplies and a description of the subcultivation procedure have previously been presented in detail (Bols and Lee, 1994; Schirmer et al., 1994).

A modification of the basal medium, L-15, was used for exposure of cells to creosote and UV radiation. This was necessary because treatment of conventional growth media with UV radiation generates toxicants that appear to arise from UV modification of medium components such as vitamins and aromatic amino acids (Lorenzen et al., 1993; Stoien and Wang, 1974). A description of the constituents of the modified L-15 medium, which was designated L-15/ex, and preparation procedures have been outlined in Chapter I and Appendix IV.

B. *UV radiation exposure*

Cells were irradiated at room temperature in an atmosphere of air and in the presence of tissue culture plate lids as described in Chapter I. UV irradiation was done with two UV-B photoreactor lamps (Southern N.E. Ultraviolet Co., Branford, CT, USA) at a photon fluence rate of 1.4 μmol m⁻² s⁻¹ UV-B. As well as UV-B (290-320 nm), the UV-B lamps emitted some visible (400-700 nm) and some UV-A (320-400 nm) radiation. However, with a visible : UV-A : UV-B ratio of 5 : 1.5 : 1, the spectrum was well weighted toward its UV-B component. Irradiation was measured with an InstaSpecTMII photodiode array spectroradiometer calibrated with a 1 kW quartz halogen lamp (Oriental corporation, Stratford, CT, USA). The values represent the photon fluence rates at the surface of the medium in the wells. A 500 μl/well aliquot of L-15/ex had previously been shown to have little discernible effect on these fluence rates (Chapter 1). The duration of irradiation was 2 hr for all experiments.

C. *Preparation of creosote in L-15/ex*

Liquid phase creosote was provided by Carbochem Ltd (Mississauga, ON, Canada) and was found to have a density of approximately 1.0 g/ml. For application to cultured fish cells, creosote was dissolved in L-15/ex by a technique recommended by Tadokoro et al. (1991) for dissolving creosote in water. This technique facilitated the solubilization of creosote in a manner that closely

reflected the solubilization process in the environment. An aliquot of 70 μl (70 mg) liquid creosote was added to 1 liter of sterile L-15/ex in a sterilized amber glass storage bottle with a Teflon lined cap (VWR Canlab, Mississauga, ON, Canada) and a sterilized, Teflon-coated magnetic stirrer (VWR Canlab, Mississauga, ON, Canada). This nominal creosote concentration was chosen because at some creosote treatment and storage sites the maximum aqueous concentration of PAHs was in this range (Environment Canada, 1993). To fully protect the solution from light, the bottle was wrapped in aluminum. The solution was stirred at room temperature and the solubilization process monitored after stirring for 1 hr, 1 day, 3 days and 7 days. At the end of each stirring period, the solution was allowed to settle for 1 hr to allow undissolved particles to settle to the bottom of the bottle before an aliquot of 150 ml was carefully removed for application to cell cultures, and for extraction and chemical analysis.

D. Extraction and chemical analysis of creosote

Aliquots of 120 ml of creosote in L-15/ex were extracted as described by Bestari et al. (1997) with minor modifications. Briefly, the samples were extracted three times with methylene chloride (Fisher Scientific, Nepean, ON, Canada) and passed into an Erlenmeyer flask through a glass wool plugged funnel with a layer of sodium sulfate to facilitate the removal of water. The Erlenmeyer beaker was then swirled several times in the presence of sodium sulfate before the samples were passed through another glass wool plugged funnel into round-bottom flasks that contained a few glass beads. The methylene chloride was evaporated with a rotary evaporator at 28°C to concentrate the samples to approximately 5 ml, followed by a stream of nitrogen to achieve dryness. The samples were then re-extracted 5 times with 1 ml of methylene chloride and stored in 5 ml amber glass vials at -20°C until chemical analysis. Naphthalene and fluoranthene could be recovered from spiked samples to, respectively, 82 % and 90 %, which is similar to the recovery rates reported by Bestari et al. (1997). The deviations between two extractions of the same stock solution were less than 12 % for all compounds.

For chemical analysis, sample aliquots of 3 μl were injected into a Hewlett Packard 5890 Gas Chromatograph (GC) equipped with an HP7673A autosampler and Flame Ionization Detector (FID). The temperature was held at 35°C for 2 min, followed by a 15°C/min increase to 165°C, followed by a 30°C/min increase to 300°C and a constant temperature of 300°C for 10 min. The carrier gas was helium with a flow rate of 30 ml/min. The injector temperature of the GC was 200°C, and the FID temperature was 300°C. The deviations between repeated measurements of the same creosote sample were less than 10 % for all chemicals.

Chemical analysis focused on PAHs because they can account for 85 % of the compounds in creosote (Environment Canada, 1993; Mueller et al., 1989). However, a few other compounds

were analyzed as well. These included the heterocyclics dibenzofuran and carbazole, and the aromatic hydrocarbons benzene, toluene and xylene. The detection limits (d.l.) of the GC method for each of the compounds are given in Table 4.1.

E. Cytotoxicity and photocytotoxicity of creosote

Confluent monolayers of RTgill-W1 cells in 48 well tissue culture plates were used to study the cytotoxicity and photocytotoxicity of creosote. Confluent cultures were achieved by plating 50,000 cells per well and allowing them to grow for 3 days. At confluency, the culture medium was removed and each well rinsed once with 500 μ l of L-15/ex. After the rinse, all wells received increasing volumes of creosote in L-15/ex together with fresh L-15/ex to yield a total volume per well of 500 μ l. To determine cytotoxicity, cells were exposed to creosote for 6 hr in the dark before the alamar Blue and CFDA-AM cytotoxicity assays were carried out as described below. For photocytotoxicity, cells were exposed to creosote for 6 hr in the dark prior to being UV irradiated for 2 hr and measured with the alamar Blue and CFDA-AM cytotoxicity assays (Figure 4.1.).

F. Cytotoxicity and photocytotoxicity of photomodified creosote

In order to obtain photomodified creosote, aliquots of creosote in L-15/ex were placed in glass jars and UV irradiated for 2 hr. Glass jars were used to reduce losses due to adsorption. The jars were covered with 48 well plate lids to achieve photon fluence rates that were similar to those obtained in UV irradiated 48 well tissue culture plates. The protocol that followed the preparation of photomodified creosote was identical to that described above for the cytotoxicity and photocytotoxicity of creosote but used photomodified creosote solution instead of intact creosote (Figure 4.1.).

G. Alamar Blue and CFDA-AM cytotoxicity assays

The alamar Blue (Immunocorp. Science Inc., Montreal, PQ, Canada) and CFDA-AM (5-carboxyfluorescein diacetate acetoxymethyl ester, Molecular Probes, Eugene, OR, USA) indicator dyes were used in combination as described in Chapter 1. Briefly, alamar Blue and CFDA-AM were prepared together in L-15/ex to give final concentrations of respectively 5% v/v and 4 μ M. After removal of the creosote solutions, aliquots of 150 μ l of the dyes were added to each well and, 2 hr later, fluorescence was quantified with the CytoFluor 2350 (PerSeptive Biosystems,

Burlington, ON, Canada) at respective excitation and emission wavelengths of 530 (± 30) and 595 (± 35) nm for alamar Blue, and 485 (± 22) and 530 (± 30) nm for CFDA-AM.

H. Data analysis

Analysis of raw data: The fluorescence readings in wells that contained creosote in L-15/ex were expressed as a percentage of the readings in control wells that received L-15/ex only. Prior to these calculations, fluorescence readings for wells without cells were subtracted from the experimental and control values with cells. Dose-response data followed a sigmoid relationship and were analyzed by nonlinear regression using the curve-fitting routine of SigmaPlot (Jandel Scientific). Data were fitted to the logistic function as described in Chapter 2 with

$$(1) \quad y(d) = 100 (\%) \{ 1 + \exp[-g(\ln(d) - \ln(EC_{50}))] \}^{-1},$$

where $y(d)$ is the % cell viability at the nominal creosote dose d , g is a slope parameter, and EC_{50} is the nominal creosote concentration that produces 50 % cell viability.

Predicting the cytotoxicity and photocytotoxicity of creosote: Predictions on the % cell viability were made for the cytotoxicity and photocytotoxicity of creosote. These predictions were based on the chemical creosote analysis in this report and on the PAH toxicity data described in Chapters 2 and 3. In accordance with these toxicity data, naphthalene and fluoranthene were used as model compounds for, respectively, the cytotoxicity and photocytotoxicity of the hydrocarbons in creosote.

Cytotoxicity: Three assumptions were made to predict the potential of creosote solutions to be directly cytotoxic. Firstly, it was assumed that all aromatic hydrocarbons and heterocyclics contribute to the direct cytotoxicity of creosote through their accumulation in cell membranes and independent of their structure (Chapter 2). Secondly, water solubility and lipophilicity were regarded as the fundamental properties of a PAH contributing to the accumulation of a PAH in cell membranes. As these two properties are interrelated and work in opposite directions, the potential ability of a PAH to accumulate in cell membranes was expressed as the product of its water solubility limit times its octanol/water partition coefficient. This is referred to as the membrane accumulation factor (MAF). Inasmuch as naphthalene was the most potent PAH to act through direct cytotoxicity and the one most likely to act in this way in the environment, the membrane accumulation factor (MAF) of each PAH was expressed relative to the MAF for naphthalene to give a naphthalene equivalent membrane accumulation factor (NEMAF) (Table 4.2.). The concentration of each PAH could be converted into a naphthalene equivalent concentration (NEC) by multiplying its concentration by its NEMAF. Thirdly, all compounds were assumed to act in membranes additively and in a manner as previously shown for naphthalene (Chapter 2). Thus the

total NEC of a creosote solution was simply the sum of the NECs for each component identified and quantified in creosote (see Table 4.3). Finally, to predict the % cell viability due to cytotoxic compounds in a creosote solution, NECs were applied to the logistic functions obtained previously for the direct cytotoxicity of naphthalene (Chapter 2). These functions were

$$(2) \quad y(d) = 100 (\%) \{ 1 + \exp[-2.035(\ln(d) - \ln(53.404))] \}^{-1} \text{ for alamar Blue, and}$$

$$(3) \quad y(d) = 100 (\%) \{ 1 + \exp[-2.846(\ln(d) - \ln(57.777))] \}^{-1} \text{ for CFDA-AM.}$$

With these functions and with NECs that would be expected at each of the applied nominal creosote concentrations, entire dose-response curves were predicted.

Photocytotoxicity: To predict the photocytotoxicity of creosote, previously obtained fluoranthene equivalent factors (FEFs, Chapter 3) were used to convert the concentrations of strictly photocytotoxic PAHs into fluoranthene equivalent concentrations (FECs). As for the cytotoxic compounds, additivity was assumed. Thus, to predict the % cell viability due to photocytotoxic compounds in creosote, the sum of FECs in each creosote sample was applied to the logistic functions obtained previously for the immediate photocytotoxicity of fluoranthene (Chapter 3). These functions were

$$(4) \quad y(d) = 100 (\%) \{ 1 + \exp[-1.568(\ln(\sum \text{FEC}) - \ln(0.289))] \}^{-1} \text{ for alamar Blue, and}$$

$$(5) \quad y(d) = 100 (\%) \{ 1 + \exp[-1.594(\ln(\sum \text{FEC}) - \ln(0.240))] \}^{-1} \text{ for CFDA-AM.}$$

With these functions and with FECs that would be expected at each of the applied nominal creosote concentrations, entire dose-response curves were predicted.

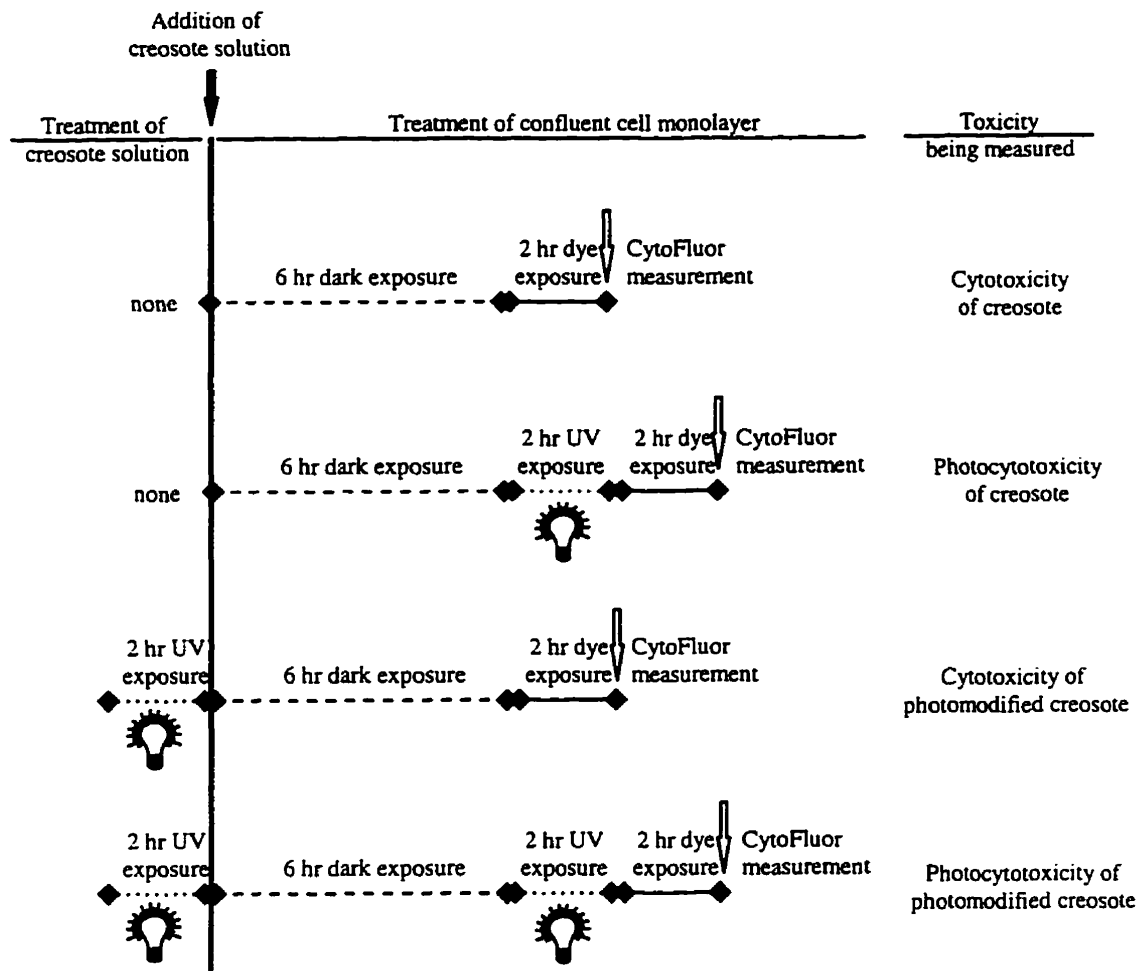


Figure 4.1. Schematic representation of the four conditions under which cells were exposed to creosote (cytotoxicity and photocytotoxicity of creosote) or photomodified creosote (cytotoxicity and photocytotoxicity of photomodified creosote).

4.4. RESULTS

A. *Preparation and chemistry of creosote solutions*

The amount of creosote that could be dissolved in L-15/ex was dependent on the time of stirring. After 1 day of stirring, all priority PAHs were found at higher concentrations in L-15/ex than after 1 hr of stirring, with the exception of naphthalene (Table 4.1., Figure 4.2.). After 3 days, some PAHs had further increased in concentration whereas others slightly decreased. In contrast, all PAH concentrations decreased between days 3 and 7 of stirring. This was also reflected in the total amount of priority PAHs detected, which was lowest after 7 days and highest after 1 and 3 days (Figure 4.2.). However, with the exception of naphthalene, the relative contribution of each PAH to the total mass detected remained relatively constant for each time point with acenaphthene, fluorene and phenanthrene being the main contributors (Figure 4.2.).

Peak concentrations were observed after 3 days of stirring for the other aromatic hydrocarbons (Table 4.1., Figure 4.3.) and for the heterocyclics (Table 4.1.). Among the heterocyclics, dibenzofuran was more abundant than carbazole while, among the aromatic hydrocarbons, 2-methyl-naphthalene + indole were the main contributors (Figure 4.3.).

If all detected compounds were added together, the highest total mass was found to be 8077 $\mu\text{g/l}$ after 3 days of stirring, followed by 6904 $\mu\text{g/l}$, 5830 $\mu\text{g/l}$, and 5571 $\mu\text{g/l}$ after, respectively, 1 day, 1 hr, and 7 days of stirring. Thus, with the method used to solubilize creosote and with taking 31 compounds into account 7.9 to 11.5 % of the 70 mg/l creosote originally added to L-15/ex could be accounted for.

Table 4.1. Chemical analysis of creosote solutions

Compound	Detection limit (d.l.; µg/l)	1 hr ⁽¹⁾	1 day ⁽¹⁾	3 days ⁽¹⁾	7 days ⁽¹⁾
		Concentration in creosote/L-15/ex stock solution (µg/l)			
<u>Priority PAHs</u>					
naphthalene	5.2	16.29	2.46 ⁽²⁾	516.7	207.8
acenaphthylene	5.2	63.62	75.70	101.0	74.96
acenaphthene	5.2	726.1	901.9	1 226	874.1
fluorene	7.3	606.5	781.0	767.6	577.7
phenanthrene	5.2	1 239	1 570	1 224	905.4
anthracene	5.2	131.5	162.5	136.2	109.6
fluoranthene	5.2	511.9	602.9	409.8	282.7
pyrene	2.1	399.8	469.2	313.7	208.0
benzo[a]anthracene	6.3	119.8	144.4	90.75	59.71
chrysene	8.3	105.5	113.4	n.d. ⁽⁴⁾	n.d.
benzo[b+k]fluoranthene ⁽³⁾	14.6	n.d.	n.d.	n.d.	n.d.
benzo[a]pyrene	14.6	n.d.	n.d.	n.d.	n.d.
indeno[1,2,3-cd]pyrene	16<d.l.<208	n.d.	n.d.	n.d.	n.d.
dibenzo[a,h]anthracene	16<d.l.<208	n.d.	n.d.	n.d.	n.d.
benzo[g,h,i]perylene	16<d.l.<208	n.d.	n.d.	n.d.	n.d.
<u>Other aromatic hydrocarbons</u>					
benzene	19.8	234.2	147.2	234.4	131.7
2-methyl-naphthalene + indole ⁽³⁾	9.4	363.2	342.9	930.3	587.4
1-methyl-naphthalene	6.3	66.96	54.17	283.3	161.2
biphenyl	5.2	168.3	186.1	319.6	218.3
<u>Heterocyclics</u>					
dibenzofuran	7.3	704.8	891.2	1 043	774.7
carbazole	9.4	372.6	459.4	481.6	397.5
<u>Other compounds analyzed for but not detected</u>					
toluene	13.5	n.d.	n.d.	n.d.	n.d.
ethylbenzene	8.3	n.d.	n.d.	n.d.	n.d.
p-m-xylenes; o-xylene	8.3	n.d.	n.d.	n.d.	n.d.
trimethylbenzenes: 1,3,5; 1,2,4; 1,2,3	9.4	n.d.	n.d.	n.d.	n.d.

(1) Time refers to the solubilization time of creosote.

(2) Value is below the detection limit of the GC method.

(3) Compounds co-eluted in the applied GC method.

(4) n.d. = not detected

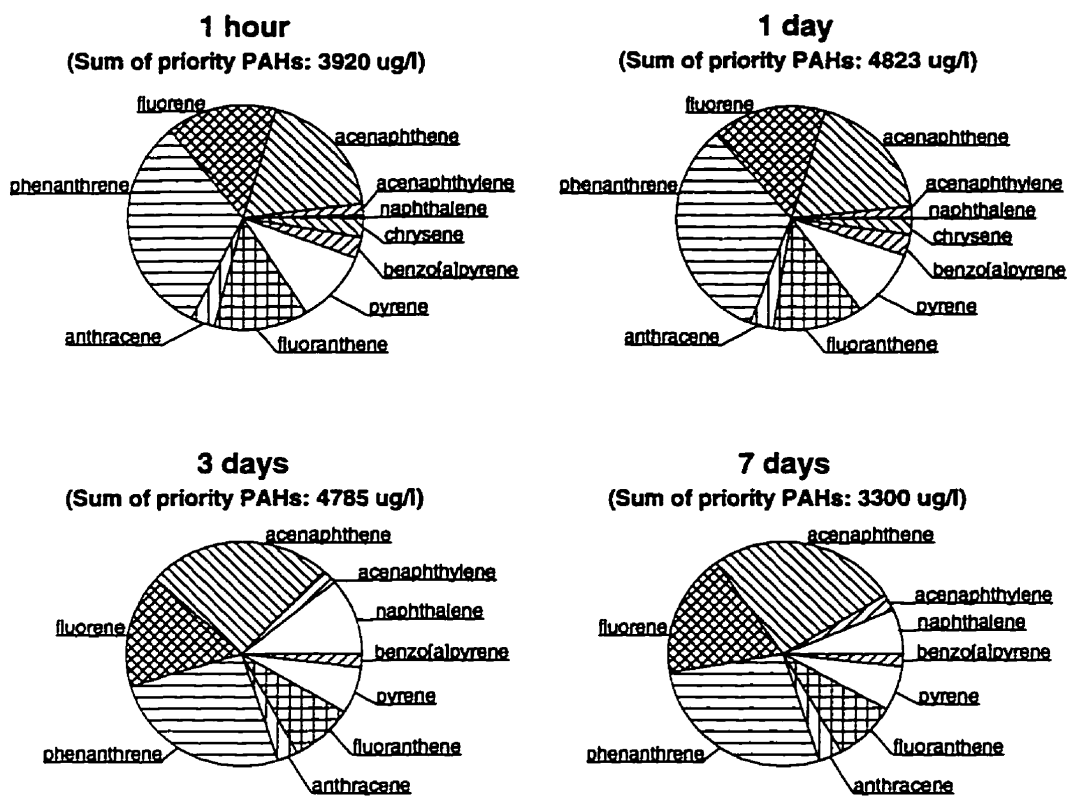


Figure 4.2. Contribution of each of the priority PAHs to the total PAH content measured by GC in the four creosote samples. Creosote was stirred in L-15/ex for 1 hour, 1 day, 3 days and 7 days before the solution was allowed to settle for 1 hour and samples were removed for extraction and chemical analysis. The total PAH content, which is given in brackets, was taken as 100 % and the % contribution of each of the PAHs was then calculated accordingly.

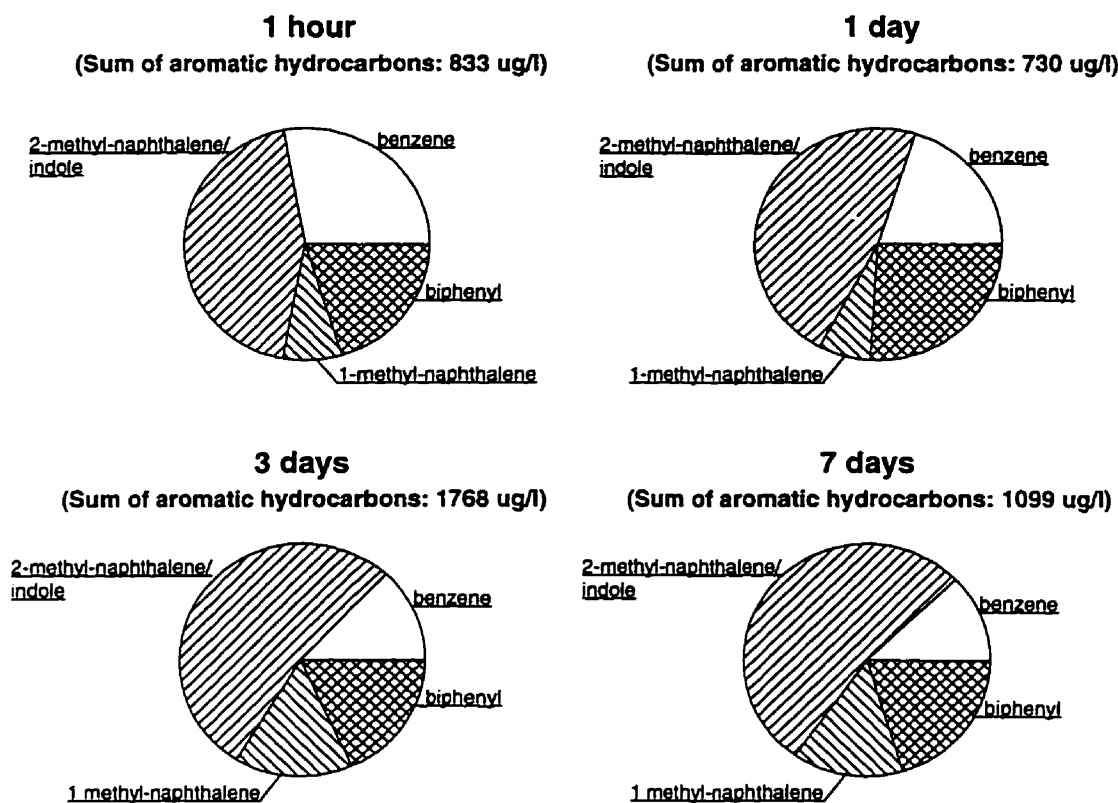


Figure 4.3. Contribution of each of the non-priority aromatic hydrocarbons to the total content of these compounds measured by GC in the four creosote samples. Creosote was stirred in L-15/ex as described in Figure 4.2. The total content of non-priority aromatic hydrocarbons, which is given in brackets, was taken as 100 % and the % contribution of each of the compounds was then calculated accordingly.

B. Cytotoxicity of creosote solutions

After RTgill-W1 cultures had been exposed to creosote solutions for 6 hr in the dark (Figure 4.1.), the two fluorescent dyes, alamar Blue and CFDA-AM, indicated cytotoxic responses. With both indicator dyes, fluorometric readings were greatly reduced at the highest nominal creosote concentration, which was 70 mg/l (Figure 4.4.). For the creosote sample that was obtained after one day of stirring, cytotoxicity was observed also at the second highest creosote concentration, 50 mg/l. For this creosote sample, EC_{50} values were 53 mg/l for alamar Blue and 52 mg/l for CFDA-AM and were the lowest observed for the creosote solutions (Figure 4.4.). In contrast, EC_{50} values were highest for the creosote sample that had been stirred for 1 hr before dosing. EC_{50} values were 71 mg/l and 77 mg/l for, respectively, the alamar Blue and the CFDA-AM cytotoxicity assay (Figure 4.4.). Differences that were observed between the alamar Blue and CFDA-AM cytotoxicity assays were minor in the creosote samples that had been stirred between 1 hr and 3 days. For the 7 day creosote sample, however, the alamar Blue assay revealed a higher level of cytotoxicity for 70 mg/l than did the CFDA-AM assay (Figure 4.4.).

The observed and predicted ability of creosote solutions to be directly cytotoxic were compared (Figure 4.5 and Table 4.4). For predicted ability, the concentrations of all identified compounds in the creosote solutions were converted to naphthalene equivalent concentrations (NECs) and summed to express each nominal creosote dose for each creosote solution as a NEC (Tables 4.2 and 4.3). The NEC of each nominal creosote dose for each creosote sample was subsequently applied to the appropriate logistic functions to yield dose-response curves of predicted direct cytotoxicity (Figure 4.5.). For the creosote solution that had been stirred for 1 hr, these predicted dose-response curves were similar to observed dose-response curves. At high concentrations of the other creosote solutions, the predicted curves were flatter and it became apparent that not all cytotoxicity could be accounted for by NECs (Figure 4.5., 3 days). If the observed direct cytotoxicity was compared to the predicted cytotoxicity at the highest nominal creosote concentration, it could be concluded that between 25 and 94 % of the observed direct cytotoxicity could be accounted for by the compounds analyzed for in the creosote samples (Table 4.4.).

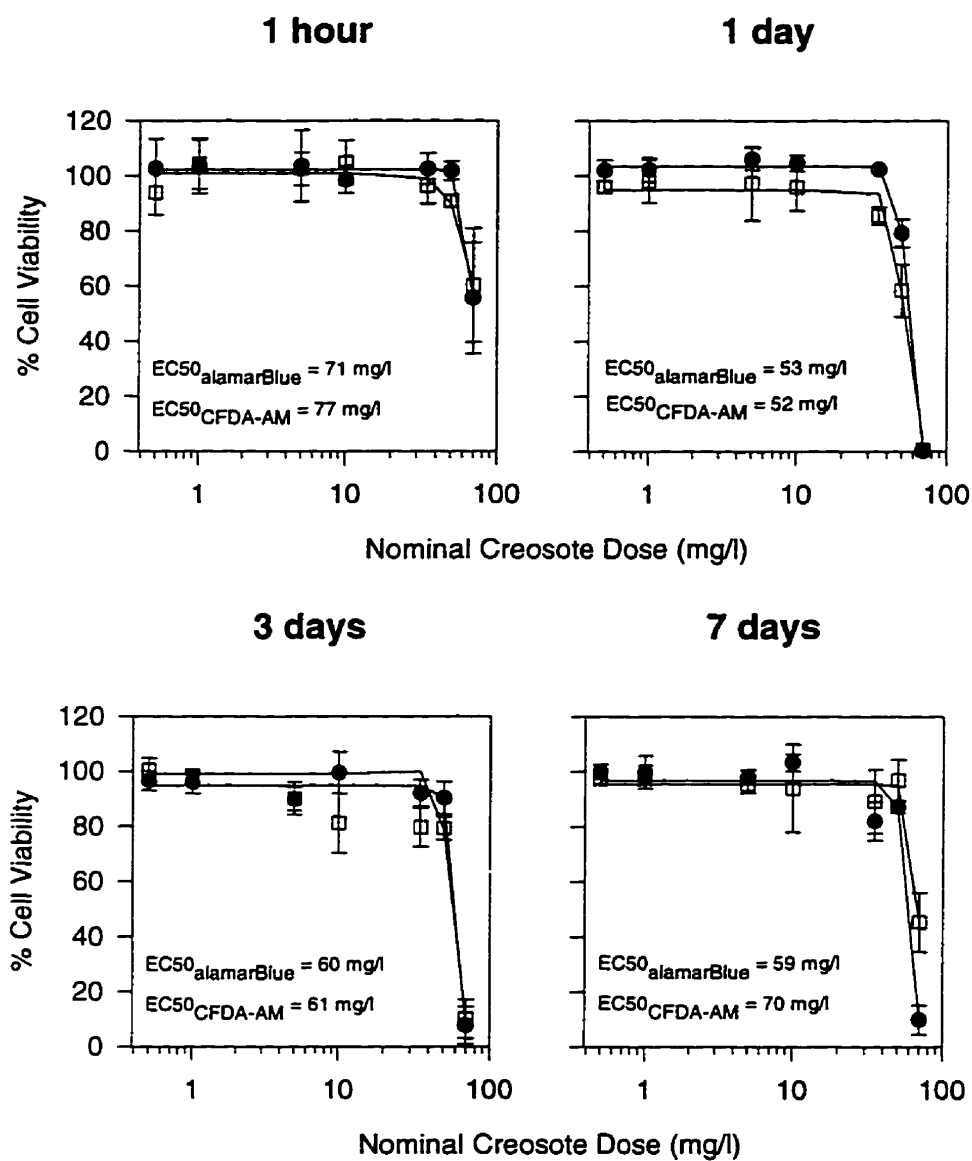


Figure 4.4. Viability of RTgill-W1 cells upon exposure to increasing concentrations of creosote in L-15/ex. Confluent cultures were exposed in the dark for 6 hr to creosote that had been stirred in L-15/ex for 1 hr, 1 day, 3 days and 7 days. Immediately after the exposure, viability was assayed with a mixture of alamar Blue (●) and CFDA-AM (□) and expressed as a percentage of the readings in control cultures that received no creosote. Each data point represents the mean of four culture wells. The vertical lines indicate the standard deviation.

Table 4.2. Derivation of naphthalene equivalent membrane accumulation factors (NEMAFs) for directly cytotoxic compounds

Compound	W.S. (uM) ⁽¹⁾	P _{ow} ⁽²⁾	W.S. x P _{ow} (MAF) ⁽³⁾	NEMAF ⁽⁴⁾
<u>Priority PAHs</u>				
naphthalene	240	1 995	478 800	1.000
acenaphthylene	26.0	12 589	327 314	0.684
acenaphthene	23.0	19 953	458 919	0.958
fluorene	12.0	15 136	181 632	0.379
phenanthrene	7.00	28 840	201 880	0.422
anthracene	0.409	28 184	11 527	0.024
fluoranthene	1.28	165 959	212 427	0.444
pyrene	0.667	75 858	50 597	0.106
benzo[a]anthracene	0.048	407 380	19 554	0.041
chrysene	0.013	812 830	10 567	0.022
<u>Other aromatic hydrocarbons</u>				
benzene	22 000	135	2 970 000	6.203
2-methyl-naphthalene + indole ⁽⁵⁾	173	7 244	1 253 212	2.617
1-methyl-naphthalene	200	7 413	1 482 600	3.096
biphenyl	48.6	12 589	611 825	1.278
<u>Heterocyclics</u>				
dibenzofuran	28.2	13 183	371 761	0.776
carbazole	6.160	5 248	32 328	0.067

(1) W.S. = Water solubility; Source: Mackay et al., 1992.

(2) P_{ow} = Octanol/water partition coefficient; Source: Mackay et al., 1992.

(3) MAF = Membrane accumulation factor.

(4) NEMAF = Naphthalene equivalent membrane accumulation factor
(MAF_{(Compound)}/MAF_{(Naphthalene)}}).}

(5) Compounds co-eluted in the applied GC method. The values in this and the following tables refer to 2-methyl-naphthalene only.

Table 4.3. Directly cytotoxic compounds in creosote and development of naphthalene equivalent concentrations (NECs)

Compound	NEMAF ⁽²⁾	1 hr ⁽¹⁾		1 day ⁽¹⁾		3 days ⁽¹⁾		7 days ⁽¹⁾	
		C ⁽³⁾ (μ M)	NEC ⁽⁴⁾ (μ M)	C ⁽³⁾ (μ M)	NEC ⁽⁴⁾ (μ M)	C ⁽³⁾ (μ M)	NEC ⁽⁴⁾ (μ M)	C ⁽³⁾ (μ M)	NEC ⁽⁴⁾ (μ M)
<u>Priority PAHs</u>									
naphthalene	1.000	0.127	0.127	0.019	0.019	4.03	4.03	1.62	1.62
acenaphthylene	0.684	0.418	0.286	0.497	0.340	0.664	0.454	0.492	0.336
acenaphthene	0.958	4.71	4.51	5.85	5.60	7.95	7.62	5.67	5.43
fluorene	0.379	3.65	1.38	4.70	1.78	4.62	1.75	3.47	1.31
phenanthrene	0.422	6.95	2.93	8.81	3.72	6.87	2.90	5.08	2.14
anthracene	0.024	0.738	0.018	0.912	0.022	0.764	0.018	0.615	0.015
fluoranthene	0.444	2.53	1.12	2.98	1.32	2.03	0.901	1.40	0.625
pyrene	0.106	1.98	0.210	2.32	0.246	1.55	0.164	1.03	0.109
benzo[a]anthracene	0.041	0.525	0.021	0.632	0.026	0.397	0.016	0.261	0.011
chrysene	0.022	0.462	0.010	0.497	0.011	n.d.	n.a.	n.d.	n.a.
<u>Other aromatic hydrocarbons</u>									
benzene	6.203	3.00	18.6	1.89	11.7	3.00	18.6	1.69	10.5
2-methyl naphthalene + indole	2.617	2.56	6.70	2.41	6.31	6.55	17.1	4.14	10.8
1-methyl-naphthalene	3.096	0.471	1.46	0.381	1.18	1.99	6.16	1.13	3.50
biphenyl	1.278	1.09	1.39	1.21	1.55	2.07	2.64	1.41	1.80
<u>Heterocyclics</u>									
dibenzofuran	0.776	4.19	3.25	5.30	4.11	6.20	4.81	4.60	3.57
carbazole	0.067	2.23	0.149	2.75	0.184	2.88	0.193	2.38	0.159
TOTAL NEC:		-	42.2	-	38.1	-	67.3	-	41.9

(1) Time refers to the solubilization time of creosote.

(2) NEMAF = Naphthalene equivalent membrane accumulation factors were obtained from Table 4.2.

(3) Concentrations (C) in μ g/l were obtained from Table 4.1. and converted into mol/l according to the molecular weight of each compound.

(4) NEC = Naphthalene equivalent concentrations were calculated by multiplying C by the corresponding NEMAF.

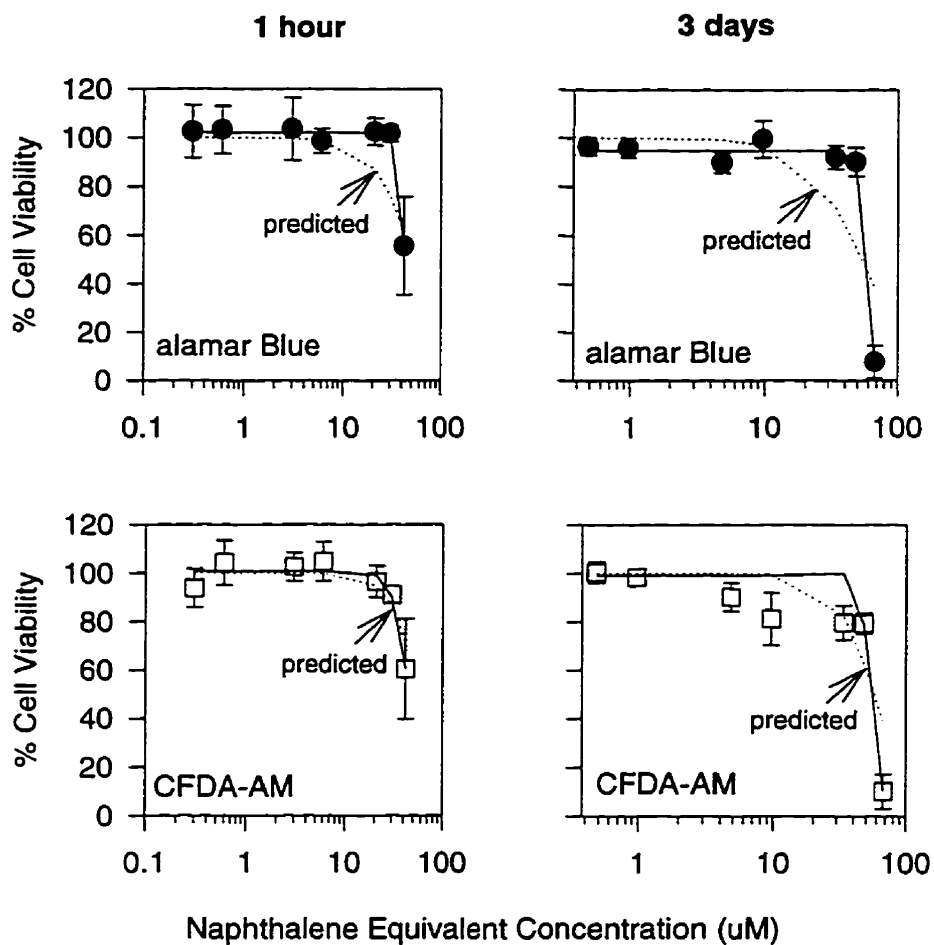


Figure 4.5. Viability of RTgill-W1 cells upon creosote exposures as described in Figure 4.4. and as predicted from previously obtained dose-response curves of naphthalene cytotoxicity using naphthalene equivalent concentrations (NECs). The obtained dose-response curves are the same as those shown for the alamar Blue (●) and CFDA-AM (□) cytotoxicity assays in the 1 hr and 3 days stirred creosote samples in Figure 4.4.. The predicted dose-response curves were obtained by converting the concentrations of hydrocarbons in the creosote samples to NECs using toxic potencies relative to naphthalene (Tables 4.2. and 4.3.). NECs were then applied to calculate the % cell viability at each concentration with the equations that were previously found to adequately describe the dose-response of naphthalene cytotoxicity. These equations are given in the Materials and Methods (equations (2) and (3)).

Table 4.4. Comparison of obtained and predicted direct cytotoxicity of creosote

Characteristics of creosote solution			Observed cytotoxicity of creosote solution (% Cell Viability) ⁽¹⁾		Predicted cytotoxicity due to low molecular weight aromatic hydrocarbons (% Cell Viability) ⁽²⁾		% Cytotoxicity unaccounted for (Predicted - observed)	
Solubilization time	Nominal concentration	NEC ⁽³⁾	alamar Blue	CFDA-AM	alamar Blue	CFDA-AM	alamar Blue	CFDA-AM
1 hour	70 mg/l	42.2 µM	56	60	62	71	6	11
1 day	70 mg/l	38.1 µM	0	1	66	76	66	75
3 days	70 mg/l	67.3 µM	8	10	38	39	30	29
7 days	70 mg/l	41.9 µM	10	45	62	71	52	26

- (1) Values correspond to the % cell viability at 70 mg/l creosote shown in Figure 4.4.
- (2) % cell viability was calculated using the estimated dose-response curves of immediate naphthalene cytotoxicity to RTgill-W1 cells as presented in Chapter 2 and as shown in Figure 4.5. The equations for adequately describing these dose-response curves are the same as equations (2) and (3) in Materials and Methods, and were $y(d) = 100\% \{1 + \exp[-2.035 (\ln(d) - \ln(53.404))]\}^{-1}$ for alamar Blue and $y(d) = 100\% \{1 + \exp[-2.846 (\ln(d) - \ln(57.777))]\}^{-1}$ for CFDA-AM.
- (3) NEC = Naphthalene equivalent concentrations were obtained from Table 4.3.

C. Photocytotoxicity of creosote solutions

When RTgill-W1 cells were UV irradiated immediately after being exposed to creosote for 6 hr in the dark (Figure 4.1.), the two fluorescent dyes, alamar Blue and CFDA-AM, indicated more pronounced cytotoxic responses than dark controls. This photocytotoxicity was observed at concentrations above 1 mg/l. Except for minor differences, the two fluorescent dyes yielded similar dose-response curves for the creosote solutions that were obtained after 1 hr to 3 days of stirring (Figure 4.6.). EC_{50} values were lowest with the 1 and 3 day creosote samples but were slightly higher in the creosote solution that was obtained after 1 hr of stirring (Figure 4.6.). For the 7 day creosote sample, the alamar Blue cytotoxicity assay yielded a dose-response curve and an EC_{50} value that were comparable to any other sample. However, the CFDA-AM assay was less sensitive, and resulted in an EC_{50} value that was three times above the EC_{50} value for alamar Blue (Figure 4.6.).

Previously, several PAHs were found to be strictly photocytotoxic, and fluoranthene was established as a reference compound for this mode of toxic action (Chapter 3). Among the photocytotoxic PAHs, four were found in all creosote samples. These PAHs were anthracene, fluoranthene, pyrene, and benzo[a]anthracene (Tables 4.1. and 4.5.). When the concentrations of these compounds in the stock solution of 70 mg/l creosote in L-15/ex were corrected by their appropriate fluoranthene equivalent factor (FEF) (Chapter 3), fluoranthene equivalent concentrations (FECs) were obtained (Table 4.5.). The sum of FECs in each creosote sample and each nominal creosote dose was subsequently applied to the appropriate logistic functions to yield dose-response curves of predicted photocytotoxicity (Figure 4.7.). If these predicted dose-response curves were compared to the actual creosote dose-response curves, a good agreement between the two was seen. This was true whether the sample contained the highest FECs (Figure 4.7., 1 day) or whether the sample with the lowest FECs was applied (Figure 4.7., 7 days). It was therefore concluded that the four photocytotoxic PAHs, anthracene, fluoranthene, pyrene and benzo[a]anthracene, fully accounted for the observed photocytotoxicity of creosote to RTgill-W1 cells.

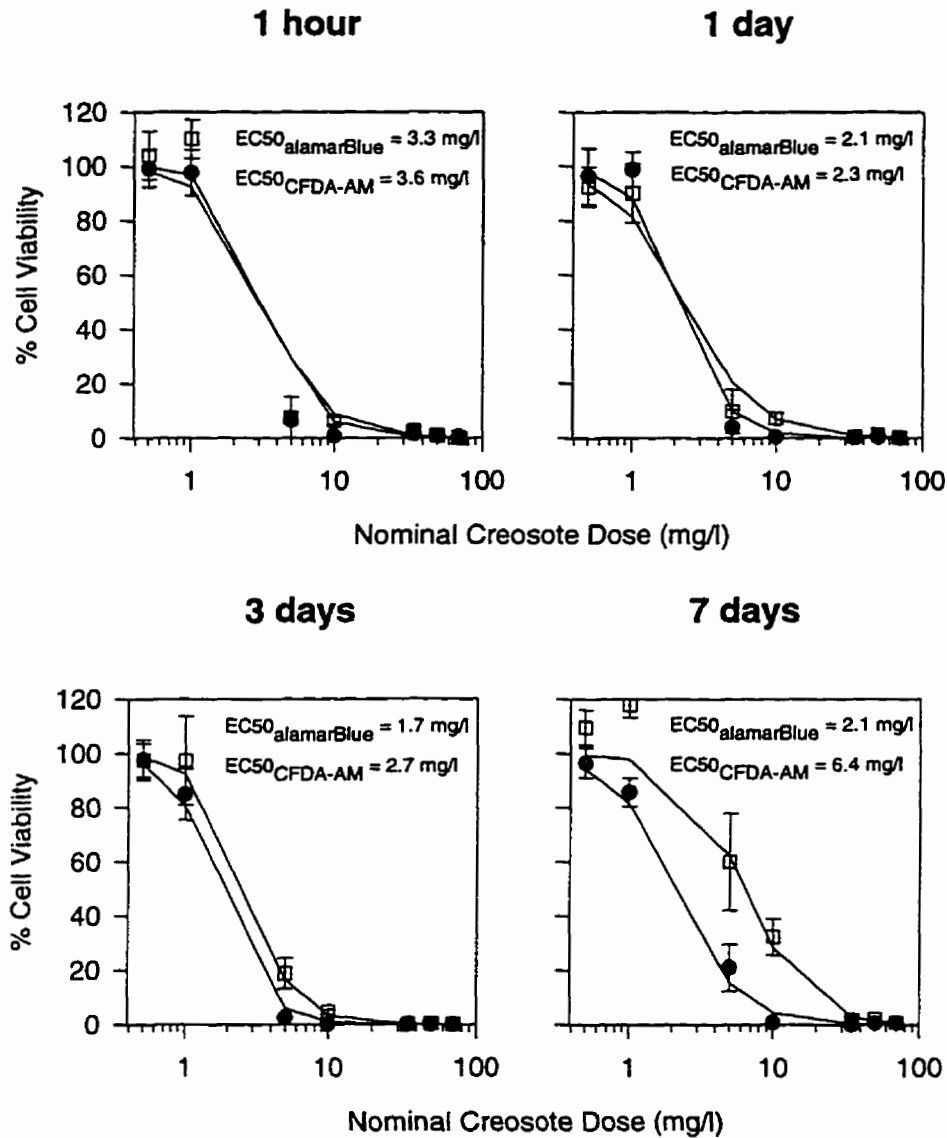


Figure 4.6. Viability of RTgill-W1 cells upon exposure to increasing concentrations of creosote in L-15/ex in the presence of UV radiation. Confluent cultures were exposed to creosote in the dark for 6 hr as described in Figure 4.4, followed by a UV radiation exposure for 2 hr. Immediately after UV irradiation viability was assayed with a mixture of alamar Blue (●) and CFDA-AM (□) and expressed as a percentage of the readings in control cultures that received UV radiation but no creosote. Each data point represents the mean of four culture wells. The vertical lines indicate the standard deviation.

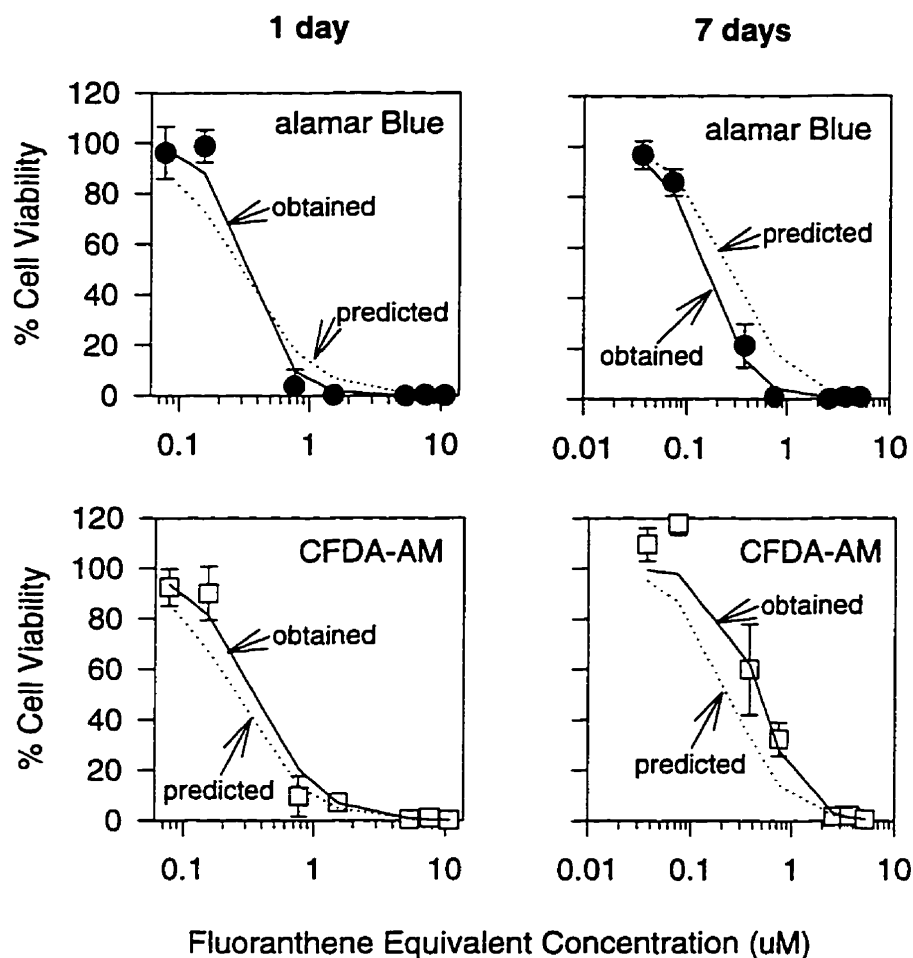


Figure 4.7. Viability of RTgill-W1 cells upon creosote exposures as described in Figure 4.6. and as predicted from previously obtained dose-response curves of fluoranthene photocytotoxicity using fluoranthene equivalent concentrations (FECs). The obtained dose-response curves are the same as those shown for the alamar Blue (●) and CFDA-AM (□) cytotoxicity assays in the 1 and 7 days stirred creosote samples in Figure 4.6.. The predicted dose-response curves were obtained by converting the concentrations of the photocytotoxic PAHs in the creosote samples to fluoranthene equivalent concentrations using previously determined fluoranthene equivalent factors. These concentrations were then applied to calculate the % cell viability at each concentration with the equations that were previously found to adequately describe the dose-response of fluoranthene photocytotoxicity. These equations are given in the Materials and Methods (equations (4) and (5)).

Table 4.5. Photocytotoxic compounds in creosote and development of fluoranthene equivalent concentrations (FECs)

Photo-cytotoxic compound	FEF ⁽²⁾	1 hr ⁽¹⁾		1 day ⁽¹⁾		3 days ⁽¹⁾		7 days ⁽¹⁾	
		C ⁽³⁾ (μ M)	FEC ⁽⁴⁾ (μ M)	C ⁽³⁾ (μ M)	FEC ⁽⁴⁾ (μ M)	C ⁽³⁾ (μ M)	FEC ⁽⁴⁾ (μ M)	C ⁽³⁾ (μ M)	FEC ⁽⁴⁾ (μ M)
anthracene	1.898	0.738	1.40	0.912	1.73	0.764	1.45	0.615	1.17
fluoranthene	1.000	2.53	2.53	2.98	2.98	2.03	2.03	1.40	1.40
pyrene	1.691	1.98	3.35	2.32	3.92	1.55	2.62	1.03	1.74
benzo[a]-anthracene	3.321	0.525	1.74	0.632	2.10	0.397	1.32	0.261	0.867
TOTAL FEC:-			9.02	-	10.73	-	7.42	-	5.18

- (1) Time refers to the solubilization time of creosote.
- (2) Fluoranthene Equivalent Factors (FEFs) were obtained from Chapter 3 (Table 3.3). Although these FEFs were obtained from cytotoxicity assays 24 hr after UV-irradiation, they varied little from the 2 hr FEFs.
- (3) Concentrations (C) in μ g/l were obtained from Table 1 and converted into mol/l according to the molecular weight of each compound.
- (4) Fluoranthene Equivalent Concentrations (FECs) were calculated by multiplying C by the corresponding FEF.

D. Cytotoxicity of photomodified creosote solutions

When RTgill-W1 cells were exposed for 6 hr in the dark to creosote solutions that previously had been UV irradiated for 2 hr (Figure 4.1.), cytotoxicity continued to be detected for all four creosote solutions and with both assays of cellular activity (Figure 4.8.). However, in contrast to the cytotoxicity of unirradiated (intact) creosote, the two assays gave quantitatively different results. For the alamar Blue assay, cytotoxicity was seen at nominal creosote concentrations above 1 mg/l. However, for the CFDA-AM assay, nominal creosote concentrations of 5 mg/l and above were necessary to elicit an appreciable response (Figure 4.8.). Consequently, the EC₅₀ values for the CFDA-AM assay were between 3.2 and 4.5 times higher than those for the alamar Blue assay.

E. Photocytotoxicity of photomodified creosote solutions

When RTgill-W1 cells were UV irradiated for 2 hr immediately after being exposed to photomodified creosote for 6 hr in the dark (Figure 4.1.), photocytotoxicity continued to be detected for all four creosote solutions and with both assays of cellular activity (Figure 4.9). In general, the alamar Blue and the CFDA-AM assays showed responses that were similar to those obtained for the cytotoxicity of photomodified creosote, although toxicity was much more

pronounced for the two endpoints (Figure 4.9.). For the alamar Blue assay, EC_{50} values were comparable to the EC_{50} values that were obtained for the photocytotoxicity of creosote and ranged from 2.1 mg/l for the creosote sample obtained after 1 day of stirring to 4.3 mg/l for the creosote sample obtained after 1 hr of stirring (Figure 4.9.). For the CFDA-AM assay, EC_{50} values were 2.2 to 3.3 times above those obtained for the alamar Blue assay and ranged from 4.6 mg/l for 1 day of stirring to 11 mg/l for 7 days of stirring (Figure 4.9.).

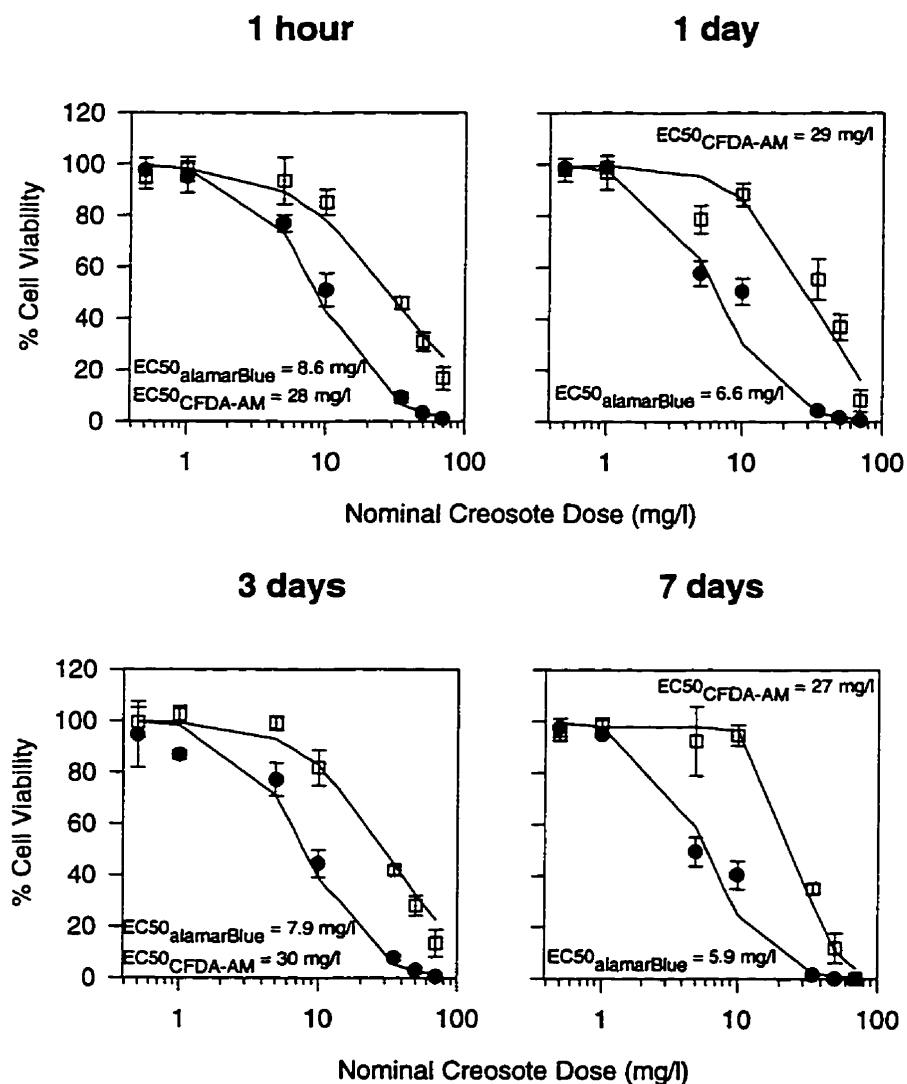


Figure 4.8. Viability of RTgill-W1 cells upon exposure to increasing concentrations of photomodified creosote in L-15/ex. Confluent cultures were exposed in the dark for 6 hr to creosote that had been stirred in L-15/ex for 1 hr, 1 day, 3 days and 7 days and subsequently modified by UV radiation exposure for 2 hr. Immediately after the exposure of this photomodified creosote to cells viability was assayed with a mixture of alamar Blue (●) and CFDA-AM (□) and expressed as a percentage of the readings in control cultures that received no creosote. Each data point represents the mean of four culture wells. The vertical lines indicate the standard deviation.

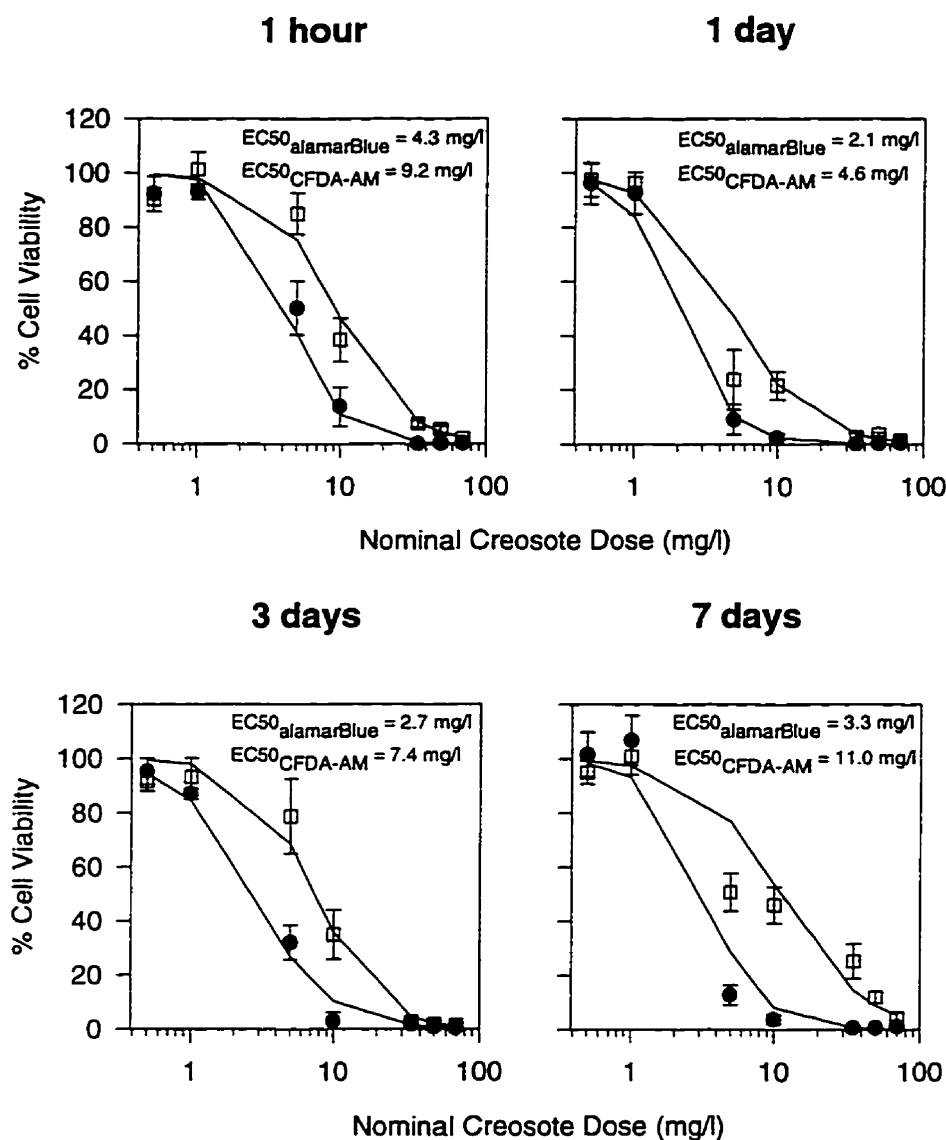


Figure 4.9. Viability of RTgill-W1 cells upon exposure to increasing concentrations of photomodified creosote in L-15/ex in the presence of UV radiation. Confluent cultures were exposed to photomodified creosote as described in Figure 4.8. followed by a UV radiation exposure for 2 hr. Immediately after UV irradiation viability was assayed with a mixture of alamar Blue (●) and CFDA-AM (□) and expressed as a percentage of the readings in control cultures that received no creosote. Each data point represents the mean of four culture wells. The vertical lines indicate the standard deviation.

F. Comparison of cyto- and photocyto-toxicity of intact and photomodified creosote solutions

The toxic potency of creosote to RTgill-W1 cells was strongly influenced by UV radiation. The most potent combination was the simultaneous presence of creosote and UV radiation, the photocytotoxicity of creosote. Compared to creosote alone, toxicity was increased 35 and 23 times in, respectively, the alamar Blue and the CFDA-AM assay in the creosote sample that was solubilized for 3 days (Table 4.6.). If the same creosote sample was photomodified prior to exposure of the cells in the dark, toxicity was 7.6 (alamar Blue) and 2.0 (CFDA-AM) times that of intact creosote, but was lower than the photocytotoxicity of either creosote or photomodified creosote (Table 4.6.). Similar ratios were obtained for the creosote samples that were obtained after 1 hr, 1 day and 7 days of solubilization. The average increase in toxicity compared to intact creosote for all creosote samples was 27 ± 5.9 and 19 ± 5.7 times for alamar Blue and CFDA-AM in the photocytotoxicity of creosote, 8.4 ± 1.1 and 2.3 ± 0.4 times for alamar Blue and CFDA-AM in the cytotoxicity of photomodified creosote, and 20 ± 4.0 and 8.5 ± 1.9 times for alamar Blue and CFDA-AM in the photocytotoxicity of photomodified creosote.

The cytotoxicity and photocytotoxicity of intact and photomodified creosote caused different changes in cell morphology as judged by phase contrast microscopy. For the cytotoxicity of intact and photomodified creosote, cells often were enlarged and their nuclei more distinct than in control cultures. However, membrane blebs were not observed and cells remained attached to the culture surface. In contrast, for the photocytotoxicity of intact and photomodified creosote at the highest concentrations, many cells rounded up and detached from the growth surface during the 2 hr of UV irradiation. At lower concentrations many cells remained attached but had blebs.

Table 4.6. EC_{50} values for the toxicity of creosote and comparison of toxic potencies⁽¹⁾

Toxicity being measured	alamar Blue		CFDA-AM	
	EC_{50} (mg/l) ⁽²⁾	~ fold increase ⁽³⁾	EC_{50} (mg/l) ⁽²⁾	~ fold increase ⁽³⁾
Cytotoxicity of creosote	60.0	1.0	61.0	1.0
Photocytotoxicity of creosote	1.7	35.0	2.7	23.0
Cytotoxicity of photomodified creosote	7.9	7.6	30.0	2.0
Photocytotoxicity of photomodified creosote	2.7	22.0	7.4	8.2

(1) Table contains values obtained in the creosote sample that had been solubilized for 3 days.

(2) Values correspond to the EC_{50} values given for the 3 day creosote sample in Figures 4.4, 4.6., 4.8., and 4.9.

(3) Factor refers to the increase in toxicity compared to the cytotoxicity of creosote (EC_{50} for the cytotoxicity of creosote/ EC_{50} for each of the other properties).

4.5. DISCUSSION

A. *Preparation and chemistry of creosote solutions*

Creosote was solubilized in this study without the aid of a carrier solvent. Although the applied nominal creosote concentration was relatively high, chemical analysis showed compounds to be present in the final creosote solution at concentrations that well reflected those found in ground water at different wood treatment sites (Goerlitz et al., 1985; Rosenfeld and Plumb, 1991). Compared to available data on the composition of the original creosote used in this study (King et al., 1995), creosote in L-15/ex was similar for major components such as phenanthrene, pyrene and anthracene. Naphthalene, however, was found at lower concentrations than expected from the original creosote composition. This confirms studies by Tadokoro et al. (1992) who found that the applied solubilization procedure led to creosote solutions that well reflected the original creosote with the exception of low boiling chemicals. Alternatively, the relatively low naphthalene concentrations found in our study could be due to losses during the storage of the creosote before its application in the experiments described in this report.

B. *Cytotoxicity of creosote solutions*

The cytotoxicity elicited by creosote was similar in many ways to the direct cytotoxicity of individual low molecular weight PAHs (Chapter 2). Similar morphological changes were observed in the cell cultures exposed in the dark to either creosote or individual low molecular weight PAHs. Both the alamar Blue and the CFDA-AM assay gave similar levels of impairment which indicates that the two assays likely were measuring the same damage. This damage would be due to the specific inhibition of membrane-integrated enzymes and/or the general disturbance of membrane properties (Chapter 2; Sikkema et al., 1994). In contrast, toxicity due to metabolic activation was unlikely to have occurred in the current experiments because of the absence of cytochrome P4501A1, and because cytotoxicity occurred within such a short period of time.

High nominal creosote doses were necessary to elicit a cytotoxic response in RTgill-W1 cells. Comparisons to other studies that have used creosote are difficult because of the different ways in which creosote has been applied to test organisms and because the composition of creosote can vary significantly between manufacturers. However, mouse embryo cultures were affected by petroleum creosote at concentrations similar to those that were effective on RTgill-W1 (Iyer et al., 1992). Moreover, the supplementation of culture medium with a rodent hepatic S9 fraction did not modify the embryotoxicity of petroleum creosote.

Additivity has been an adequate model in the past for explaining the toxicity of mixtures of several creosote components, but in the current study such a model described the cytotoxicity of

only one creosote solution. In the past, benzene, naphthalene, acenaphthene and 1-chloronaphthalene were shown to act additively in inhibiting mitochondrial respiration in vitro (Beach and Harmon, 1992; Chapter 2). Naphthalene, acenaphthene, phenanthrene and anthracene were slightly less than additive at equitoxic concentrations in eliciting acute toxicity to *Daphnia magna*, but additivity was still thought a sufficient model (Muñoz and Tarazona, 1993). In the current study an additive model described the cytotoxicity of just the creosote solution that had been stirred for 1 h and not the creosote solutions that had been stirred from 1 to 7 days. Presumably longer stirring dissolved additional compounds, which were not analyzed for chemically. These additional compounds could cause the additive model to under estimate the cytotoxic potential of the creosote solutions in several ways.

The simplest cause of under estimation would be if any of the additional compounds were directly cytotoxic. In favor of this possibility is the fact that the chemistry of creosote is extremely complex, with up to 200 different compounds (Mueller et al., 1989), whereas only 15 to 16 chemicals were identified in the current study and considered in the additive model. The phenols are one chemical class to consider. Phenols are frequently found in creosote (Mueller et al., 1989), and have been shown to be cytotoxic to cultured fish cells (Babich and Borenfreund, 1987; Bols et al., 1985; Schürmann et al., 1997) as well as to fish (Hattula et al., 1981; Hodson et al., 1984; Veith and Broderius, 1990). Another chemical class of potential importance are the polycyclic nitroaromatic hydrocarbons. In studies on the in vitro embryotoxicity of petroleum creosote, Iyer et al. (1992) suggested that polycyclic nitroaromatic hydrocarbons were major contributors to the direct embryotoxicity. A different explanation for the under estimation is that the additional compounds might not be directly cytotoxic, but they could potentiate the cytotoxic actions of other compounds. Only further research with other complex solutions of aromatic hydrocarbons and more complete chemical analysis will allow these possibilities to be distinguished.

C. Photocytotoxicity of creosote solutions

The photocytotoxicity of creosote appeared to arise from photosensitized reactions that led to the formation of reactive oxygen species (Chapters 1 and 3; Valenzo, 1987). This was because the responses of cells to UV irradiation and creosote solutions was similar to the responses to UV irradiation and individual PAH congeners, which appeared to be photocytotoxic through the production of reactive oxygen species (Chapters 1 and 3). The similar responses were the morphological changes of cells and the decline in cellular activities that occurred to the same extent in either the alamar Blue or CFDA-AM assays. The photosensitized reactions potentially could be due to intact PAHs or products that arise from the photomodification of the original sensitizing compound. Alternatively, photomodification products could be cytotoxic directly. However, if cytotoxic photomodification products should indeed arise, they appear to be less

important in the presence of UV radiation. This is because if the creosote solution was photomodified prior to being added to the cells in the dark, toxicity was less than for the photocytotoxicity of creosote and the two fluorescent indicator dyes showed significantly different results. One exception in the photocytotoxicity of creosote is seen in the sample that was solubilized for 7 days. The different responses in the alamar Blue and CFDA-AM assays hint at the formation of photomodification products whose impairment of the mitochondrial electron transport system occurs before general membrane damage.

The photocytotoxicity of creosote solutions could be fully accounted for by four PAHs, using previously developed fluoranthene equivalent factors (FEFs; Chapter 3). These four PAHs were anthracene, fluoranthene, pyrene, and benzo[a]anthracene. In a study on the phototoxicity of several coal tar constituents to guinea-pig skin, Kochevar et al. (1982) found anthracene, fluoranthene and pyrene to be most potent, whereas phenanthrene, chrysene and carbazole were not phototoxic. Other researchers have found relatively high phototoxic potencies for anthracene, fluoranthene, pyrene, and/or benzo[a]anthracene in a variety of biological systems (reviewed by Arfsten et al., 1996). However, it has not been shown previously that these four compounds can account for the photocytotoxicity of a complex mixture such as creosote. This is particularly intriguing as two of the above congeners, namely fluoranthene and pyrene, are prevalent not only in creosote contaminated aquatic environments (Bestari et al., 1997; Rosenfeld and Plumb, 1991) but also in air ambient to aluminum plants, wood heating sources, rural or urban areas, as well as in contaminated fresh water and sediments (Environment Canada, 1994).

The application of FEFs in our study was done under the assumption that the phototoxic compounds act in an additive fashion. Research on the phototoxicity of defined mixtures has just begun. Hatch and Burton (1996) have recently shown that fluoranthene and anthracene were additive in their phototoxicity to benthic organisms. This is in agreement with the proposed similar mode of phototoxic action for PAHs, the generation of reactive oxygen species upon absorption of UV radiation. Hence, higher concentrations of a phototoxic compound or mixtures of phototoxic compounds will give rise to higher concentrations of reactive oxygen species and consequently enhanced toxicity.

D. Cytotoxicity of photomodified creosote solutions

Photomodifying creosote through UV irradiation must have generated cytotoxic products because irradiation caused the creosote solutions to be more cytotoxic. Previously, fluoranthene was shown to be extensively photomodified under similar experimental conditions (Chapter 1), and because fluoranthene has a half-life in solar radiation that is intermediate among the detected PAHs (Huang et al., 1997; Mackay et al., 1992), significant modifications of other PAHs in creosote can be expected as well. Most commonly, the photomodification of a single PAH leads to

a complex mixture that contains, amongst other classes of compounds, quinones and diols (Mallakin et al., 1997; McConkey et al., 1997; Nikolaou et al., 1984). For example, 9,10-phenanthrenequinone (PHEQ), was found to be the major component and primary toxicant in phenanthrene-containing solutions that were exposed to actinic radiation (McConkey et al., 1997). PHEQ was unique in that it not only was resistant to further photooxidation but also in that it did not support photosensitized reactions. With phenanthrene being the most abundant PAH in all creosote samples, PHEQ thus likely contributes to the cytotoxicity of photomodified creosote in the current study.

The alamar Blue assay was more sensitive than the CFDA-AM assay in detecting an inhibition of cellular activity by the photomodified creosote solutions. The EC_{50} s were 3 to 4 fold lower with alamar Blue. This indicates that photomodification products had specific actions in mitochondria. Such an impairment could be due to compounds that structurally mimic components of the electron transport chain. For example, quinones can receive electrons from NADH that are normally donated to ubiquinone. Alamar Blue and natural receptors would then compete for electrons with the quinones of the photomodified creosote solution, which potentially leads to a decreased reduction of alamar Blue and thus decreased fluorescent readings. The reduced quinone can pass on its electron to oxygen, forming superoxide radical and the parent quinone. The quinone can then repeat the cycle while superoxide radical is converted into hydrogen peroxide by superoxide dismutase and/or into hydroxyl radical in the presence of iron by the Fenton reaction (Di Giulio et al., 1989). Thus, quinones can lead to yields of oxygen radicals that exceed the capabilities of cellular antioxidant defense mechanisms and result in a more general damage to cell membranes and proteins. This general damage due to oxidative stress has been measured with CFDA-AM in this report and with Neutral Red in previous reports that used cultured fish cells (Babich et al., 1993; Babich et al., 1994).

E. Photocytotoxicity of photomodified creosote solutions

As with the photocytotoxicity of the original creosote solution, the photocytotoxicity of photomodified creosote appears to arise from photosensitized reactions. Support for this comes from the fact that in combination with UV irradiation both the intact and photomodified creosote solutions caused similar changes in cellular morphology and a level of impairment that was the same with either the alamar Blue or CFDA-AM assays. These photosensitized reactions would have been initiated by parent compounds that remained after the photomodification process or by photomodification products that themselves act as photosensitizers. One such photomodification product that has recently been identified is 2-hydroxyanthraquinone (Mallakin et al., 1997).

F. Comparison of cyto-and photocyto-toxicity of intact and photomodified creosote solutions

The results of this study indicate that assessing the environmental impact of creosote is complex. UV-irradiation consistently increased the toxicity of creosote to fish cells in culture and, at least in the case of the photocytotoxicity of creosote, this was attributable to PAHs. A positive association in fish between high PAH exposures near creosote contaminated sites and the induction of cytochrome P4501A1 (Schoor et al., 1991) or the occurrence of liver neoplasms (Vogelbein et al., 1990) has been reported and constitute other ways in which creosote can be toxic to aquatic organisms. For the UV radiation exposures, the highest toxicity was seen when creosote and the fish gill cells were present simultaneously. This photocytotoxicity of creosote led to a 35-fold increase in toxic potency. Exposure conditions in which photocytotoxicity would be expected to occur in the environment are near the waste water efflux of wood treatment facilities. It is wood treatment and storage facilities that are major contributors of creosote entry into the environment (Environment Canada, 1993). Furthermore, the toxicity of creosote was enhanced when creosote was photomodified prior to exposure to the cell culture system. This cytotoxicity of photomodified creosote led to an 8-fold increase in toxic potency and implies that UV irradiation does not necessarily result in the toxicity deactivation of complex mixtures. Borthwick and Patrick (1982) tested the deactivation of creosote in saltwater due to exposure to direct sunlight and measured a half-life of less than a week. This study indicates that prolonged UV radiation exposures will likely lead to a significant decrease in toxic potency under static conditions. However, if the supply of creosote contaminated water is continuous, as would be expected at wood treatment sites, deactivation due to UV irradiation is not likely to occur but in contrast, can lead to a further activation of toxicity.

The RTgill-W1 cell bioassay allowed the study of a complex chemical mixture, creosote, with respect to its toxicity in the absence or presence of UV radiation. Together with chemical analysis, the assay made it possible to fully determine the compounds that gave rise to the most toxic combination studied here, the simultaneous presence of creosote and UV radiation or the photocytotoxicity of creosote. Furthermore, by combining two fluorescent indicator dyes, alamar Blue and CFDA-AM, responses of cell cultures could be quantified rapidly and reliably with a fluorescent plate reader, and different modes of creosote cytotoxicity identified. Thus, the assay is useful in screening environmental samples for the presence of compounds that are toxic directly or by a concurrent or prior UV irradiation, and in understanding the modes of toxic action of these compounds on a cellular level.

4.6. ACKNOWLEDGMENTS

We would like to thank Kimberly Hamilton for helping with the chemical analysis of the creosote solutions. This research was supported by a Strategic Grant from the Natural Sciences and Engineering Research Council of Canada and by the Canadian Network of Toxicology Centers.

4.7. REFERENCES

- Ankley, G.T., Erickson, R.J., Phillipps, G.L., Mattson, V.R., Kosian, P.A., Sheedy, B.R. and Cox, J.S. (1995) Effects of light intensity on the phototoxicity of fluoranthene to a benthic macroinvertebrate. *Environmental Science and Technology* **29**, 2828-2833.
- Ankley, G. T., Erickson, R.J., Sheedy, B.R., Kosian, P.A., Mattson, V.R. and Cox, J.S. (1997) Evaluation of models for predicting the phototoxic potency of polycyclic aromatic hydrocarbons. *Aquatic Toxicology* **37**, 37-50.
- Arfsten, D. P., Schaeffer, D. J. and Mulveny, D. C. (1996) The effects of near ultraviolet radiation on the toxic effects of polycyclic aromatic hydrocarbons on animals and plants: a review. *Ecotoxicology and Environmental Safety* **33**, 1-24.
- Babich, H. and Borenfreund, E. (1992) Neutral Red assay for toxicology in vitro. In: *In vitro methods of toxicology*, R.R. Watson (Ed), CRC Press, Boca Raton, Chapter 17.
- Babich, H. and Borenfreund, E. (1987) Structure-activity relationship (SAR) models established in vitro with the Neutral Red cytotoxicity assay. *Toxicology in Vitro* **1**, 3-9.
- Babich H., Palace, M.R., Borenfreund, E. and Stern, A. (1994) Naphthoquinone cytotoxicity to bluegill sunfish BF-2 cells. *Archives of Environmental Contamination and Toxicology* **27**, 8-13.
- Babich H., Palace, M.R. and Stern, A. (1993) Oxidative stress in fish cells: *In vitro* studies. *Archives of Environmental Contamination and Toxicology* **24**, 173-178.
- Beach, A.C. and Harmon, H.J. (1992) Additive effects and potential inhibitory mechanism of some common aromatic pollutants on in vitro mitochondrial respiration. *Journal of Biochemical Toxicology* **7**, 155-161.
- Bestari, K.T., Robinson, R.D., Solomon, K.R., Steele, T.S. and Day, K.E. (1997) Distribution and dissipation of polycyclic aromatic hydrocarbons within experimental microcosms treated with liquid creosote. *Environmental Toxicology and Chemistry*, submitted.
- Bols, N.C., Barlian, A., Chirino-Trejo, S.J., Caldwell, S.J., Goegan, P. and Lee, L.E.J. (1994) Development of a cell line from primary cultures of rainbow trout, *Oncorhynchus mykiss* (Walbaum), gills. *Journal of Fish Diseases* **17**, 601-611.
- Bols, N.C., Boliska, S.A., Dixon, D.G., Hodson, P.V. and Kaiser, K.L.E. (1985) The use of fish cell cultures as an indication of contaminant toxicity to fish. *Aquatic Toxicology* **6**, 147-155.
- Bols, N.C. and Lee L.E.J. (1994) Cell lines: availability, propagation and isolation. In: *Biochemistry and molecular biology of fishes*. P.W. Hochachka and T.P. Mommsen (Eds), Elsevier Science, Amsterdam, Vol. 3, 145-159.
- Borthwick, P. and Patrick, J.M. (1982) Use of aquatic toxicology and quantitative chemistry to estimate environmental deactivation of marine-grade creosote in seawater. *Environmental Toxicology and Chemistry* **1**, 281-288.

- Bowling, J. W., Leversee, G. J., Landrum, P. F. and Giesy, J. P. (1983) Acute mortality of anthracene-contaminated fish exposed to sunlight. *Aquatic Toxicology* **3**, 79-90.
- Di Giulio, R.T., Washburn, P.C., Wenning, R.J., Winston, G.W. and Jewell, C.S. (1989) Biochemical responses in aquatic animals: a review of determinants of oxidative stress. *Environmental Toxicology and Chemistry* **8**, 1103-1123.
- Environment Canada (1994) Polycyclic aromatic hydrocarbons. Environmental Protection Act, Report En40-215/42E, Ottawa, ON, Canada.
- Environment Canada (1993) Creosote-impregnated waste materials. Environmental Protection Act, Report En40-215/13-E, Ottawa, ON, Canada.
- Goerlitz, D.F., Troutman, D.E., Godsy, E.M. and Franks, B.J. (1985) Migration of wood-preserving chemicals in contaminated groundwater in a sand aquifer at Pensacola, Florida. *Environmental Science and Technology* **19**, 955-961.
- Hatch, A.C. and Burton, G.A. (1996) Responses of *Chironomus tentans* and *Hyaella azteca* to polycyclic aromatic hydrocarbons. SETAC, 17th annual meeting abstract book, Washington, D.C., November 17-21, 167.
- Hattula, M.L., Wasenius, V.M., Reunanen, H. and Arstila, A.U. (1981) Acute toxicity of some chlorinated phenols, catechols and cresols to trout. *Bulletin of Environmental Contamination and Toxicology* **26**, 295-298.
- Hill, J.O., Royer, R.E., Mitchell, C.E. and Dutcher, J.S. (1983) In vitro cytotoxicity to alveolar macrophages of tar from a low-Btu coal gasifier. *Environmental Research* **31**, 484-492.
- Hodson, P.V., Dixon, D.G. and Kaiser, K.L.E. (1984) The measurement of median lethal doses (LD50s) as a rapid indication of contaminant toxicity to fish. *Environmental Toxicology and Chemistry* **3**, 243-254.
- Huang, X.D., Dixon, D.G. and Greenberg, B.M. (1995) Increased polycyclic aromatic hydrocarbon toxicity following their photomodification in natural sunlight: Impacts on the Duckweed *Lemna gibba* L. G-3. *Ecotoxicology and Environmental Safety* **32**, 194-200.
- Huang, X.D., Dixon, D.G. and Greenberg, B.M. (1993) Impacts of UV radiation and photomodification on the toxicity of PAHs to the higher plant *Lemna gibba* (Duckweed). *Environmental Toxicology and Chemistry* **12**, 1067-1077.
- Huang, X.D., Krylov, S.N., Ren, L., McConkey, B.J., Dixon, D.G. and Greenberg, B.M. (1997) Mechanistic QSAR model for the photoinduced toxicity of polycyclic aromatic hydrocarbons: II. An empirical model for the toxicity of 16 PAHs to the Duckweed *Lemna gibba* L. G-3. *Environmental Toxicology and Chemistry*, in press.
- Iyer, P., Martin, J.E. and Irvin, T.R. (1992) In vitro embryotoxicity of petroleum creosote monitored via mouse preimplantation embryo culture. *Journal of Toxicology and Environmental Health* **37**, 231-245.

- Kagan, J., Kagan, E. D., Kagan, I. A., Kagan, P. A. and Quigley, S. (1985) The phototoxicity of non-carcinogenic polycyclic aromatic hydrocarbons in aquatic organisms. *Chemosphere* **14**, 1829-1834.
- King, M.W.G., Malcolmson, H. and Barker J.F. (1995) Groundwater plume development from a complex organic mixture. API and NGWA conference - Petroleum hydrocarbons and organic chemicals in ground water: prevention, detection and restoration, November 2-4, Houston, Texas.
- Kochevar, I.E., Armstrong, R.B., Einbinder, J., Walther, R.R. and Harber, L.C. (1982) Coal tar phototoxicity: active compounds and action spectra. *Photochemistry and Photobiology* **36**, 65-69.
- Lewis, M.R. (1935) The photosensitivity of chick-embryo cells growing in media containing certain carcinogenic substances. *American Journal of Cancer* **25**, 305-309.
- Lorenzen, A., James, C.A. and Kennedy, S.W. (1993) Effects of UV irradiation of cell culture medium on PCB-mediated porphyrin accumulation and EROD induction in chick embryo hepatocytes. *Toxicology in Vitro* **7**, 159-166.
- Mackay, D., Shiu, W.Y. and Ma, K.C. (1992) Illustrated handbook of physical-chemical properties and environmental fate for organic chemicals (2). Lewis Publishers, Chelsea, MI, 57-367.
- Mallakin, A., McConkey, B.J., Miao G., Mckibben, B., Sniekus, V., Dixon, D.G. and Greenberg, B.M. (1997) Involvement of structural photomodification on the impacts of environmental contaminants: Toxicology of specific anthracene photooxidation products. *Environmental Toxicology and Chemistry*, submitted.
- McCloskey, J. T. and Oris, J. T. (1993) Effect of anthracene and solar ultraviolet radiation exposure on gill ATPase and selected hematologic measurements in the bluegill sunfish (*Lepomis macrochirus*). *Aquatic Toxicology* **24**, 207-218.
- McConkey, B.J., Duxbury, C.L., Dixon, D.G. and Greenberg, B.M. (1997) Toxicity of a PAH photooxidation product to the bacteria *Photobacterium Phosphoreum* and the Duckweed *Lemna Gibba*: Effects of phenanthrene and its primary photoproduct, phenanthrenequinone. *Environmental Toxicology and Chemistry* **16**, 892-899.
- Mueller, J.G., Chapman, P.J. and Pritchard, P.H. (1989) Creosote-contaminated sites: Their potential for bioremediation. *Environmental Science and Technology* **23**, 1197-1201.
- Muñoz, M.J. and Tarazona, J.V. (1993) Synergistic effect to two- and four component combinations of the polycyclic aromatic hydrocarbons: Phenanthrene, anthracene, naphthalene and acenaphthene on *Daphnia magna*. *Bulletin of Environmental Contamination and Toxicology* **50**, 363-368.

- Newsted, J.L. and Giesy, J.P. (1987) Predictive models for photoinduced acute toxicity of polycyclic aromatic hydrocarbons to *Daphnia Magna*, Strauss (Cladocera, Crustacea). *Environmental Toxicology and Chemistry* **6**, 445-461.
- Nicolaou, K., Masclet, P. and Mouvier, G. (1984) Sources and chemical reactivity of polynuclear aromatic hydrocarbons in the atmosphere - a critical review. *The Science of the Total Environment* **32**, 103-132.
- Oris, J.T. and Giesy, J.P. (1987) The photo-induced toxicity of polycyclic aromatic hydrocarbons to larvae of the fathead minnow (*Pimephales promelas*). *Chemosphere* **16**, 1395-1404.
- Oris, J. T. and Giesy, J. P. (1986) Photoinduced toxicity of anthracene to juvenile bluegill sunfish (*Lepomis Macrochirus Rafinesque*): photoperiod effects and predictive hazard evaluation. *Environmental Toxicology and Chemistry* **5**, 761-768.
- Oris, J. T. and Giesy, J. P. (1985) The photoenhanced toxicity of anthracene to juvenile sunfish (*Lepomis* spp.). *Aquatic Toxicology* **6**, 133-146.
- Ren, L., Huang, X.D., McConkey, B.J., Dixon, D.G. and Greenberg, B.M. (1994) Photoinduced toxicity of three polycyclic aromatic hydrocarbons (fluoranthene, pyrene, and naphthalene) to the Duckweed *Lemna gibba* L. G-3. *Ecotoxicology and Environmental Safety* **28**, 160-171.
- Ren, L., Zeiler, L.F., Dixon, D.G. and Greenberg, B.M. (1996) Photoinduced effects of polycyclic aromatic hydrocarbons on *Brassica napus* (Canola) during germination and early seedling development. *Ecotoxicology and Environmental Safety* **33**, 73-80.
- Rosenfeld, J.K. and Plumb, R.H. (1991) Ground water contamination at wood treatment facilities. *GWMR Winter*, 133-140.
- Schirmer, K., Ganassin, R.C., Brubacher, J.L. and Bols, N.C. (1994) A DNA fluorometric assay for measuring fish cell proliferation in microplates with different well sizes. *Journal of Tissue Culture Methods* **16**, 133-142.
- Schoor, W.P., Williams, D.E. and Takahashi, N. (1991) The induction of cytochrome P-450-1A1 in juvenile fish by creosote-contaminated sediment. *Archives of Environmental Contamination and Toxicology* **20**, 497-504.
- Schüürmann, G., Segner, H. and Jung, K. (1997) Multivariate mode-of-action analysis of acute toxicity of phenols. *Aquatic Toxicology* **38**, 277-296.
- Sikkema, J., de Bont, J.A.M. and Poolman, B. (1994) Interactions of cyclic hydrocarbons with biological membranes. *Journal of Biological Chemistry* **269**, 8022-8028.
- Stoien, J.D. and Wang, R.J. (1974) Effect of near-ultraviolet and visible light on mammalian cells in culture. II Formation of toxic photoproducts in tissue culture medium by blacklight. *Proceedings of the National Academy of Science of the U.S.A.* **71**, 3961-3965.

- Tadokoro, H., Maeda, M., Kawashima, Y., Kitano, M., Hwang, D.-F. and Yoshida, T. (1991) Aquatic toxicity testing for multicomponent compounds with special reference to preparation of test solution. *Ecotoxicology and Environmental Safety* **21**, 57-67.
- Valenzo, D.P. (1987) Photomodification of biological membranes with emphasis on singlet oxygen mechanisms. *Photochemistry and Photobiology* **46**, 147-160.
- Veith, G.D. and Broderius, S.J. (1990) Rules for distinguishing toxicants that cause type I and type II narcosis syndromes. *Environmental Health Perspectives* **87**, 207-211.
- Vogelbein, W. K., Fournie, J.W., Van Veld, P.A. and Huggett, R.J. (1990) Hepatic neoplasms in the mummichog *Fundulus heteroclitus* from a creosote-contaminated site. *Cancer Research* **50**, 5978-5986.
- Weinstein, J.E., Oris, J.T. and Taylor, D.H. (1997) An ultrastructural examination of the mode of UV-induced toxic action of fluoranthene in fathead minnows, *Pimephales promelas*. *Aquatic Toxicology*, in press.

CONCLUDING REMARKS AND FUTURE DIRECTIONS

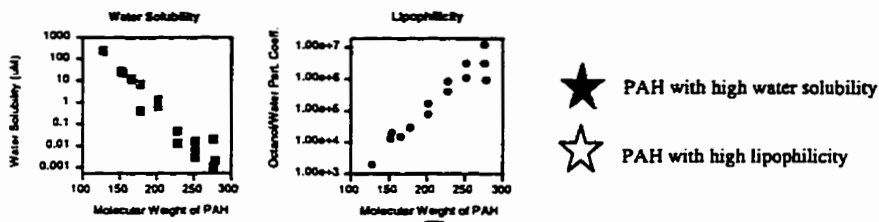
Polycyclic aromatic hydrocarbons (PAHs) are a group of chemicals whose toxicology is difficult to study for at least three reasons. Firstly, PAHs are structurally, and thus physically and chemically, diverse. Secondly, PAHs occur in the environment as complex mixtures and thirdly, PAHs can elicit toxicity in a variety of ways. Two ways in which PAHs can be toxic to aquatic organisms have been studied with continuous fish cell cultures in this thesis: their direct cytotoxicity and their toxicity in the presence of UV radiation, or their photocytotoxicity.

The direct cytotoxicity of PAHs (Figure B.I.) was found to depend on two physical-chemical parameters. These were water solubility and lipophilicity, which work in opposite ways. PAHs with a relatively high water solubility (and a low lipophilicity) provide a large number of molecules in the aqueous phase to be potentially taken up into their cellular target sites, the membranes. However, the low lipophilicity allows only a small portion of the available molecules to accumulate. In contrast, few molecules are soluble in the aqueous phase for PAHs with a low water solubility, providing only a limited number of molecules to be potentially taken up by cells. However, the high lipophilicity favors the cellular uptake of a large portion of the few available PAH molecules. Therefore, if a PAH is equally more water soluble than another PAH is more lipophilic, the net result in the cell is the same. Although the mode of the directly cytotoxic action has not been studied directly, the different fluorescent dyes indicated a general disruption of membrane integrity in the presence of the PAHs but an early inhibition of specific membrane enzymes could not be ruled out.

The photocytotoxicity of PAHs (Figure B.II.) was found to depend on four physical-chemical parameters. These were water solubility and lipophilicity but additionally, the ability of each PAH to absorb UV radiation and to form the electronically excited triplet state, which is needed for photochemical reactions to occur. The transfer of energy from an excited triplet state PAH to oxygen yields singlet oxygen, which beside catalyzing other oxidative reactions, is a prime initiator of lipid peroxidation. Lipid peroxidation is known to lead to membrane blebbing (Halliwell and Gutteridge, 1985) and this has consistently been observed in this study for the photocytotoxicity of PAHs. Furthermore, the transfer of an electron from an excited triplet state PAH to cellular substrates or oxygen can lead to extensive radical formation. Finally, the direct chemical reaction of excited triplet state PAHs with oxygen leads to the formation of oxidized PAH products, such as quinones. Quinones are capable of redox cycling in which enzymes, such as the NADH dehydrogenase of the mitochondrial electron transport chain, serve as electron and hydrogen donors to yield quinone radicals that pass the extra electron to oxygen while returning to their original state. Redox cycling thus can yield radical formation in the presence as well as in the

absence of UV radiation and was thought to be the cause of the specific inhibition of mitochondrial activity in the cytotoxicity of photomodified creosote.

FACTORS AFFECTING CYTOTOXICITY



1. Accumulation of PAH molecules in:

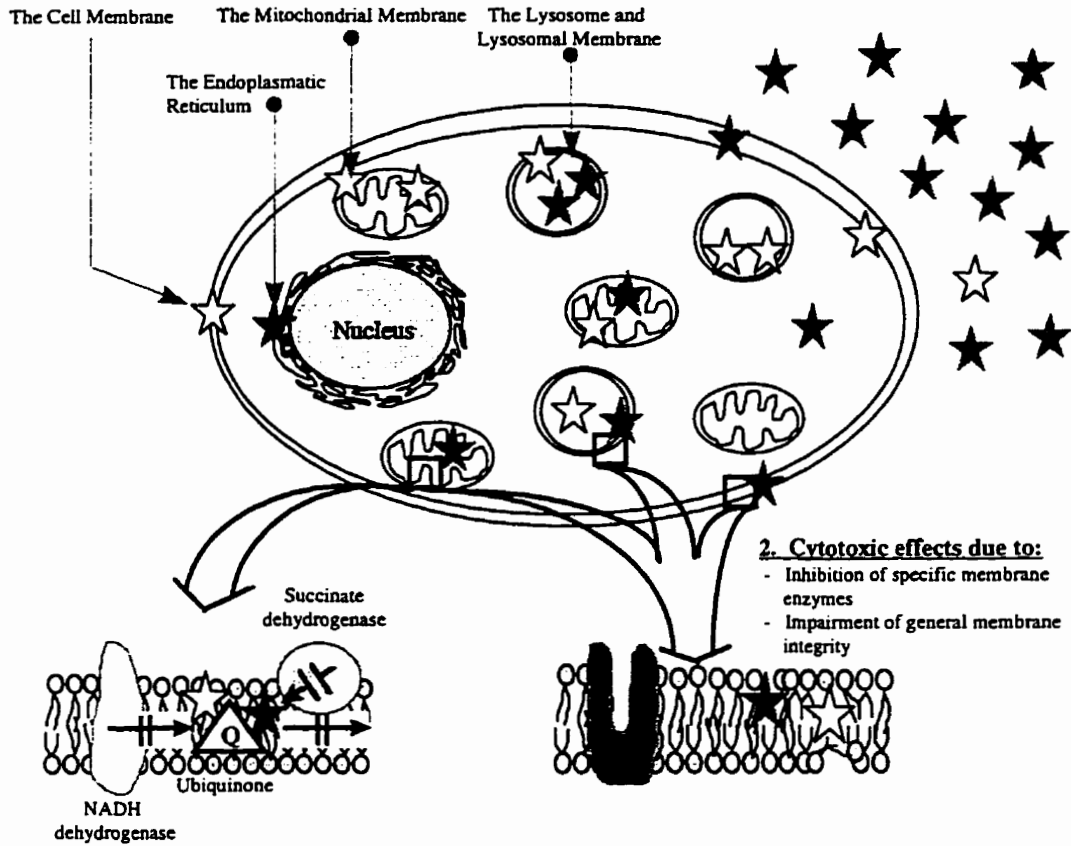


Figure B.I. Schematic representation of the direct cytotoxicity of PAHs.

FACTORS AFFECTING PHOTOCYTOTOXICITY

1. Accumulation of PAH molecules in:

- The Cell Membrane
- The Endoplasmatic Reticulum
- The Mitochondrial Membrane
- The Lysosome and Lysosomal Membrane

★ PAH with high water solubility

☆ PAH with high lipophilicity

2. Absorption of UV radiation by PAH molecules and excited triplet state formation

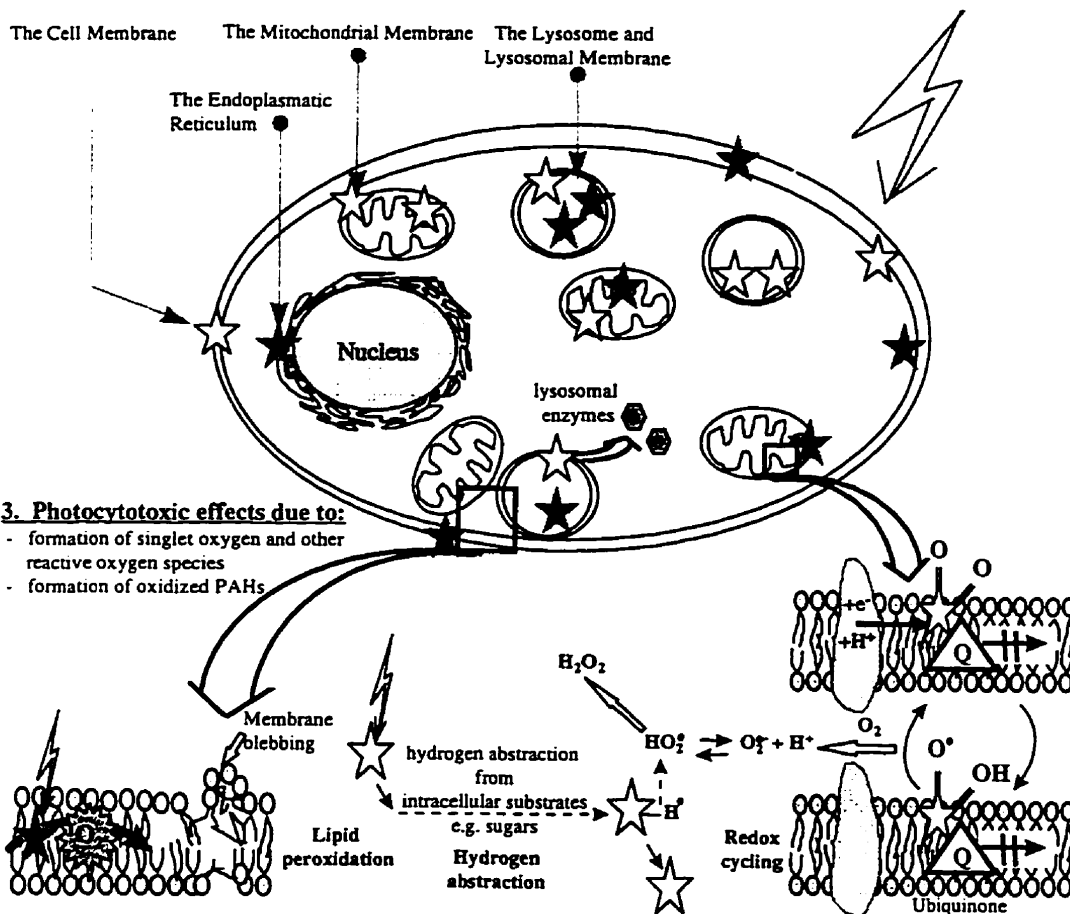
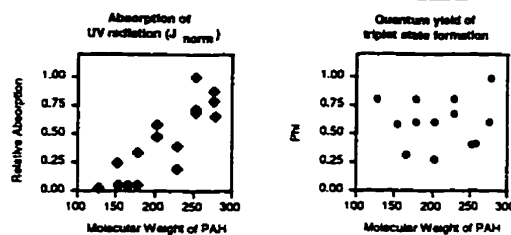


Figure B.II. Schematic representation of the photocytotoxicity of PAHs

Many new questions arose from the results of this work related to the cytotoxicity and photocytotoxicity of PAHs and other ways in which PAHs are toxic. For example, both UV radiation and the PAH fluoranthene have been shown, in separate studies, to induce apoptosis at relatively high doses (Godar and Lucas, 1995; Yamaguchi et al., 1996). Thus, it would be interesting to investigate whether a combination of the two leads to apoptosis at much lower concentrations than previously observed or even at concentrations below those that elicited photocytotoxicity in this thesis. The success with the indicator dyes, alamar Blue and CFDA-AM, suggests that they could be used successfully along with the neutral red to study additional modes of PAH cytotoxicity. One is the cytotoxicity due to metabolic activation. These indicator dyes could be used on cells with an active cytochrome P450-dependent mono-oxygenase system to conveniently screen priority PAHs for their potential to give rise to cytotoxic products through cell metabolism. In addition, the sensitivity of alamar Blue in detecting responses to photomodified creosote suggests that this assay could be used to screen PAHs after they have been UV irradiated for their propensity to give rise to cytotoxic products with a mitochondrial mode of action. In these ways a complete profile of the toxic actions of the priority PAHs could be developed.

The methodological developments that led to the *in vitro* toxicity assays for the direct and photoinduced toxicity of PAHs to the rainbow trout gill cell line, RTgill-W1, have shown that environmentally important features can be incorporated into studies with microwell plates. Previously, the water solubility limits of environmental contaminants have rarely been considered *in vitro*. However, the importance of such considerations has become clear in this study in at least two ways. Firstly, high contaminant concentrations can lead to different mechanisms of toxicity as was seen in the U- or L-shaped dose-response curves for the photocytotoxicity of selected PAHs in the neutral red assay. Secondly, by taking the water solubility limits of PAHs into account, compounds that are the most likely to cause cytotoxicity and/or photocytotoxicity in the environment could be determined. Thus, naphthalene could serve as an indicator of potential cytotoxicity in aqueous environmental samples, whereas fluoranthene and pyrene are indicators of photocytotoxicity.

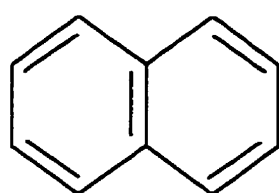
The developed assay procedures are simple, inexpensive and rapid. Both individual PAHs as well as a complex mixture were tested reliably, making the assays a useful tool for testing effluents or environmental samples, as well as for toxic identification evaluations. Furthermore, the assays can be useful in engineering approaches that aim to reduce the toxicity of effluents. Finally, the *in vitro* assays have the potential to lead to new sampling and monitoring techniques.

REFERENCES

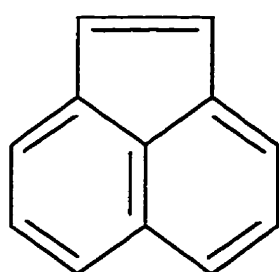
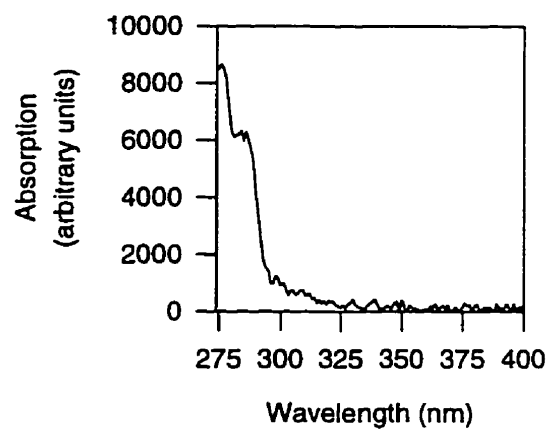
- Godar, D.E. and Lucas, A.D. (1995) Spectral dependence of UV-induced immediate and delayed apoptosis: the role of membrane and DNA damage. *Photochemistry and Photobiology* **62**, 108-113.
- Halliwell, B. and Gutteridge, J.M.C. (1985) Lipid peroxidation: a radical chain reaction. In: *Free radicals in biology and medicine*. Clarendon Press, Oxford, pg. 156.
- Yamaguchi, K., Near, R., Shneider, A., Cui, H., Ju, S.-T. and Sherr, D.H. (1996) Fluoranthene-induced apoptosis in murine T cell hybridomas is independent of the aromatic hydrocarbon receptor. *Toxicology and Applied Pharmacology* **139**, 144-152.

APPENDIX I

CHEMICAL CONFIGURATION AND ABSORPTION SPECTRA OF THE 16 PRIORITY PAHs



NAPHTHALENE



ACENAPHTHYLENE

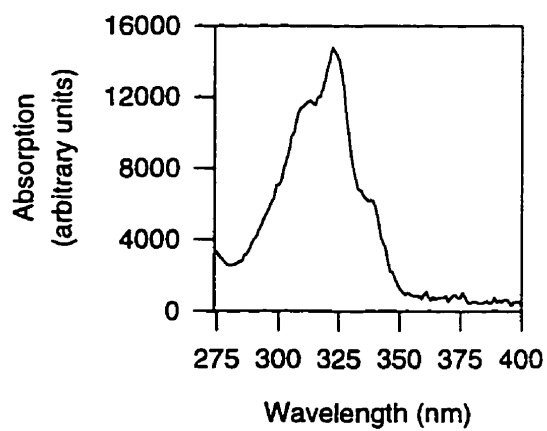
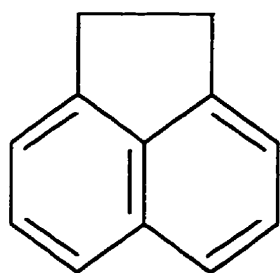
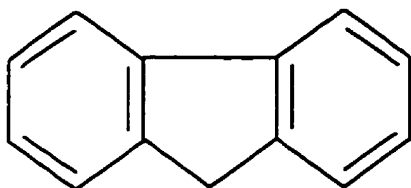
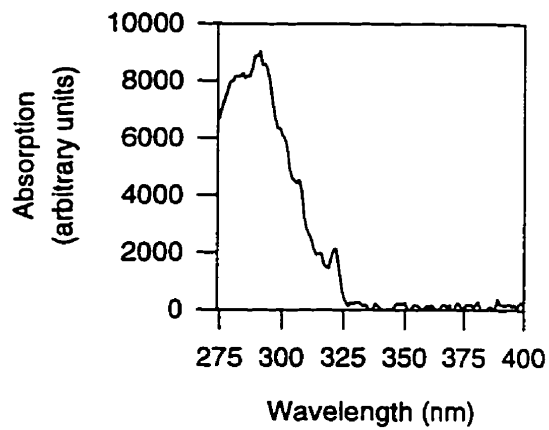


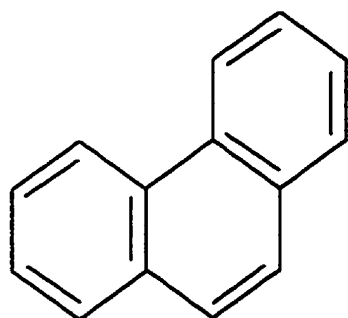
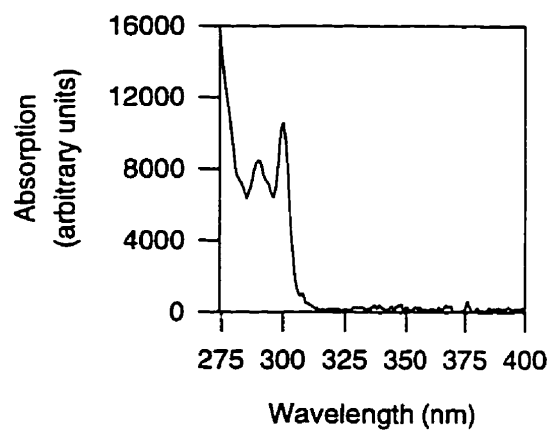
Figure C.I. Representation of the chemical configuration and absorption spectrum for each of the 16 priority PAHs. This figure continues over the next 5 pages.



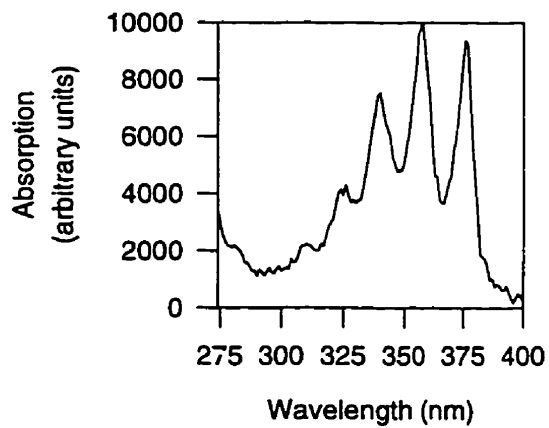
ACENAPHTHENE

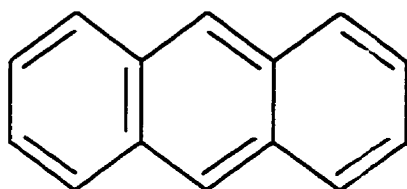


FLUORENE

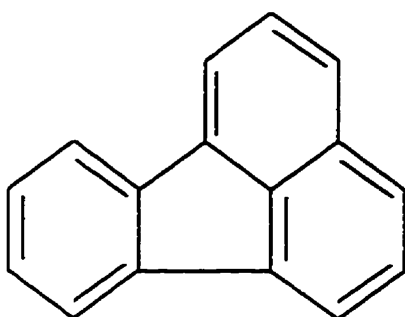
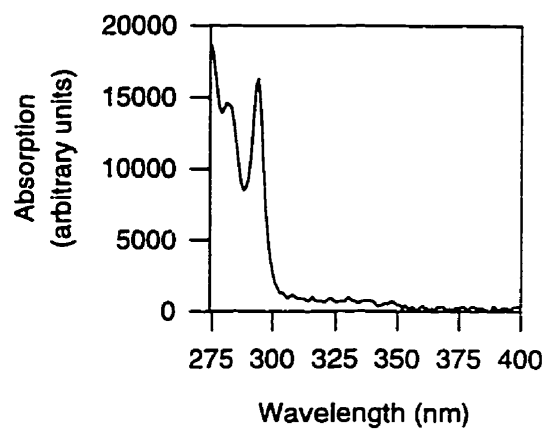


PHENANTHRENE

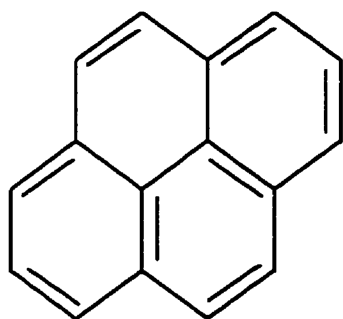
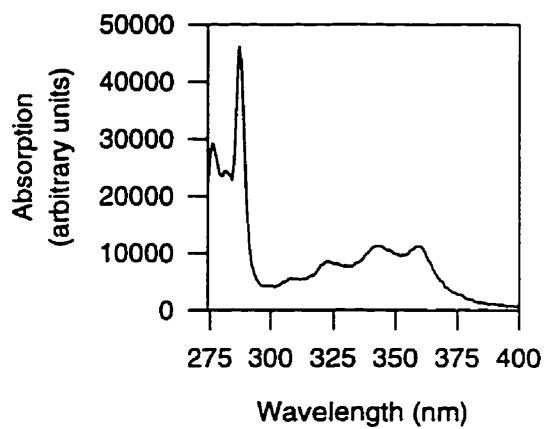




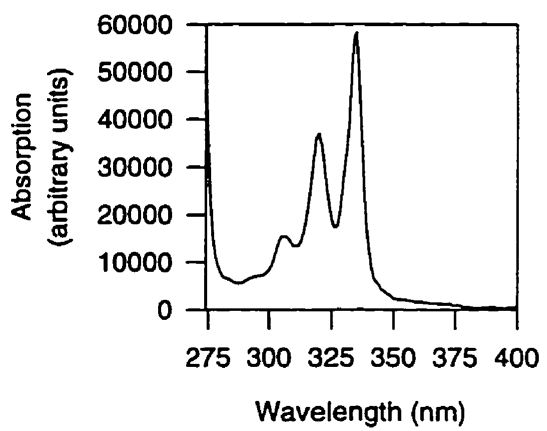
ANTHRACENE

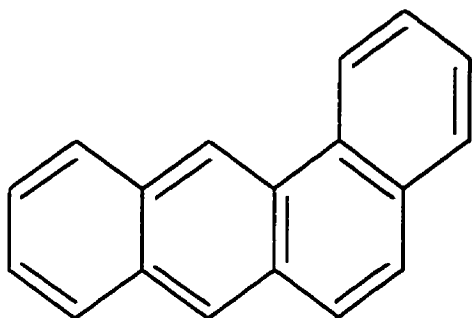


FLUORANTHENE

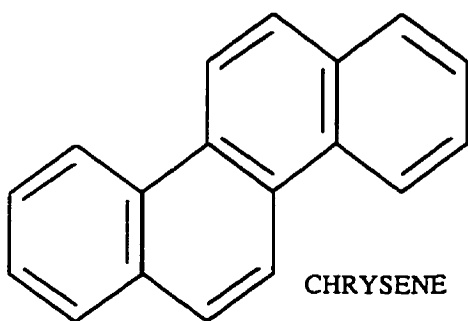
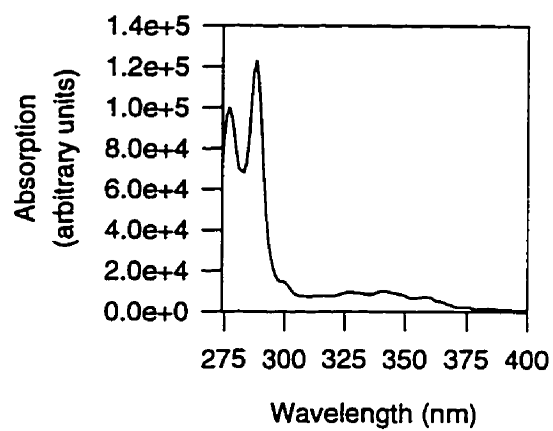


PYRENE

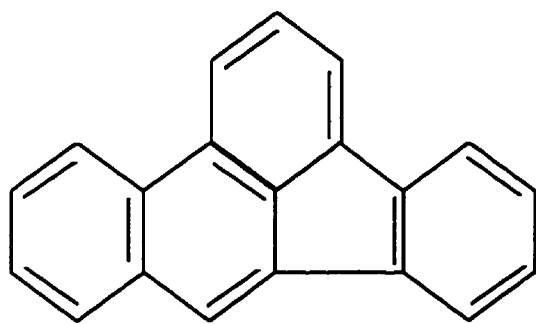
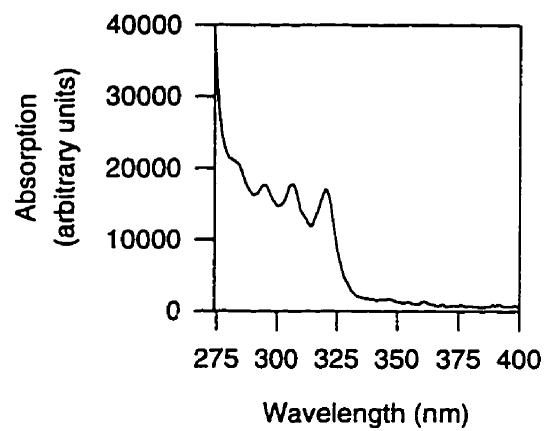




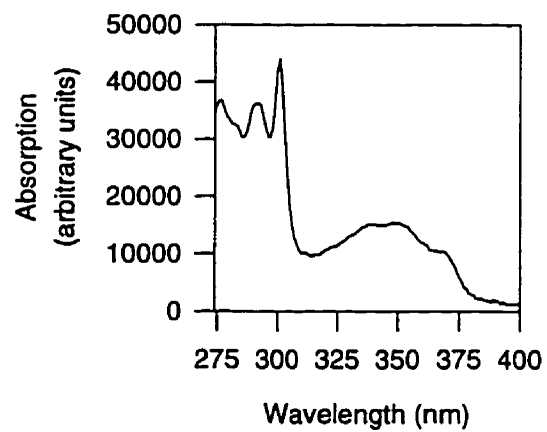
BENZO[a]ANTHRACENE

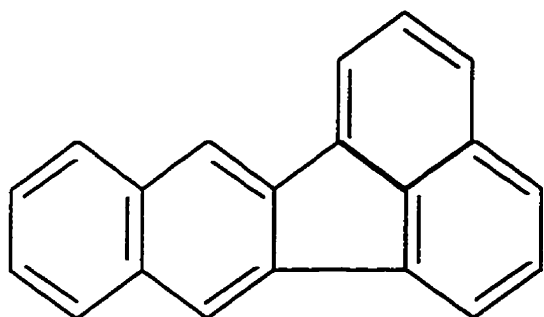


CHRYSENE

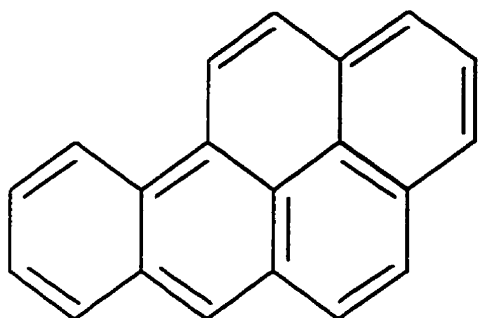
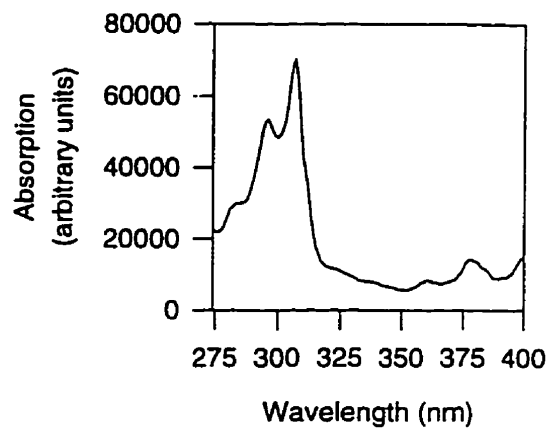


BENZO[b]FLUORANTHENE

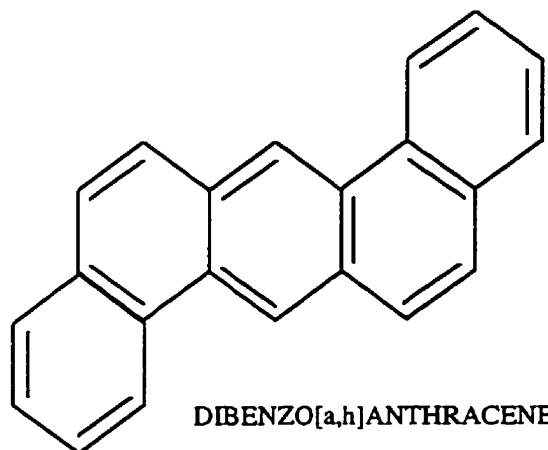
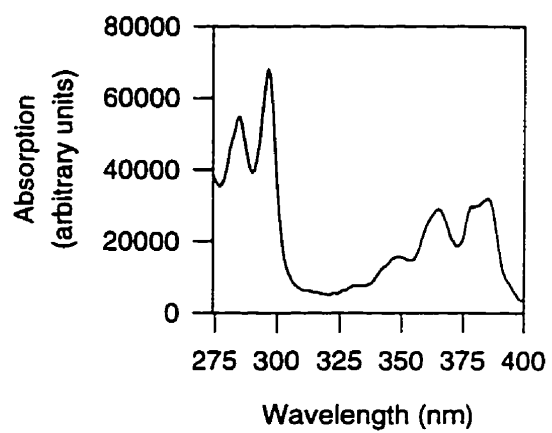




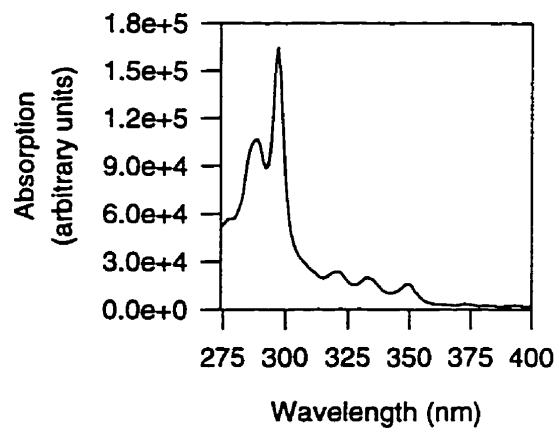
BENZO[k]FLUORANTHENE

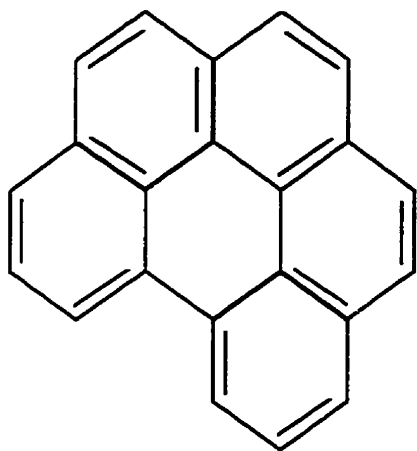


BENZO[a]PYRENE

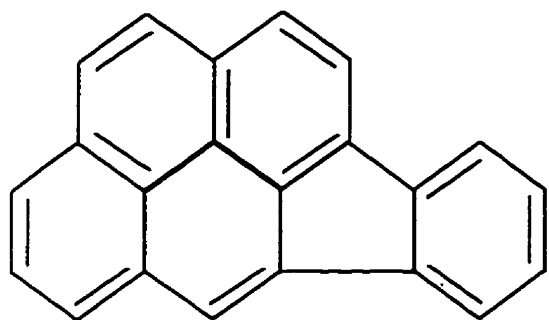
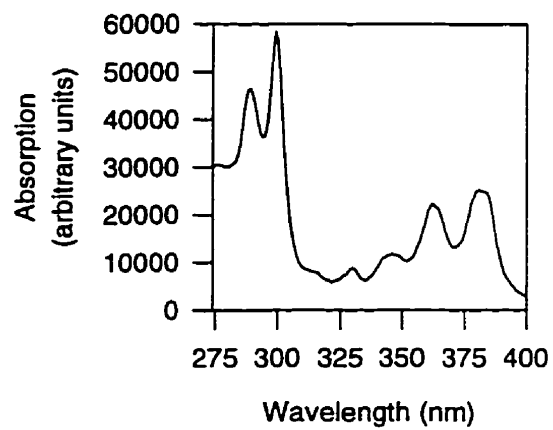


DIBENZO[a,h]ANTHRACENE

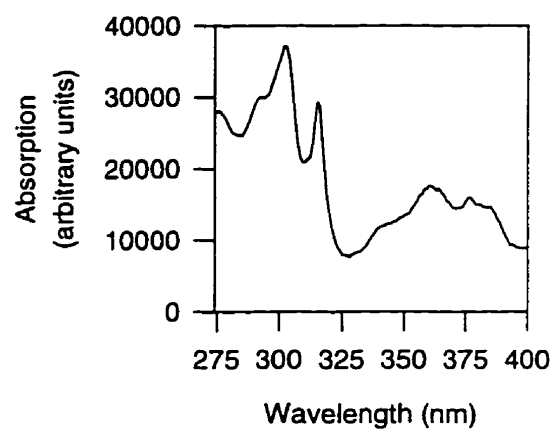




BENZO[g,h,i]PERYLENE



INDENO[1,2,3-cd]PYRENE



APPENDIX II

EMISSION OF UV RADIATION BY UV-B AND UV-A PHOTOREACTOR LAMPS

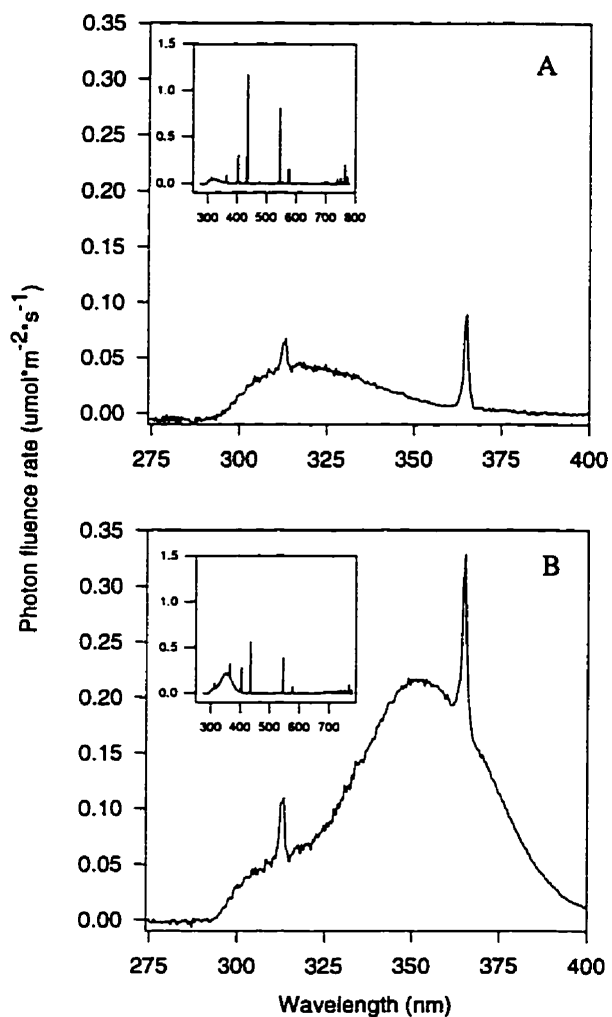


Figure C.II. Emission of UV radiation from 274 to 400 nm by two UV-B photoreactor lamps (A) or one UV-B and one UV-A photoreactor lamp (B), measured after passage through a 48-well culture plate lid. With two UV-B lamps, the photon fluence rate was $1.4 \mu\text{mol m}^{-2} \text{s}^{-1}$ UV-B (UV-A : UV-B, 1.5). With one UV-B and one UV-A lamp, the photon fluence rate was $1.1 \mu\text{mol m}^{-2} \text{s}^{-1}$ UV-B (UV-A : UV-B, 9.7). The inserts show the spectrum emitted between 274 and 778 nm.

APPENDIX III

RTgill-W1 CELL BIOASSAY FOR MEASURING THE CYTOTOXICITY AND PHOTOCYTOTOXICITY OF PAHs

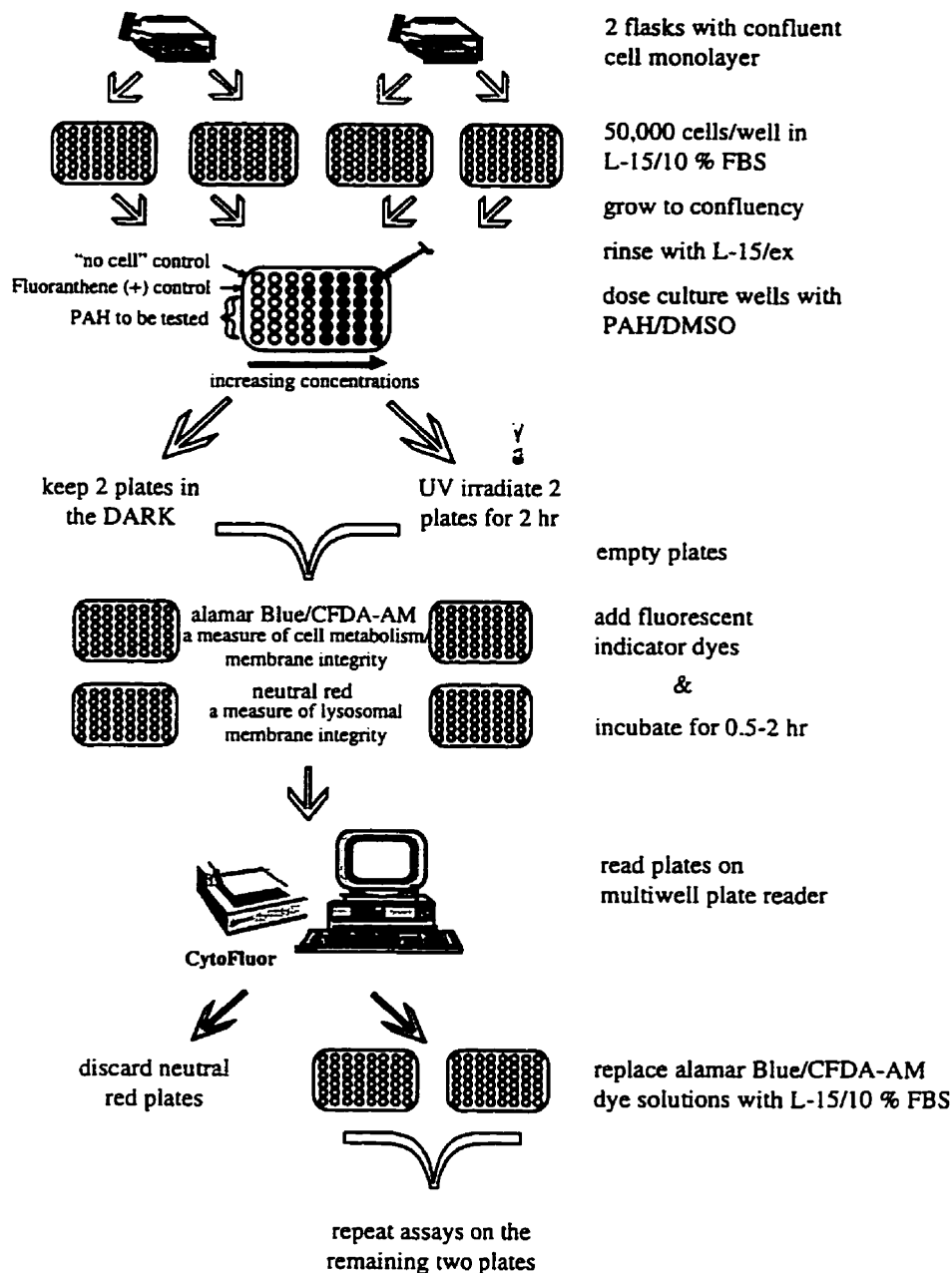


Figure C.III. Schematic representation of the standard assay procedure.

APPENDIX IV

PREPARATION OF THE MODIFIED CULTURE MEDIUM, L-15/ex, AND ALAMAR BLUE, CFDA-AM, AND NEUTRAL RED DYE SOLUTIONS

IV.1. PREPARATION OF L-15/ex

A. *Preparation of constituents of L-15/ex*

The preparation of constituents for L-15/ex follows the procedure outlined by Leibovitz, A. (1963), *American Journal of Hygiene* 78, 173. All components are cell culture grade (Sigma, St. Louis, MO, USA) and are prepared in cell culture grade, distilled water (Canadian Life Technologies, Burlington, ON, Canada).

Salt solution A: To 600 ml water add:

1. 80 g NaCl
2. 4.0 g KCl
3. 2.0 g MgSO₄
4. 2.0 g MgCl₂

Salt solution B: To 100 ml water add;

1. 1.4 g CaCl₂

Salt solution C: To 300 ml water add,

1. 1.9 g Na₂HPO₄
2. 0.6 g KH₂PO₄

Each solution is autoclaved separately and stored at room temperature.

Sodium pyruvate: To 100 ml of water add,

1. 5.5 g sodium pyruvate
2. filter-sterilize (0.2 µm)
3. dispense in 12 ml amounts and store at -20°C

Galactose solution: To 100 ml of water add,

1. 9.0 g galactose
2. filter-sterilize (0.2 μm)
3. dispense in 12 ml amounts and store at -20°C

B. Preparation of L-15/ex

To 1 liter of cell culture grade distilled water add aseptically:

1. 68.0 ml Salt Solution A
2. 11.4 ml Salt Solution B
3. 34.0 ml Salt Solution C
4. 11.4 ml sodium pyruvate
5. 11.4 ml galactose

Store at room temperature.

IV.2. Preparation of dye working solutions

A. Preparation of alamar Blue

Dilute alamar Blue solution (Immunocorp. Science Inc., Montreal, PQ, Canada) in L-15/ex to a final concentration of 5 % v/v. Always prepare fresh.

B. Preparation of CFDA-AM

CFDA-AM stock solution: To the crystalline CFDA-AM (Molecular Probes, Eugene, OR, USA) add DMSO to give 4 mM CFDA-AM. Store at -20°C .

CFDA-AM working solution: Thaw stock solution at room temperature and dilute 1 : 1000 in L-15/ex to yield 4 μM . If alamar Blue and CFDA-AM are being used together, dilute the CFDA-AM stock solution 1 : 1000 in the alamar Blue working solution to yield 4 μM CFDA-AM. Always prepare fresh. Re-freeze stock solution.

C. Preparation of neutral red

Neutral red stock solution: Dissolve 50 mg neutral red (94 %, Sigma Chemical Co., St. Louis, MO, USA) in 10 ml of ddH₂O. Store this stock solution at room temperature and protected from light.

Neutral red working solution: Dilute stock solution 1 : 100 in L-15/ex to give 50 µg/ml neutral red in L-15/ex. Vortex well and filter-sterilize (0.2 µm). Always prepare fresh.

Neutral red fixative: Prepare 0.5 % v/v formaldehyde and 1 % w/v CaCl₂ in ddH₂O. Store at room temperature.

Neutral red extraction solution: Prepare 1 % v/v acetic acid and 50 % v/v ethanol in ddH₂O. Store at room temperature.